

**International  
Progress Report**

**IPR-07-21**

# **Äspö Hard Rock Laboratory**

## **Temperature Buffer Test**

**Sensors data report  
(Period 030326-070701)  
Report No:10**

Reza Goudarzi

Mattias Åkesson

Harald Hökmark

Clay Technology AB

July 2007

***Svensk Kärnbränslehantering AB***

Swedish Nuclear Fuel  
and Waste Management Co  
Box 5864  
SE-102 40 Stockholm Sweden  
Tel 08-459 84 00  
+46 8 459 84 00  
Fax 08-661 57 19  
+46 8 661 57 19





Report no.	No.
IPR-07-21	F12K
Author	Date
Reza Goudarzi	July 2007
Mattias Åkesson	
Harald Hökmark	
Checked by	Date
Bertrand Vignal	2007-12-11
Approved	Date
Anders Sjöland	2008-01-16

# Äspö Hard Rock Laboratory

## Temperature Buffer Test

**Sensors data report  
(Period 030326-070701)  
Report No:10**

Reza Goudarzi  
Mattias Åkesson  
Harald Hökmark

Clay Technology AB

July 2007

**Keywords:** Field test, Data, Repository, Bentonite, Rock, Canister, Measurements, Water pressure, Total pressure, Relative humidity, Temperature, Displacements

This report concerns a study which was conducted for SKB. The conclusions and viewpoints presented in the report are those of the author(s) and do not necessarily coincide with those of the client.



# Résumé

TBT (Test de Barrière ouvragée en Température) est un projet mené par SKB et l'ANDRA, soutenu par ENRESA (en modélisation) et DBE (en instrumentation) qui vise à comprendre et modéliser le comportement thermo-hydro-mécanique de barrières ouvragées à base d'argile gonflante soumises à des températures élevées ( $> 100^{\circ}\text{C}$ ) pendant leur hydratation.

L'essai est conduit dans le HRL d'Äspö dans une alvéole verticale de 8 m de profondeur et 1,75 m de diamètre. Deux sondes chauffantes (chacune de 3 m de long et 0,6 m de diamètre) sont entourées d'argile gonflante, une bentonite MX 80 qui est confinée par un bouchon ancré dans la roche par 9 câbles. L'essai fonctionne depuis le printemps 2003. Les sondes ont été chauffées chacune à la puissance nominale de 1500 W du 15<sup>ème</sup> au 1171<sup>ème</sup> jour et à 1600 W depuis.

Ce rapport présente les données de TBT enregistrées depuis son début le 26 mars 2003 jusqu'au premier juillet 2007.

Dans la bentonite la pression totale est mesurée en 29 points, la pression de pore en 8 points et l'humidité relative en 35 points. La température est mesurée en 92 points et aussi à l'emplacement de chaque capteur dont la mesure nécessite d'être compensée en température.

Des mesures additionnelles sont faites : température en 40 points dans la roche alentour, en 11 points à la surface et 6 à l'intérieur des sondes. La force de confinement est mesurée sur trois des neuf câbles. Le déplacement vertical du bouchon est mesuré en trois points. Le débit et la pression d'eau fournie au système sont également mesurés.

Des mesures de température et de pression dans les zones chaudes du test obtenues par des capteurs à fibres optiques installés par DBE sont rapportées dans l'Appendix B.

Globalement, le système de mesure et de transmission des données fonctionne bien et les capteurs fournissent des valeurs fiables. Une exception concerne la mesure d'humidité relative au droit de la sonde inférieure où plusieurs capteurs ne fonctionnent plus.

La densité des dispositifs de mesure de température par thermocouples à mi-hauteur de chaque sonde chauffante s'est révélée utile pour observer de façon qualitative les cycles saturation - désaturation. Dans la section du bas des indications claires de désaturation sont apparues très tôt dans l'expérience sur une zone annulaire de 0.15 m autour de la sonde chauffante. Cette partie se resature très lentement à l'heure actuelle.

Dans la bentonite, la plupart des mesures d'humidité ne sont plus significatives, car le matériau est désormais trop proche de la saturation. Cependant dans la section supérieure (au Ring 9), le fait que les pressions de pore tendent à s'équilibrer avec la pression d'eau du filtre de sable indique une quasi saturation de l'argile.

Ce filtre de sable disposé entre la roche et la colonne de bentonite permet une alimentation artificielle du système en eau. Plus de la totalité de l'eau théoriquement nécessaire au remplissage du filtre et à la saturation de la bentonite a été injectée, ce qui montre que le système n'est pas hydrauliquement clos mais fuit dans l'environnement rocheux (EDZ). La pression croissante nécessaire pour maintenir le débit d'injection prouve la fragilité du système d'injection (colmatage des embouts des injecteurs).

Depuis le dernier rapport, une action de décolmatage a été entreprise avec une injection d'eau déminéralisée en remplacement de l'eau de site utilisée depuis le début de l'expérience. Cette action s'est révélée fructueuse et depuis il est possible de maintenir la pression hydraulique dans le filtre autour de 4 bar absolu.

La baisse de pression totale et la hausse de la succion observées entre le 225<sup>ème</sup> et le 370<sup>ème</sup> jour autour de la sonde supérieure ont été provoquées par un déficit en eau inattendu du haut du filtre de sable. Lorsque ce filtre a été de nouveau rempli, la pression totale dans la bentonite s'est rétablie et la succion s'est remise à décroître.

# Abstract

TBT (Temperature Buffer Test) is a joint project between SKB/ANDRA and supported by ENRESA (modeling) and DBE (instrumentation), which aims at understanding and modeling the thermo-hydro-mechanical behavior of buffers made of swelling clay submitted to high temperatures (over 100°C) during the water saturation process.

The test is carried out in Äspö HRL in a 8 meters deep and 1.75 m diameter deposition hole, with two canisters (3 m long, 0.6 m diameter), surrounded by a MX 80 bentonite buffer and a confining plug on top anchored with 9 rods. It was installed during spring 2003. The canisters were heated with 1500 W power from day 15 to day 1171. The power was raised to 1600 W since day 1171.

This report presents data from the measurements in the Temperature Buffer Test from 030326 to 070701 (26 March 2003 to 01 July 2007).

The following measurements are made in the bentonite: Temperature is measured in 92 points, total pressure in 29 points, pore water pressure in 8 points and relative humidity in 35 points. Temperature is also measured by all gauges as an auxiliary measurement used for compensation.

The following additional measurements are done: Temperature is measured in 40 points in the rock, in 11 points on the surface of each canister and in 6 points inside each canister. The force on the confining plug is measured in 3 of the 9 rods and its vertical displacement is measured in three points. The water inflow and water pressure in the outer sand filter is also measured.

Temperature and total pressure measurements obtained in the hot parts of the system with fiber optic sensors installed by DBE are reported in Appendix B.

A general conclusion is that the measuring systems and transducers work well and almost all sensors deliver reliable values. An exception is the Relative Humidity sensors in the high temperature area around the lower canister, where sensors have failed.

The dense arrays of thermocouples at the mid-height of the two heaters appear to be useful for examining the dehydration/hydration process qualitatively. In the lower section there are clear signs of early dehydration in a 0.15 m annular zone around the heater. Resaturation of this part is now slowly in progress.

In the bentonite buffer, most humidity sensors measurements are now insignificant, the material being too close to saturation. However in the upper section (Ring 9), the fact that pore pressure start equilibrating with the water pressure in the sand slot indicates a quasi saturation of the clay material.

This sand slot set between the bentonite column and the surrounding rock is used for artificial wetting. More than the water theoretically needed to fill up the sand slot and to saturate the bentonite has already been injected, which proves that the system is not hydraulically closed but leaks towards the rock (EDZ). The high sand slot injection pressure required to maintain the inflow shows the weakness of the injection system (clogging of the filter tips). Since the last report, an unclogging action has been taken by injecting demineralised water instead of ground water, as it was done since the beginning of the experiment. This action proved successful, and it is now possible to maintain the hydraulic pressure in the filter around 4 bar absolute.

The decrease in total pressure and increase in suction that was recorded around the upper canister from day 225 to day 370 has been caused by an unexpected lack of water supply in the upper part of the sand slot. When this slot got filled again with water, the total pressure resumed and increased and the suction decreased again.

# Sammanfattning

TBT (Temperature Buffer Test) är ett gemensamt SKB/ANDRA projekt med deltagande av ENRESA (modellering) och DBE (instrumentering). Syftet är att öka förståelsen för de termiska, hydrauliska och mekaniska processerna i en buffert gjord av svällande lera som utsätts för höga temperaturer (över 100 °C) under vattenmättnadsfasen och att kunna modellera dessa processer.

Försöket görs på 420-metersnivån i Äspö HRL i ett 8 m djupt deponeringshål med diametern 1,75 m, där två kapslar, omgivande bentonitbuffert och en ovanliggande plugg, som förankrats med 9 stag, installerades våren 2003. Kapslarna värmdes med en effekt på 1500 W från dag 15 till dag 1171. Effekten på kapslarna ökades till 1600 W dag 1171.

I denna rapport presenteras data från mätningar i TBT under perioden 030326-070701.

Följande mätningar görs i bentoniten: Temperaturen mäts i 92 punkter, totaltryck i 29 punkter, porvattentryck i 8 punkter och relativa fuktigheten i 35 punkter. Temperaturen mäts även i alla relativa fuktighetsmätare, för att kompensera för temperaturens inverkan på mätresultaten.

Följande övriga mätningar görs: Temperaturen mäts i 40 punkter i berget, i 11 punkter på ytan av varje kapsel och i 6 punkter inne varje kapsel. Kraften på den ovanliggande pluggen mäts i 3 av de 9 stagen och vertikala förskjutningen av pluggen mäts i tre punkter. Vatteninflödet och vattentrycket i den yttre sandfyllda spalten mäts också.

Temperaturer och totaltryck registrerade med fiberoptiska sensorer, installerade av DBE, rapporteras i Appendix B.

En generell slutsats är att mätsystemen och givarna fungera bra och i stort sett alla givare leverar pålitliga mätvärden. Ett undantag är mätningarna av relativa fuktigheten i högtemperaturområdet runt den nedre kapseln, där ett flertal givare inte fungerar.

De tätta linjerna av termoelement vid de två värmarnas höjdcentrum visar sig vara användbara för att undersöka torkning/mättnadsprocessen kvalitativt. I den undre sektionen finns det tydliga tecken på uttorkning inom ett avstånd av 0,15 m från värmarytan. En långsam återmättnad av denna zon pågår

Resultaten från de flesta relativ fuktighetsmätarna är nu mindre signifikanta, eftersom bentonitbufferten är för nära mättnad. Portrycksgivarna i Ring 9 börjar emellertid komma i jämvikt med vattentrycket i sandfiltret, vilket indikerar att full mättnad har uppnåtts i denna del.

Sandfiltret mellan bentonitblocken och omgivande berg används för artificiell bevätning. Mer vatten än den teoretiska mängden som behövs för att mätta hela systemet har nu tillförts. Detta visar att systemet inte är hydrauliskt stängt, utan att det finns ett läckage (sannolikt ut i berget). Det injekteringstryck i sandspalten som fordras för att upprätthålla inflödet visar på en svaghet hos injekteringssystemet. Detta beror sannolikt på en igensättning av filterspetsarna.

Den sänkning av totaltrycket och höjning av buffertens *suction* som noterats runt den översta kapseln mellan dag 225 och dag 370 orsakades av en brist på vattentillgång i övre delen av sandfiltret. När sandfiltret vattenfylldes och trycksattes höjdes totaltrycket åter medan buffertens *suction* minskade.

# Contents

<b>1</b>	<b>Introduction</b>	<b>11</b>
<b>2</b>	<b>Comments</b>	<b>13</b>
2.1	General	13
2.2	Total pressure, Geokon (App. A, pages 49-57)	15
2.3	Suction, Wescore Psychrometers (App. A, pages 58-62)	15
2.4	Relative humidity, Vaisala and Rotronic (App. A, pages 63-68)	15
2.5	Pore water pressure, Geokon (App. A, pages 69-70)	16
2.6	Water flow and water pressure in the sand (App. A, pages 71-72)	16
2.7	Forces on the plug (App. A, page 73)	16
2.8	Displacement of the plug (App. A, page 74)	17
2.9	Canister power (App A, page 75-76)	17
2.10	Temperature in the buffer (App. A, pages 77-82)	17
2.11	Temperature in the rock (App. A, pages 83-86)	18
2.12	Temperature on the canister surface (App. A, pages 87-88)	18
2.13	Temperature inside the canister (App. A, pages 89-90)	18
<b>3</b>	<b>Coordinate system</b>	<b>19</b>
<b>4</b>	<b>Location of instruments</b>	<b>21</b>
4.1	Brief description of the instruments	21
	Measurements of temperature	21
	Measurement of total pressure in the buffer	21
	Measurement of pore water pressure in the buffer	21
	Measurement of the water saturation process	21
	Measurements of forces on the plug	22
	Measurements of plug displacement	22
	Measurement of water flow into the sand	22
4.2	Strategy for describing the position of each device	22
4.3	Position of each instrument in the bentonite	23
4.4	Instruments in the rock	28
	Temperature measurements	28
4.5	Instruments in the canister	29
4.6	Instruments on the plug	31
<b>5</b>	<b>Discussion of results</b>	<b>33</b>
5.1	General	33
5.2	Total inflow of water	33
5.3	Temperatures	38
5.4	Relative humidity/suction	41
5.5	Pore pressure	42
5.6	Total pressure	43
<b>References</b>		<b>45</b>
<b>Appendix A</b>		<b>47</b>
<b>Appendix B</b>		<b>91</b>



# 1 Introduction

The installation of the Temperature Buffer Test was made during spring 2003 in Äspö Hard Rock Laboratory, Sweden.

The Temperature Buffer Test, TBT, is a full-scale experiment that ANDRA and SKB carry out at the SKB Äspö Hard Rock Laboratory. In addition ENRESA supports TBT with THM modelling and DBE has installed a number of optic pressure sensors.

The test aims at understanding and modelling the thermo-hydro-mechanical behaviour of buffers made of swelling clay submitted to high temperatures (over 100°C) during the water saturation process. No other full scales tests have been carried out with buffer temperatures exceeding 100°C so far.

The test consists of a full-scale KBS3 deposition hole, 2 steel canisters equipped with electrical heaters simulating the power of radioactive decay and a mechanical plug at the top. Figure 1-1 shows the layout and denomination of blocks and canisters. The canisters are embedded in dense clay buffer consisting of blocks (cylindrical and ring shaped) of compacted bentonite powder.

An artificial water pressure is applied in the outer slot between the buffer and the rock, which is filled with compacted sand and functions as a filter.

The upper canister is surrounded by sand in order to reduce the temperature in the bentonite.

The buffer material is instrumented with pressure cells (total and water pressure), thermocouples and moisture gauges. Thermocouples are also installed in the rock.

A retaining plug is built in order to confine the buffer swelling.

Measured results and general comments concerning the collected data are given in chapter 2. A test overview with the positions of the measuring points and a brief description of the instruments are presented in chapters 3 and 4. Finally analyses and discussions of the results are given in chapter 5.

In general the data in this report are presented in diagrams covering the time period 030326 to 070701<sup>1</sup>. The time axis in the diagrams represents days from 030326. The diagrams are attached in Appendix A.

Results regarding the fibre optic sensing system are attached in Appendix B.

---

<sup>1</sup> YYMMDD (Swedish way of expressing dates implying that the first two numbers are the year, the next two numbers are the month and the final two numbers are the date)

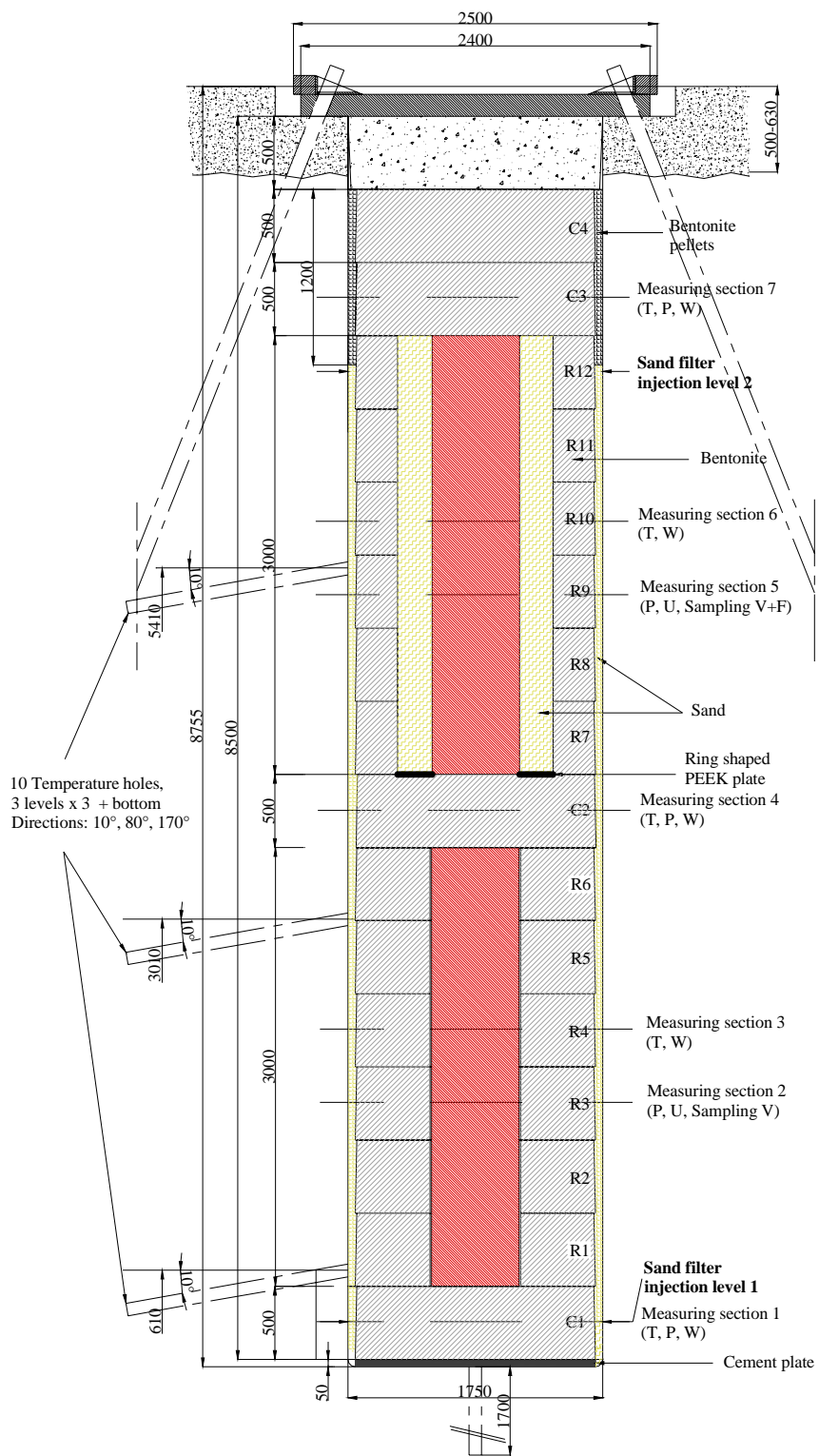


**Figure 1-1.** Schematic view showing the layout of the experiment and the numbering of bentonite blocks. The lower heater is denominated No. 1 and the upper heater is No. 2.

## 2 Comments

### 2.1 General

In this chapter short comments on general trends in the measurements are given. Sensors that are not delivering reliable data or no data at all are noted and comments on the data in general are given but no evaluation or comparison with predictions will be given here.

The heating of both canisters started with an initially applied constant power of 900 W on 030326. This date is also marked as start date. The power was raised to 1200 W on 030403. The power was further raised to 1500 W on 030410. Several power failures have occurred. The power was raised to 1600 W at 20060609 (day 1171).

Important events and dates are shown in Table 2-1.

**Table 2-1. Key dates for TBT.**

Activity	Date (time)	Day No.
900 W power applied	030326	0
Start water filling of filter	030327	1
1200 W power applied	030403	8
1500 W power applied	030410	15
Finished water filling	~030604	~70
Power failure heater 1	030423 (~20.00)-030424 (~10.00)	27-28
Power failure heater 1	030527 (~01.00)-030527 (~12.00)	62
Power failure heater 1	030603 (~12.00)-030603 (~14.00)	69
Power failure heater 1	030606 (~19.00)-030609 (~10.00)	72-75
Power failure heater 1	030612 (~12.00)-030612 (~14.00)	78
Power failure heaters 1 and 2	030923 (~12.00 <sup>1)</sup> )-030923 (~18.00 <sup>1)</sup> )	181
Power failure heaters 1 and 2	031028 (~18.00 <sup>1)</sup> )-031029 (~11.00 <sup>1)</sup> )	216
Injection pump replaced by gas tube	031104	223
Power failure heater 1	040120 (~16.00)-040120 (~19.00)	300
Power failure heater 2	040120 (~18.00)-040120 (~20.00)	300
Filling and pressurisation of the sand filter also through the upper tubes	040406	377

Flushing and pressurisation of filters through both upper and lower tubes (160 kPa)	040615-040616	448-449
Pressurisation of filters through both upper and lower tubes	041011-041014	565-568
Filling and pressurisation of the sand filter through AS205 and AS207	041014	568
Filling and pressurisation of the sand filter through AS201, AS202, AS204, AS205, AS206 and AS208	041110	595
Power failure heater 2 50 w more power	050629-050706	826- 833
Filling and pressurisation of the sand filter through AS201, AS203, AS204, AS205, AS207 and AS208	050728	856
Water filling of filter mats.	051209	989
Airvents AS212-AS215 closed.		
AS209 connected to artificial saturation.		
AS210 connected to artificial saturation.	051212	992
Back flushing of filters through both upper and lower tubes. Only AS203 is still closed.	060517-060614	1148- 1176
1600 W power applied	060609-	1171-
Power failure heater 1	060903-060904	1257-1258
Change in water quality for injection	070417	1483

1) The duration of the power loss is not known since no data was recorded between the times noted.

The water filling was done through four tubes leading to the bottom of the sand filter. The filling was slow due to flow resistance in the sand and the rate was increased by pressurizing the water (see chapter 2.6). The filling was completed after 60-80 days. The water pressure in the bottom of the sand filter has been kept with periodical interruptions (see chapter 2.6) but the valves to the 4 upper tubes leading out water from the top of the sand filter have been open at all times until 040615.

On day 377 (040406) water was supplied to the sand filter also through the tubes leading to the top of the sand filter and a small pressure applied. On days 448-449 the filters were flushed and a water pressure of 160 kPa was applied on the sand filter through both the top tubes and the bottom tubes.

This report is the tenths one and covers the results up to 070701.

## **2.2 Total pressure, Geokon (App. A, pages 49-57)**

The measured pressure ranges from 6.0 to 9.0 MPa. The start of the pressure increase takes place shortly after the water filling has reached the level of the different transducer.

Notable is that all transducers in ring 9 around heater 2 except the one at the rock are recording decreasing total pressure in a period between day ~230 and day ~370. The reason for this and other observations are discussed in chapter 5.

The pressure increase by sensor placed in Cyl.3 at 20051209 (day 989) due to water filling of the filter mats between Cyl.3 and Cyl.4.

Nine transducers are out of order.

## **2.3 Suction, Wescore Psychrometers (App. A, pages 58-62)**

Wescor psychrometers are only working at suction below ~7000 kPa, which correspond to high relative humidity (higher than 95%).

Ten of twelve transducers have yielded interpretable values, which means that they are close to water saturation. Notable is that two transducers around heater 2 are yielding increasing suction (drying) during a period of about 80 days, which is consistent with the measured decrease in total pressure. On the other hand the suction of those transducers is again dropping in suction during the last 2 months, which is also in consistence with the total pressure observations.

WB233 placed in Cyl.3 began to react during the previous measuring period due to water injection to the mat between Cyl.3 and Cyl.4.

## **2.4 Relative humidity, Vaisala and Rotronic (App. A, pages 63-68)**

Relative humidity and temperature measured with Vaisala and Rotronic transducers are shown on pages 63-68. For most transducers RH starts to increase just after the filling of water has reached the sensor level. Only one sensor in the buffer shows an obvious reduction in RH, namely WB206, which is located in the high temperature zone close to the lower heater. Sensors WB221 and WB222 are located in the sand in contact with the bentonite rings 9 and 10. The high initial RH measured by WB221 may be caused by the free water in the sand that had the water content of about 1% from start.

WB206 indicate an increasing from 62% to 78% during this measuring period (from day 860).

8 of 23 sensors are presently out of order for other reasons than high degree of saturation. Four of them are placed in ring 4.

## **2.5 Pore water pressure, Geokon (App. A, pages 69-70)**

Transducers UB206, UB207 and UB208 placed in Ring 9 show pore water pressure about 0.3 MPa to 0.5 MPa at the end of this measuring period.

Transducer UB204 placed in Ring 3 shows pore pressure about 0.1 MPa at the end of this measuring period.

The other water pressure sensors yield pressure close to zero.

## **2.6 Water flow and water pressure in the sand (App. A, pages 71-72)**

Water filling and measurement of water inflow into the sand started on 030327. The total inflow to the sand has since that date been 3530 litre. The total volume of voids in the sand filter was initially about 790 litres. The inflow rate has been in average about 1.56 l/day since day 110. The inflow rate has been in average about 0.29 l/day in the last sex month.

There was also an outflow that started after completed filling since the valves from the top of the sand filter was kept open. The outflow stopped rather early and the total outflow of water has been 44 litres.

The water injection pressure upstream the filter tips is shown on page 72. The water pressure was increased to 800 – 900 kPa during the first 50 days and then kept “constant” until day ~370. However, problems with the water pump have lead to many interruptions in the applied pressure. At day 377 the water pressure was reduced in connection with the start of water supply also from the tubes leading to the top of the filter.

It should be noted that the actual water pressure in the sand filter is only measured at those injection points that are closed to the atmosphere and not pressurized, at present (2007-07-01) points AS203, AS206 and AS207.

## **2.7 Forces on the plug (App. A, page 73)**

The forces on the plug have been measured since 030404. The total force is about 14130 kN at 070701. The influence of the additional water supply from the upper tubes after ~370 days is clearly seen.

During the first about 15 days the plug was only fixed with 3 rods. When the total force exceeded 1100 kN the rest of the 9 rods were fixed in a prescribed manner. This procedure took place 10-11 April 2003 that is 15-16 days after test start. From that time only every third anchor is measured and the results should thus be multiplied with 3. The diagram shows both the actual measurements and after multiplication with 3.

One of the force transducers displayed some irregular trends during this measuring period.

## **2.8 Displacement of the plug (App. A, page 74)**

The three displacement gauges were placed and started to measure displacements from 030409 (day 14) (except for zero reading that was done day 0). One of them (DP201) did not work well and was replaced on 030923 with a new transducer.

Transducer DP203 is out of order.

The measured displacements are in good agreement with the measured forces.

## **2.9 Canister power (App A, page 75-76)**

The heating of both canisters started with an initially applied constant power of 900 W on 030326 and was raised to 1500 W according to Table 2-1. Only one out of three heaters in each canister is presently used (RAH1 and RAH2).

The failure in one of heater (RCH2) in canister 2 caused increasing of power with 50 W on 2005-06-29 to 2005-07-05.

The power has increased to 1600 W in both canisters on 2006-06-09 (day1171).

## **2.10 Temperature in the buffer (App. A, pages 77-82)**

Temperature is measured in a large number of points. The plotting of results is done so that the effect of wetting and cracking can be traced, since sensors placed close to each other are collected in the same diagrams.

The highest measured temperature in the bentonite is 138 °C by sensor TB215 located in the midplane of canister 1 at the distance 15 mm from the canister surface. The corresponding temperature on the canister surface is 140 °C, which shows that the temperature drop at the slot between the canister and the bentonite ring is very small.

Temperature is also measured (TB254, TB255 and TB256) in the sand around canister 2 (page 82), where the temperature drop is rather large (~2.5 °C/cm).

The increase in temperature with about one degree °C seen in the upper part of the buffer in the beginning of June (day ~435) is judged to be caused by the increase in tunnel air temperature that takes place in the summer (page 84).

On day ~335 three additional transducers (TB290, TB291 and TB292) placed in Ring 12 were connected to the data scanner and are reported on page 83. One of them was out of order from start.

The increase in temperature in the beginning of June 2006 (day ~1171) depends to increasing of power with 100 W.

9 of 92 transducers are out of order.

## **2.11 Temperature in the rock (App. A, pages 83-86)**

The maximum temperature measured in the rock (71 degrees) is measured in the central section on the surface of the deposition hole. The deviation from axial symmetry of the temperature measured in the rock is caused by the influence from the heating of the neighbouring Canister Retrieval Test.

On October 11 (day 930) the power in Canister Retrieval Test was switched off.

## **2.12 Temperature on the canister surface (App. A, pages 87-88)**

The maximum temperature measured on the surface of canister 1 is about 140 °C and on the surface of canister 2 about 134 °C on 070701. There are strong temperature differences in the canisters, both radial and axial. The highest measured difference on the surface is 22 °C on canister 1 and 35 °C on canister 2.

The steady increase in temperature of heater 1 has turned into a slow decrease. The temperature of heater 2 has decreased since day 50.

The decreasing temperatures on the surface of canister 2 on day 1505 were a result of 30 litres of water injection into the sand shield.

One sensor (TH1 SE0) has stopped to work since day 1234.

## **2.13 Temperature inside the canister (App. A, pages 89-90)**

The maximum temperature measured inside canister 1 is about 165 °C and about 161 °C in canister 2 on 070701.

The very high value from sensor TH2 SI3 0° is not reliable before day 1080.

### 3 Coordinate system

Measurements are done in 7 measuring sections placed on different levels (see Figure 1-1). On each level, sensors are placed in eight main directions A, AB, B, BC, C, CD, D and DA according to Figure 3-1. Direction A and C are placed in the tunnels axial direction with A headed against the end of the tunnel i.e. almost to the South (see Figure 1-1, 3-1 and 4-1). The angle  $\alpha$  is counted anti-clockwise from direction A. The z-coordinate is counted from the bottom of the deposition hole (the cement base).

The bentonite blocks are called cylinders and rings. The cylinders are numbered C1-C4 and the rings R1-R12 respectively (see Figure 1-1).

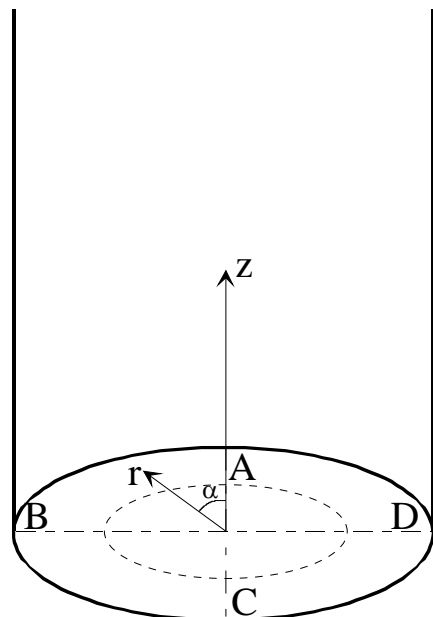


**Figure 3-1.** Figure describing the coordinate system used when determining the instrument positions.



## 4 Location of instruments

### 4.1 Brief description of the instruments

The different instruments that are used in the experiment are briefly described in this chapter. For additional information, see /4-1/.

#### Measurements of temperature

##### *Buffer*

Thermocouples from Pentronic have been installed for measuring temperature in the buffer. Measurements are done in 92 points in the test hole. In addition, temperature gauges are built in into the capacitive relative humidity sensors (23 sensors) as well as in the pressure gauges of vibrating wire type (37 gauges). Temperature is also measured in the psychrometers.

##### *Canister*

Temperature is measured in 11 points on the surface of each canister. Temperature is also measured in each canister insert in 6 points.

##### *Rock*

Temperature in the rock and on the rock surface of the hole is measured in 40 points with thermocouples from Pentronic.

#### Measurement of total pressure in the buffer

Total pressure is the sum of the swelling pressure and the pore water pressure. It is measured with Geokon total pressure cells with vibrating wire transducers. 29 cells of this type have been installed.

#### Measurement of pore water pressure in the buffer

Pore water pressure is measured with Geokon pore pressure cells with vibrating wire transducer. 8 cells of this type have been installed.

#### Measurement of the water saturation process

The water saturation process is recorded by measuring the relative humidity in the pore system, which can be converted into water ratio or total suction (negative water pressure). The following techniques and devices are used:

- Vaisala relative humidity sensor of capacitive type. 29 cells of this type have been installed. The measuring range is 0-100 % RH.
- Wescor psychrometers measure the dry and the wet temperature in the pore system. The measuring range is 95.5-99.6 % RH corresponding to the pore water pressure -0.5 to -6MPa. 12 cells of this type have been installed.

### **Measurements of forces on the plug**

The force on the plug caused by the swelling pressure of the bentonite is measured in 3 of the 9 anchors. The force transducers are of the type GLÖTZL.

### **Measurements of plug displacement**

Due to straining of the anchors the swelling pressure of the bentonite will cause not only a force on the plug but also displacement of the plug. The displacement is measured in three points with transducers of the type LVDT with the range 0 – 50 mm.

### **Measurement of water flow into the sand**

An artificial water pressure is applied in the outer slot, which is filled with sand. Titanium tubes equipped with filter tips are placed in the sand on two levels, 250 mm and 6750 mm from bottom (four at each level).

## **4.2 Strategy for describing the position of each device**

Every instrument is named with a unique name consisting of 1 letter describing the type of measurement, (T-Temperature, P-Total Pressure, U-Pore Pressure, W-Relative Humidity, C-Chemical sampling, D-Displacement and A-Artificial water), 1 letter describing where the measurement takes place (B-Buffer, H-Heater, S-Sand, R-Rock and P-plug), 1 figure denoting the deposition hole (1 is used for the CRT test and 2 is used for this experiment), and 2 figures specifying the position in the buffer according to a separate list (see Table 4-1 to 4-7). Every instrument position is described with three coordinates according to Figure 3-1. The r-coordinate is the horizontal distance from the centre of the hole and the z-coordinate is the height from the bottom of the hole (the block height is set to 500mm). The coordinate is the angle from the vertical direction A (almost South).

The position of each instrument is described in the legend in the diagrams according to the following strategy:

**Buffer:** Three positions according to Figure 3-1: ( $z \setminus \alpha \setminus r$ ) meaning (z-coordinate in m. from the bottom \ the angle  $\alpha$  \ the radius in m.)

The cells measuring total pressure have been installed in three different directions in order to measure the radial stress (R), the axial stress (A) and the tangential stress (T). The direction of the pressure measurement is added in Table 4-2 and in the legend for each cell.

**Rock:** Three positions with the following meaning: (distance in meters from the bottom \  $\alpha$  according to Fig 3-1 \ distance in meters from the rock surface)

The bentonite blocks are called cylinders and rings. The cylinders are numbered C1-C4 and the rings R1-R12 respectively (Figure 1-1).

**Canister:** The denomination of the instruments in the canister differs a little from the other instruments. At first there are two letters and one figure describing the type of measurement and the place (TH for temperature and heater) and which heater (1 for lower heater and 2 for upper). Then there are again two letters describing if it is an external or internal sensor (SE or SI) and one figure describing the position on the canister (0-4 according to Figure 4-2). Finally the angle clockwise from direction A is written.

### 4.3 Position of each instrument in the bentonite

Measurements are done in 7 measuring sections placed on different levels (see Figure 1-1). On each level, sensors are placed in eight main directions A, AB, B, BC, C, CD, D and DA according to Figure 4-1. The bentonite blocks are called cylinders and rings. The cylinders are numbered C1-C4 and the rings R1-R12 respectively (see Figure 1-1).

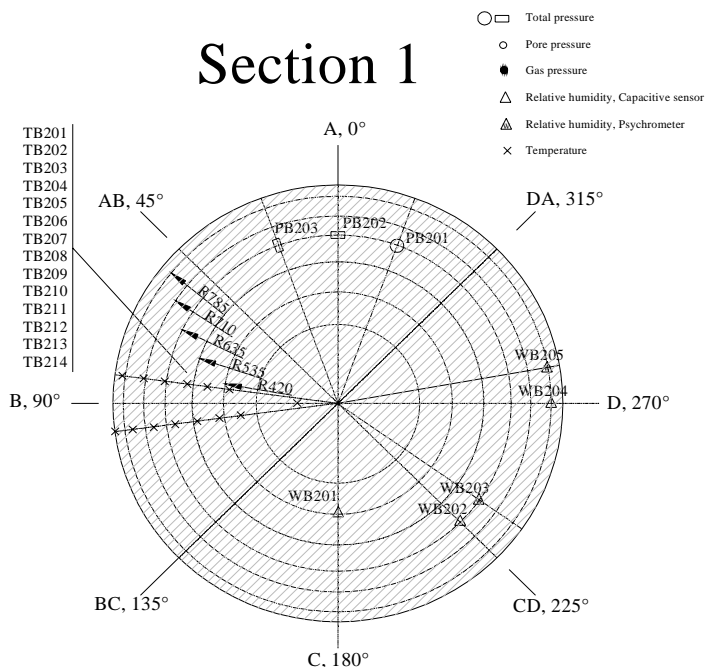


**Figure 4-1.** Schematic view, showing the main directions of the instrument positioning. The drawing shows the instrumentation in measuring section 1.

An overview of the positions of the instruments is shown in Fig 1-1 and 4-1. Exact positions are described in Tables 4-1 to 4-6. These tables have been updated since the last report and the measured exact position of the transducers have been inserted.

The instruments are located in three main levels in each instrumented block, the surface of the block (only total pressure cells measuring the horizontal pressure) and 50 mm and 250 mm from the upper block surface. The thermocouples and the total pressure cells are placed in the 50 mm level by practical reasons and the other sensors in the 250 mm level.

**Table 4-1. Numbering and position of instruments for measuring temperature (T).**

Type and number	Measuring section	Block	Instrument position in block				Instrument Fabricate
			Direction	$\alpha$ degree	r m	Z m	
TB201	1	Cyl. 1	B	90	0,150	0,452	Pentronic
TB202	1	Cyl. 1	B	95	0,360	0,452	Pentronic
TB203	1	Cyl. 1	B	85	0,400	0,452	Pentronic
TB204	1	Cyl. 1	B	95	0,440	0,452	Pentronic
TB205	1	Cyl. 1	B	85	0,480	0,452	Pentronic
TB206	1	Cyl. 1	B	95	0,520	0,452	Pentronic
TB207	1	Cyl. 1	B	85	0,560	0,452	Pentronic
TB208	1	Cyl. 1	B	95	0,600	0,452	Pentronic
TB209	1	Cyl. 1	B	85	0,640	0,452	Pentronic
TB210	1	Cyl. 1	B	95	0,680	0,452	Pentronic
TB211	1	Cyl. 1	B	85	0,720	0,452	Pentronic
TB212	1	Cyl. 1	B	95	0,760	0,452	Pentronic
TB213	1	Cyl. 1	B	85	0,800	0,452	Pentronic
TB214	1	Cyl. 1	B	95	0,840	0,452	Pentronic
TB215	3	Ring 4	B	97,5	0,320	2,469	Pentronic
TB216	3	Ring 4	B	82,5	0,360	2,469	Pentronic
TB217	3	Ring 4	B	97,5	0,390	2,469	Pentronic
TB218	3	Ring 4	B	92,5	0,420	2,469	Pentronic
TB219	3	Ring 4	B	87,5	0,435	2,469	Pentronic
TB220	3	Ring 4	B	82,5	0,450	2,469	Pentronic
TB221	3	Ring 4	B	97,5	0,465	2,469	Pentronic
TB222	3	Ring 4	B	92,5	0,480	2,469	Pentronic
TB223	3	Ring 4	B	87,5	0,495	2,469	Pentronic
TB224	3	Ring 4	B	82,5	0,510	2,469	Pentronic
TB225	3	Ring 4	B	97,5	0,525	2,469	Pentronic
TB226	3	Ring 4	B	92,5	0,540	2,469	Pentronic
TB227	3	Ring 4	B	87,5	0,555	2,469	Pentronic
TB228	3	Ring 4	B	82,5	0,570	2,469	Pentronic
TB229	3	Ring 4	B	97,5	0,585	2,469	Pentronic
TB230	3	Ring 4	B	92,5	0,600	2,469	Pentronic
TB231	3	Ring 4	B	87,5	0,615	2,469	Pentronic
TB232	3	Ring 4	B	82,5	0,630	2,469	Pentronic
TB233	3	Ring 4	B	97,5	0,645	2,469	Pentronic
TB234	3	Ring 4	B	92,5	0,660	2,469	Pentronic
TB235	3	Ring 4	B	87,5	0,690	2,469	Pentronic
TB236	3	Ring 4	B	92,5	0,720	2,469	Pentronic
TB237	3	Ring 4	B	87,5	0,750	2,469	Pentronic
TB238	3	Ring 4	B	92,5	0,780	2,469	Pentronic
TB239	3	Ring 4	B	87,5	0,810	2,469	Pentronic
TB240	4	Cyl. 2	B	90	0,150	3,983	Pentronic
TB241	4	Cyl. 2	B	95	0,360	3,983	Pentronic
TB242	4	Cyl. 2	B	85	0,400	3,983	Pentronic
TB243	4	Cyl. 2	B	95	0,440	3,983	Pentronic
TB244	4	Cyl. 2	B	85	0,480	3,983	Pentronic
TB245	4	Cyl. 2	B	95	0,520	3,983	Pentronic

Type and number	Measuring section	Block	Instrument position in block			Instrument Fabricate	
			Direction	$\alpha$	r		
			degree	m	m		
TB246	4	Cyl. 2	B	85	0,560	3,983	Pentronic
TB247	4	Cyl. 2	B	95	0,600	3,983	Pentronic
TB248	4	Cyl. 2	B	85	0,640	3,983	Pentronic
TB249	4	Cyl. 2	B	95	0,680	3,983	Pentronic
TB250	4	Cyl. 2	B	85	0,720	3,983	Pentronic
TB251	4	Cyl. 2	B	95	0,760	3,983	Pentronic
TB252	4	Cyl. 2	B	85	0,800	3,983	Pentronic
TB253	4	Cyl. 2	B	95	0,825	3,983	Pentronic
TB254	6	Ring 10	B	90	0,343	6,056	Pentronic
TB255	6	Ring 10	B	90	0,400	6,056	Pentronic
TB256	6	Ring 10	B	90	0,463	6,056	Pentronic
TB257	6	Ring 10	B	97,5	0,540	6,006	Pentronic
TB258	6	Ring 10	B	92,5	0,555	6,006	Pentronic
TB259	6	Ring 10	B	87,5	0,570	6,006	Pentronic
TB260	6	Ring 10	B	82,5	0,585	6,006	Pentronic
TB261	6	Ring 10	B	97,5	0,600	6,006	Pentronic
TB262	6	Ring 10	B	92,5	0,615	6,006	Pentronic
TB263	6	Ring 10	B	87,5	0,630	6,006	Pentronic
TB264	6	Ring 10	B	82,5	0,645	6,006	Pentronic
TB265	6	Ring 10	B	97,5	0,660	6,006	Pentronic
TB266	6	Ring 10	B	92,5	0,675	6,006	Pentronic
TB267	6	Ring 10	B	87,5	0,690	6,006	Pentronic
TB268	6	Ring 10	B	82,5	0,705	6,006	Pentronic
TB269	6	Ring 10	B	97,5	0,720	6,006	Pentronic
TB270	6	Ring 10	B	92,5	0,735	6,006	Pentronic
TB271	6	Ring 10	B	87,5	0,750	6,006	Pentronic
TB272	6	Ring 10	B	82,5	0,765	6,006	Pentronic
TB273	6	Ring 10	B	97,5	0,780	6,006	Pentronic
TB274	6	Ring 10	B	92,5	0,795	6,006	Pentronic
TB275	6	Ring 10	B	87,5	0,810	6,006	Pentronic
TB276	7	Cyl. 3	B	90	0,150	7,524	Pentronic
TB277	7	Cyl. 3	B	95	0,360	7,524	Pentronic
TB278	7	Cyl. 3	B	85	0,400	7,524	Pentronic
TB279	7	Cyl. 3	B	95	0,440	7,524	Pentronic
TB280	7	Cyl. 3	B	85	0,480	7,524	Pentronic
TB281	7	Cyl. 3	B	95	0,520	7,524	Pentronic
TB282	7	Cyl. 3	B	85	0,560	7,524	Pentronic
TB283	7	Cyl. 3	B	95	0,600	7,524	Pentronic
TB284	7	Cyl. 3	B	85	0,640	7,524	Pentronic
TB285	7	Cyl. 3	B	95	0,680	7,524	Pentronic
TB286	7	Cyl. 3	B	85	0,720	7,524	Pentronic
TB287	7	Cyl. 3	B	95	0,760	7,524	Pentronic
TB288	7	Cyl. 3	B	85	0,800	7,524	Pentronic
TB289	7	Cyl. 3	B	95	0,825	7,524	Pentronic
TB290		Ring 12	B	90	0,360	6,881	Pentronic
TB291		Ring 12	B	90	0,420	6,881	Pentronic
TB292		Ring 12	B	90	0,480	6,881	Pentronic

**Table 4-2. Numbering and position of instruments measuring total pressure (P).**

Type and number	Measuring section	Block	Instrument position in block				Instrument Fabricate	Direction of pressure measurement
			Direction	$\alpha$	r	z		
				degree	m	m		
PB201	1	Cyl. 1	A	340	0,635	0,502	Geokon	Axial
PB202	1	Cyl. 1	A	0	0,635	0,452	Geokon	Radial
PB203	1	Cyl. 1	A	20	0,635	0,452	Geokon	Tangential
PB204	2	R3	D	250	0,420	1,968	Geokon	Radial
PB205	2	R3	D	290	0,420	2,018	Geokon	Axial
PB206	2	R3	A	8	0,535	1,968	Geokon	Radial
PB207	2	R3	A	20	0,535	1,968	Geokon	Tangential
PB208	2	R3	AB	45	0,585	2,018	Geokon	Axial
PB209	2	R3	B	100	0,635	1,968	Geokon	Tangential
PB210	2	R3	C	170	0,710	1,968	Geokon	Tangential
PB211	2	R3	C	180	0,710	1,968	Geokon	Radial
PB212	2	R3	D	260	0,748	2,018	Geokon	Axial
PB213	2	R3	D	270	0,875	1,950	Geokon	Radial on rock
PB214	4	Cyl. 2	A	340	0,635	4,033	Geokon	Axial
PB215	4	Cyl. 2	A	0	0,635	3,983	Geokon	Radial
PB216	4	Cyl. 2	A	20	0,635	3,983	Geokon	Tangential
PB217	5	Ring 9	D	270	0,535	5,319	Geokon	Radial,against sand
PB218	5	Ring 9	A	340	0,635	5,554	Geokon	Axial
PB219	5	Ring 9	A	0	0,635	5,504	Geokon	Radial
PB220	5	Ring 9	A	20	0,635	5,504	Geokon	Tangential
PB221	5	Ring 9	B	70	0,710	5,554	Geokon	Axial
PB222	5	Ring 9	B	110	0,710	5,504	Geokon	Radial
PB223	5	Ring 9	C	160	0,745	5,554	Geokon	Axial
PB224	5	Ring 9	C	180	0,770	5,504	Geokon	Radial
PB225	5	Ring 9	C	200	0,740	5,504	Geokon	Tangential
PB226	5	Ring 9	D	270	0,875	5,450	Geokon	Radial on rock
PB227	7	Cyl. 3	A	340	0,635	7,574	Geokon	Axial
PB228	7	Cyl. 3	A	0	0,635	7,524	Geokon	Radial
PB229	7	Cyl. 3	A	20	0,635	7,524	Geokon	Tangential
PB230	2	R3	C	180	0,315	1,968	DBE	Radial
PB231	5	R9	C	180	0,535	5,504	DBE	Radial

**Table 4-3. Numbering and position of instruments measuring pore pressure (U).**

Type and number	Measuring section	Block	Instrument position in block				Instrument Fabricate	Remark
			Direction	$\alpha$	r	z		
				degree	m	m		
UB201	2	Ring 3	D	270	0,420	1,768	Geokon	
UB202	2	Ring 3	A	350	0,535	1,768	Geokon	
UB203	2	Ring 3	B	90	0,635	1,768	Geokon	
UB204	2	Ring 3	D	280	0,785	1,768	Geokon	
US205	5	Ring 9	D	270	0,510	5,304	Geokon	In sand
UB206	5	Ring 9	DA	315	0,635	5,304	Geokon	
UB207	5	Ring 9	B	90	0,710	5,304	Geokon	
UB208	5	Ring 9	CD	225	0,785	5,304	Geokon	
UB209	2	Ring 3	C	200	0,315	1,968	DBE	
UB210	5	Ring 9	C	150	0,510	5,304	DBE	

**Table 4-4. Numbering and position of instruments measuring water content (W).**

Type and number	Measuring section	Block	Instrument position in block				Instrument Fabricate	Remark
			Direction	$\alpha$ degree	r m	Z m		
WB201	1	Cyl.1	C	180	0,420	0,252	Rotronic	
WB202	1	Cyl.1	CD	225	0,635	0,252	Vaisala	
WB203	1	Cyl.1	CD	235	0,635	0,252	Wescor	
WB204	1	Cyl.1	D	270	0,785	0,252	Rotronic	
WB205	1	Cyl.1	D	280	0,785	0,252	Wescor	
WB206	3	Ring 4	BC	135	0,360	2,269	Vaisala	
WB207	3	Ring 4	C	180	0,420	2,269	Rotronic	
WB208	3	Ring 4	CD	225	0,485	2,269	Vaisala	
WB209	3	Ring 4	D	270	0,560	2,269	Rotronic	
WB210	3	Ring 4	DA	315	0,635	2,269	Vaisala	
WB211	3	Ring 4	DA	325	0,635	2,269	Wescor	
WB212	3	Ring 4	A	0	0,710	2,269	Rotronic	
WB213	3	Ring 4	A	10	0,710	2,269	Wescor	
WB214	3	Ring 4	AB	45	0,785	2,269	Vaisala	
WB215	3	Ring 4	AB	55	0,785	2,269	Wescor	
WB216	4	Cyl.2	C	180	0,420	3,783	Rotronic	
WB217	4	Cyl.2	CD	225	0,635	3,783	Vaisala	
WB218	4	Cyl.2	CD	235	0,635	3,783	Wescor	
WB219	4	Cyl.2	D	270	0,785	3,783	Rotronic	
WB220	4	Cyl.2	D	280	0,785	3,783	Wescor	
WS221	5	Ring 9	BC	135	0,525	5,304	Vaisala	In sand
WS222	6	Ring 10	BC	135	0,525	5,806	Vaisala	In sand
WB223	6	Ring 10	C	180	0,585	5,806	Rotronic	
WB224	6	Ring 10	CD	225	0,635	5,806	Vaisala	
WB225	6	Ring 10	D	270	0,685	5,806	Rotronic	
WB226	6	Ring 10	D	280	0,685	5,806	Wescor	
WB227	6	Ring 10	DA	315	0,735	5,806	Vaisala	
WB228	6	Ring 10	DA	325	0,735	5,806	Wescor	
WB229	6	Ring 10	A	0	0,785	5,806	Rotronic	
WB230	6	Ring 10	A	10	0,785	5,806	Wescor	
WB231	7	Cyl.3	C	180	0,420	7,374	Rotronic	
WB232	7	Cyl.3	CD	225	0,635	7,374	Vaisala	
WB233	7	Cyl.3	CD	235	0,635	7,374	Wescor	
WB234	7	Cyl.3	D	270	0,785	7,374	Rotronic	
WB235	7	Cyl.3	D	280	0,785	7,374	Wescor	

## 4.4 Instruments in the rock

### Temperature measurements

40 thermocouples are located in ten boreholes in the rock (see Figure 1-1). The depth of each borehole is 1.5 m. In each borehole 4 thermocouples are placed at different distances from the rock surface. Observe that the coordinate system does not count the radius but the radial distance from the rock surface of the deposition hole. The position of each instrument is described in Table 4-5.

**Table 4-5. Numbering and positions of thermocouples in the rock.**

Mark	Level	Direction	Distance from rock surface	Instrument Fabricate
	m	degree	m	
TR201	0	Center	0,000	Pentronic
TR202	0	Center	0,375	Pentronic
TR203	0	Center	0,750	Pentronic
TR204	0	Center	1,500	Pentronic
TR205	0,61	10°	0,000	Pentronic
TR206	0,61	10°	0,375	Pentronic
TR207	0,61	10°	0,750	Pentronic
TR208	0,61	10°	1,500	Pentronic
TR209	0,61	80°	0,000	Pentronic
TR210	0,61	80°	0,375	Pentronic
TR211	0,61	80°	0,750	Pentronic
TR212	0,61	80°	1,500	Pentronic
TR213	0,61	170°	0,000	Pentronic
TR214	0,61	170°	0,375	Pentronic
TR215	0,61	170°	0,750	Pentronic
TR216	0,61	170°	1,500	Pentronic
TR217	3,01	10°	0,000	Pentronic
TR218	3,01	10°	0,375	Pentronic
TR219	3,01	10°	0,750	Pentronic
TR220	3,01	10°	1,500	Pentronic
TR221	3,01	80°	0,000	Pentronic
TR222	3,01	80°	0,375	Pentronic
TR223	3,01	80°	0,750	Pentronic
TR224	3,01	80°	1,500	Pentronic
TR225	3,01	170°	0,000	Pentronic
TR226	3,01	170°	0,375	Pentronic
TR227	3,01	170°	0,750	Pentronic
TR228	3,01	170°	1,500	Pentronic
TR229	5,41	10°	0,000	Pentronic
TR230	5,41	10°	0,375	Pentronic
TR231	5,41	10°	0,750	Pentronic
TR232	5,41	10°	1,500	Pentronic
TR233	5,41	80°	0,000	Pentronic
TR234	5,41	80°	0,375	Pentronic
TR235	5,41	80°	0,750	Pentronic
TR236	5,41	80°	1,500	Pentronic
TR237	5,41	170°	0,000	Pentronic
TR238	5,41	170°	0,375	Pentronic
TR239	5,41	170°	0,750	Pentronic
TR240	5,41	170°	1,500	Pentronic

## 4.5 Instruments in the canister

Temperature is measured both on the canister surface and inside the canister /4-2/. Eleven thermocouples are installed on each canisters surface. Three groups of three thermocouples are installed 100 mm from each heater end, and in the middle of the heater, with a distribution of 120°. Two additional thermocouples are installed in the centre of the bottom lid and the top cover. Temperature inside the canister insert is measured at 6 points with thermocouples.

Figure 4-2 shows how these thermocouples are placed (see also chapter 4.2). Table 4-6 and 4-7 show the positions.

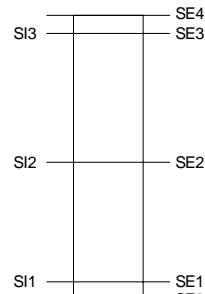
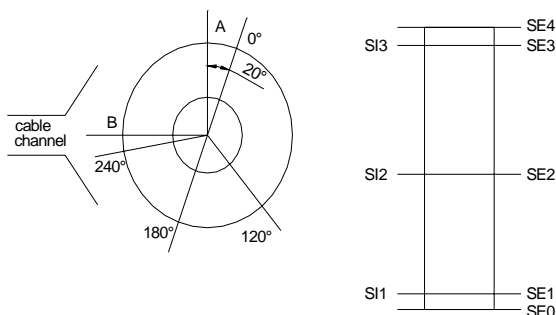
**Table 4-6. Numbering and position of instruments for measuring the temperature on the heaters surface (T).**

Type and number	Heater	Instruments coordinates				Instrument Fabricate	Remark
		Position	α degree	r m	z m		
TH1 SE0	1	Bottom	0	0,000	0,500		
TH1 SE1 0°	1	Lower sec.	0	0,305	0,600		
TH1 SE1 240°	1	Lower sec.	240	0,305	0,600		
TH1 SE1 120°	1	Lower sec.	120	0,305	0,600		
TH1 SE2 0°	1	Middle sec.	0	0,305	2,000		
TH1 SE2 240°	1	Middle sec.	240	0,305	2,000		
TH1 SE2 120°	1	Middle sec.	120	0,305	2,000		
TH1 SE3 0°	1	Upper sec.	0	0,305	3,400		
TH1 SE3 240°	1	Upper sec.	240	0,305	3,400		
TH1 SE3 120°	1	Upper sec.	120	0,305	3,400		
TH1 SE4	1	Top	0	0,000	3,500		
TH2 SE0	2	Bottom	0	0,000	4,000		
TH2 SE1 0°	2	Lower sec.	0	0,305	4,100		
TH2 SE1 240°	2	Lower sec.	240	0,305	4,100		
TH2 SE1 120°	2	Lower sec.	120	0,305	4,100		
TH2 SE2 0°	2	Middle sec.	0	0,305	5,500		
TH2 SE2 240°	2	Middle sec.	240	0,305	5,500		
TH2 SE2 120°	2	Middle sec.	120	0,305	5,500		
TH2 SE3 0°	2	Upper sec.	0	0,305	6,900		
TH2 SE3 240°	2	Upper sec.	240	0,305	6,900		
TH2 SE3 120°	2	Upper sec.	120	0,305	6,900		
TH2 SE4	2	Top	0	0,000	7,000		

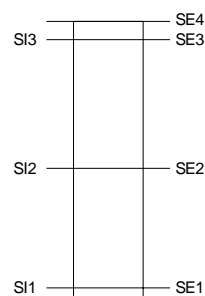
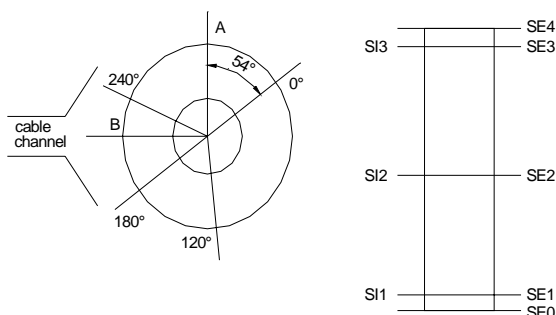
**Table 4-7. Numbering and position of instruments for measuring the temperature inside the heaters (T).**

Type and number	Heater	Instruments coordinates			Instrument Fabricate	Remark
		Position	$\alpha$ degree	Z m		
TH1 SI1 0°	1	Lower sec.	0	0,60		
TH1 SI1 180°	1	Lower sec.	180	0,60		
TH1 SI2 0°	1	Middle sec.	0	2,00		
TH1 SI2 180°	1	Middle sec.	180	2,00		
TH1 SI3 0°	1	Upper sec.	0	3,40		
TH1 SI3 180°	1	Upper sec.	180	3,40		
TH2 SI1 0°	2	Lower sec.	0	0,60		
TH2 SI1 180°	2	Lower sec.	180	0,60		
TH2 SI2 0°	2	Middle sec.	0	2,00		
TH2 SI2 180°	2	Middle sec.	180	2,00		
TH2 SI3 0°	2	Upper sec.	0	3,40		
TH2 SI3 180°	2	Upper sec.	180	3,40		

**Heater 2**



**Heater 1**



**Figur 4-2. Location of thermocouples inside (SI) and on (SE) the canisters.**

## 4.6 Instruments on the plug

Three force transducers and three displacement transducers have been placed on the plug to measure the force of the anchors and the displacement of the plug. The location of these transducers can be described in relation to Fig 4-3, which shows a schematic view of the plug with the slots, rods and cables.

The rods are numbered 1-9 anti-clockwise and number 1 is the northern rod 18 degrees from direction A. The force transducers are placed on rods 3, 6, and 9. The displacement transducers are placed between the rods on the steel ring in the periphery of the plug. They are fixed on the rock surface and measure thus the displacement relative to the rock.

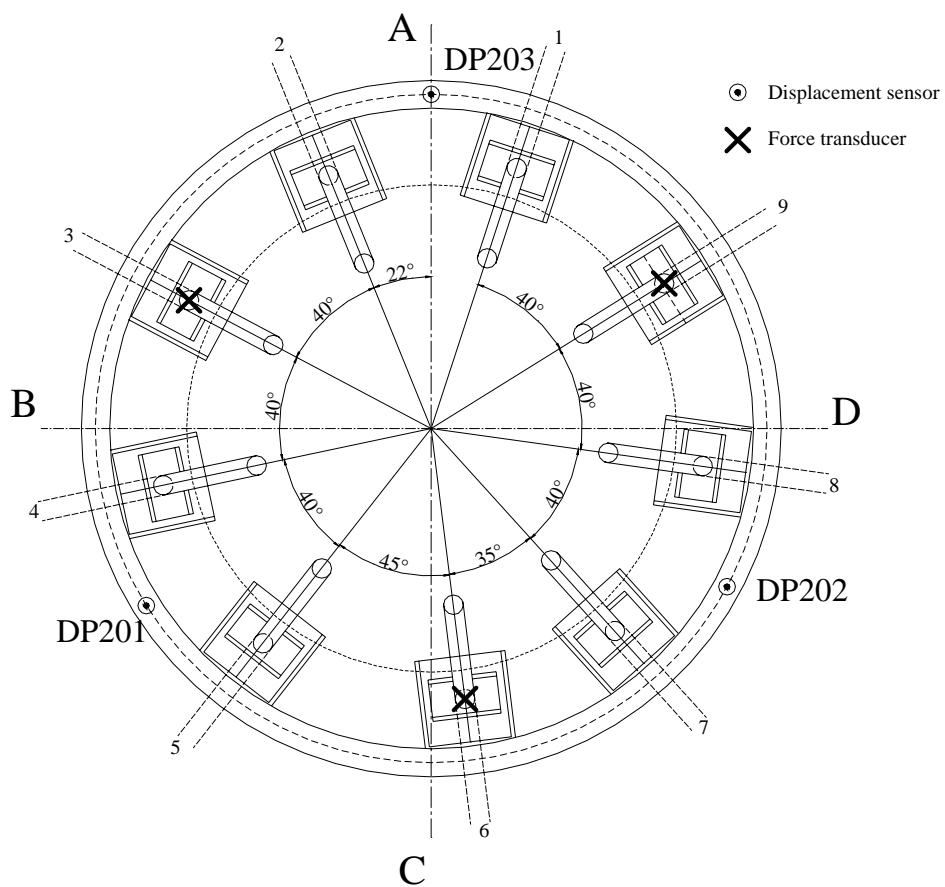


**Figure 4-3.** Schematic view showing the positions of the rods and the displacement and force transducers on the retaining plug.



## 5 Discussion of results

### 5.1 General

The aim of this chapter is two-parted: (i) to give an updated interpretation of the project as a whole; and (ii) to highlight the latest developments. More detailed discussions of earlier results can be found in previous data reports.

### 5.2 Total inflow of water

The total injected water volume is shown in (App.A\page71) and was slightly higher than  $3.5 \text{ m}^3$  at July 1, 2007. Table 5-1 shows the pore space available at the beginning of the test. The calculated available pore volume has thereby been exceeded with  $0.8 \text{ m}^3$ . This discrepancy appears to be caused by a water leakage, possibly into the rock. This is elaborated below.

The inflow has varied significantly during the test period. During the first 75 days the inflow was about 15 l/d, while it dropped to about 1.3 l/d during the subsequent 250 days. On average during the period from July 1, 2006 to July 1, 2007, the inflow was 0.5 l/d.

Two major events can be noticed in the applied scheme for pressurization (Table 5-2):

- During the first 377 days, the sand filter was only pressurized through the lower injection points, while the upper were open to the atmosphere. After this day, upper injection points have also been pressurized while none of the injection points has been open to the atmosphere.
- The second event was the installation of equipment for measuring pressure at each injection point at October 8, 2004 (day 562) (see Figure 5-1.). Since then, at least one out of eight injection points have been closed and used for monitoring of the actual pressure in the sand filter.

#### Change of water quality

A third event that appears to be of major importance for the function of the injection system was the change of water quality. The background for this was that the injection points in the sand filter have exhibited a high flow resistance during the operation phase of the test. In order to reduce this resistance, the quality of the water used for hydration of the buffer was changed on April 17 2007. The formation water used earlier was replaced by de-ionized water.

The effect of this modification, with increasing inflow, was noticed almost immediately. Two ports used earlier for injection were closed in order to avoid frequent refilling of the rather small pressure tank in use at that time (see Table 5-2). Later on (on August 13) the small tank has been replaced by a larger tank which enabled a higher inflow without the need of frequent refilling. This change enabled the control of the filter pressure of 3 bar with an injection pressure of 5 bar (relative). This will be described in the next data report.

**Table 5-1. TBT Pore space.**

	Available at test start [m <sup>3</sup> ]	
Sand filter	0.77	
Pellets filling	0.24	1.38
Bentonite	1.08	
Heater/bentonite clearance	0.06	
Sand shield	0.55	
Total	2.70	

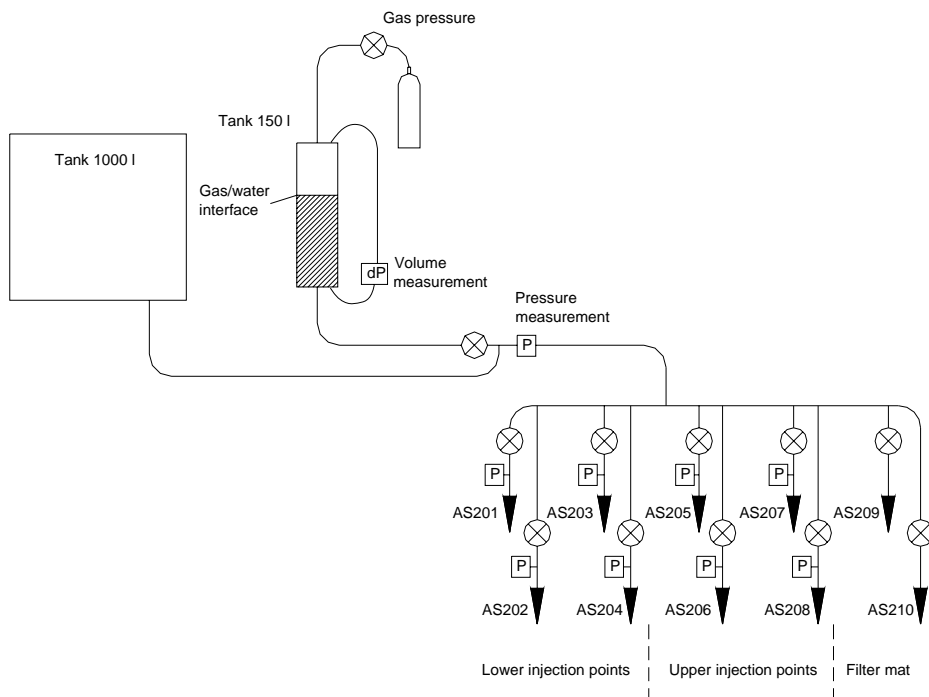


**Figure 5-1.** Schematic view of injection system.

Small tank has been replaced by a larger tank which enabled a higher inflow without the need of frequent refilling. This change enabled the control of the filter pressure of 3 bar with an injection pressure of 5 bar (relative). This will be described in the next data report.

In a previous Sensor data report (/5-1/), a model for the relation between filter pressure, the inflow and an outflow was suggested. Since the inflow and the filter pressure was highly correlated from July 2005 to July 2006 (see Figure 5-2), it was suggested that the actual water uptake during this period was very limited and nearly all injected water was lost though leakage. From this followed that the conductivity of the leakage was approx. 1 l/d,bar.

After the increase of the injection pressure in August 2006, the relation between the filter pressure and the inflow has changed. Still, they are correlated which suggests that the main part of the injected volume is lost through a leakage. The estimated cumulative water uptake of approx. 2.3 m<sup>3</sup>, reported in /5-1/, therefore still appears to be relevant. With an initial available pore volume of 2.7 m<sup>3</sup>, this would imply a remaining pore volume of 0.4 m<sup>3</sup> which is quite close to the initial available pore volume of the sand shield.

**Table 5-2. Injection point pressurization scheme (values are relative pressures). The actual water pressure in the sand filter is only measured at those points that are closed.**

Intervals	Lower injection points				Upper injection points				Filter mat		p (bar)
	201	202	203	204	205	206	207	208	209	210	
030326 – 040406 <i>Day 0 – 377</i>	O	O	O	O	⊕	⊕	⊕	⊕	⊗	⊗	7
040406 – 040615 <i>Day 377 – 447</i>	O	O	O	O	O	O	O	O	⊗	⊗	0
040615 – 040616 <i>Day 447 – 448</i>	Hydraulic test I										
040616 – 041008 <i>Day 448 – 562</i>	O	O	O	O	O	O	O	O	⊗	⊗	1.5
041008 – 041014 <i>Day 562 – 568</i>	Hydraulic test II										
041014 – 041110 <i>Day 568 – 595</i>	⊗	⊗	⊗	⊗	O	⊗	O	⊗	⊗	⊗	5
041110 – 050728 <i>Day 595 – 856</i>	O	O	⊗	O	O	O	⊗	O	⊗	⊗	5
050728 – 051209 <i>Day 856 – 989</i>	O	⊗	O	O	O	⊗	O	O	⊗	⊗	5
051209 – 051212 <i>Day 989 – 992</i>	O	⊗	O	O	O	⊗	O	O	O	⊗	5
051212 – 060517 <i>Day 992 – 1148</i>	O	⊗	O	O	O	⊗	O	O	O	O	5
060517 – 060614 <i>Day 1148 – 1176</i>	Back flushing of injection points										
060614 – 060807 <i>Day 1176 – 1230</i>	O	O	⊗	O	O	O	O	O	O	O	5
060807 – 060811 <i>Day 1230 – 1234</i>	Increase of injection pressure										
060811 – 070417 <i>Day 1234 – 1483</i>	O	O	⊗	O	O	O	O	O	O	O	9
070417 <i>Day 1483</i>	Change in water quality										
070417 – 070423 <i>Day 1483 – 1489</i>	O	O	⊗	O	O	O	O	O	O	O	9
070423 – 070509 <i>Day 1489 – 1505</i>	O	O	⊗	O	O	O	⊗	O	O	O	9
070509 – 070701 <i>Day 1505 – 1558</i>	O	O	⊗	O	O	⊗	⊗	O	O	O	9

O = Open and pressurized

⊕ = Open to atmosphere

⊗ = Closed

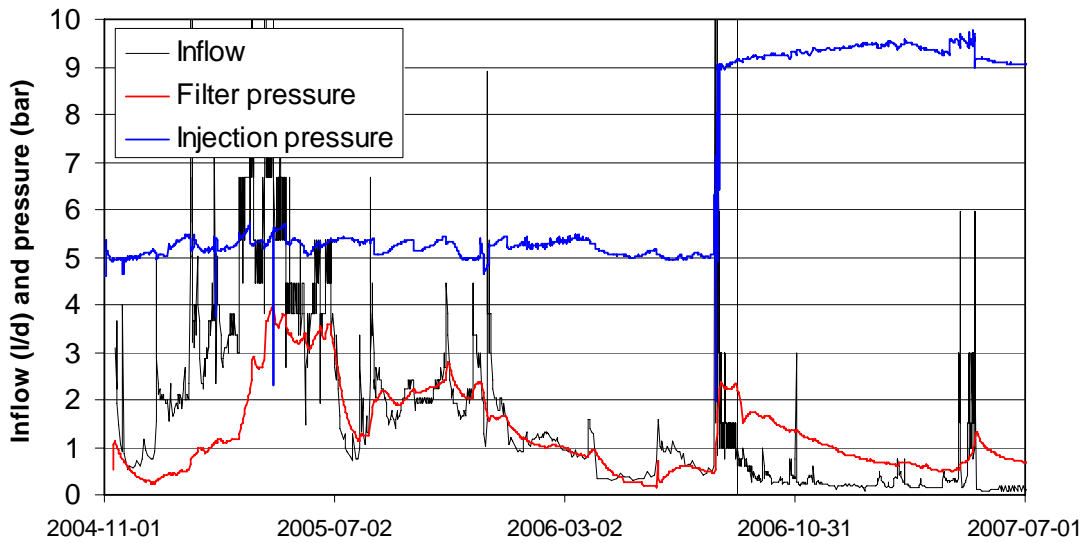


**Figure 5-2.** Development of relative pressures (injection and in sand filter) and inflow since the second hydraulic test.

### Shield hydration

A number of preparatory activities for a future gas migration test have been conducted since the previous data report. In order to facilitate a gas test in the upper package of the experiment, it is essential to ensure that complete water saturation can be achieved in this part. This can supposedly be attained by water injection and pressurization of the sand shield.

The first step was to sample and analyze the gas in the shield. The sampling was made on January 25. The result from the gas analysis is shown in Table 5-3. The most striking observation is the content of CO<sub>2</sub>, which corresponds to 35 vol% of the dry gas. The content of O<sub>2</sub> and N<sub>2</sub> is 2 and 57 vol%, respectively. It appears as if most of the O<sub>2</sub> has been consumed and is now found as CO<sub>2</sub>, but an additional input of CO<sub>2</sub> is needed to account for the measured content. The helium content was also very high (6 vol%).

The second step was the program for venting dry gas from the sand shield. A major concern for the gas migration test and thus for the filling of the sand shield is to make sure that no pockets of dry gas (i.e. all gases except from water vapor) remains in the shield. Such a situation could potentially imply that the volume of pressurized gas during the migration test would be unsafely large.

The basic idea behind the program for venting the dry gas was to inject batches of de-ionized water through one of the injection points in the shield. The gas pressure was expected to increase during this procedure since the system is closed. The vapor was subsequently planned to be flushed through the other injection point. At the same time a significant part of remaining dry gas would be vented. By iterating this procedure a number of times, the amount of dry gas was expected to reduce to insignificant levels.

**Table 5-3. Composition of dry gas (analysis by Microbial Analysis Sweden AB).**

Gas	Sample (ppm)	Dry air* (ppm)
Hydrogen	128	0.55
Helium	57 700	5.24
Argon	3 590	9 340
Oxygen	20 000	209 460
Nitrogen	566 000	780 840
Carbon monoxide	30.9	Trace
Carbon dioxide	353 000	383
Methane	581	1.745
Ethane	37.8	-
Ethane+Ethylene	9.4	-
Propane	0	-
Propene	16.6	-

\* From Wikipedia

**Table 5-4. Volumes injected into and extracted from the sand shield.**

Date	Injected water volume (liters)	Extracted water volume (liters)	Extracted gas volume (liters)
2007-05-09	4.5	0.1	37
2007-05-10	6.1	0.5	21
2007-05-11	19.6	1.8	>> 2
2007-05-25	0.1	0.6	>> 5
<b>Total</b>	<b>30.3</b>	<b>3.0</b>	<b>&gt;&gt; 65</b>

**Table 5-5. Pressurization tests with GDS.**

Date	Port CS202	Port CS203
	Maximum pressure & flow rate	Maximum pressure & flow rate
2007-06-08	20 bar & 0.6 ml/h	25 bar & 20 ml/h
2007-06-29	60 bar & 0.4 ml/h	40* bar & 150 ml/h

\* The target value was 60 bar, but the maximum flow rate was reached at 40 bar.

The method was however found to be inadequate, on the first hand because the prevailing vapor pressure and thus the water content of the shield was lower than expected. The water content was therefore increased through injecting water into the shield. At the same time gas was extracted with vacuum. The amounts of injected and extracted water and gas are shown in Table 5-4.

During the course of injecting water into the system, both injection points (or their surrounding) started to exhibit a high flow resistance. The ports were therefore pressurized with GDS in two attempts to purge the injection points (Table 5-5). The inflow through one of the ports (CS203) was found to increase significantly when the pressure was raised to 40 bar. This pressure level has later on (during the autumn of 2007) been sustained by continuous pressurization of the shield. This will be described in the next data report.

The injection of water influenced the conditions around the upper heater and this is reflected by some of the sensor data. The temperatures on the upper heater (App.A\page88) tended to decrease whereas the temperatures in Ring 10 tended to increase (App.A\page80). This change can be explained as an increased heat transport through the sand shield.

A second effect of the injection of water was the decrease in total pressure and pore pressure in Ring 9 (App.A\ pages54-56 and page70). This could be an effect of swelling of the buffer into the sand shield. If this is the case, then this could explain the increase of flow resistance of the injection points. An alternative explanation for the pressure drop is that this was a thermal effect. The opposite response, so that pressures would increase rather than decrease, could however be expected if the thermal change would be the cause.

### 5.3 Temperatures

Temperatures are monitored by use of thermocouples in three cylinders (C1, C2 and C3) and two rings (R4 and R10), cf. Figure 1-1. In addition, temperature readings are provided by the capacitance-type relative humidity (RH) sensors. In general, the temperature results exhibit consistent trends up to maximum values after about 200 days (App.A\pages77-82). A few exceptions have occurred for inner parts in Cyl 2 and the inner sand shield at Ring 10, where the maximum temperatures were reached after only about 40 and 60 days, respectively (App.A\pages79-80).

The TBT experiment is located 6 m from the CRT experiment. The latter was initiated approximately 880 days before the start of the TBT experiment and has therefore contributed with a certain heat flux. The CRT was terminated in October 2005. In order to compensate for this loss, the power output from the TBT heaters was increased from 1500 to 1600 W on June 9, 2006.

The temperature readings from July 1 2007 are compiled in Figure 5-3. It can be noted that the highest temperatures in the bentonite blocks are found in Ring 4, whereas the lowest can be found in cylinder C3. The most significant change from the previous data report was the decrease in temperature around the upper heater caused by the injection of water into the shield (see Section 5.2). The temperature on the mid-section of the heater surface was 146 °C on January 1, whereas it had dropped to 133 °C on July 1. This decrease is shown in the temperature profiles in Figure 5-4.

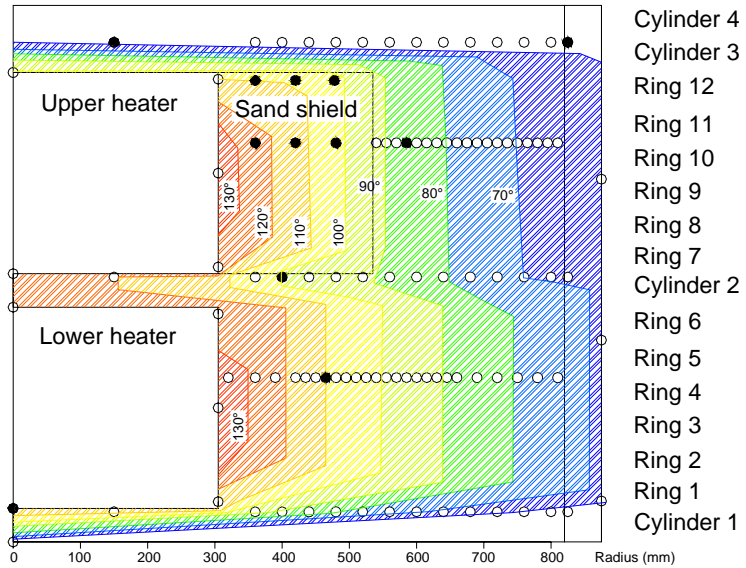


**Figure 5-3.** Temperature distribution at July 1, 2007. Rings indicate sensor positions. Filled rings indicate sensors out of order.

The temperature distributions enable evaluations of the apparent thermal conductivity of the buffer materials. Distributions of such conductivities were presented in a previous Sensor data report (/5-1/). The development of conductivities at different radii in Ring 4 is shown in Figure 5-5. It can be noted that the innermost point, at 35 mm from the heater surface, dropped immediately after test start, but has thereafter increased to the value of 1 W/mK. This occurred in the beginning of 2007. The conductivity in this point appears to have remained constant since then. In contrast, a point at 155 mm from the heater appears to have undergone a rapid increase in the beginning and has thereafter remained fairly constant.

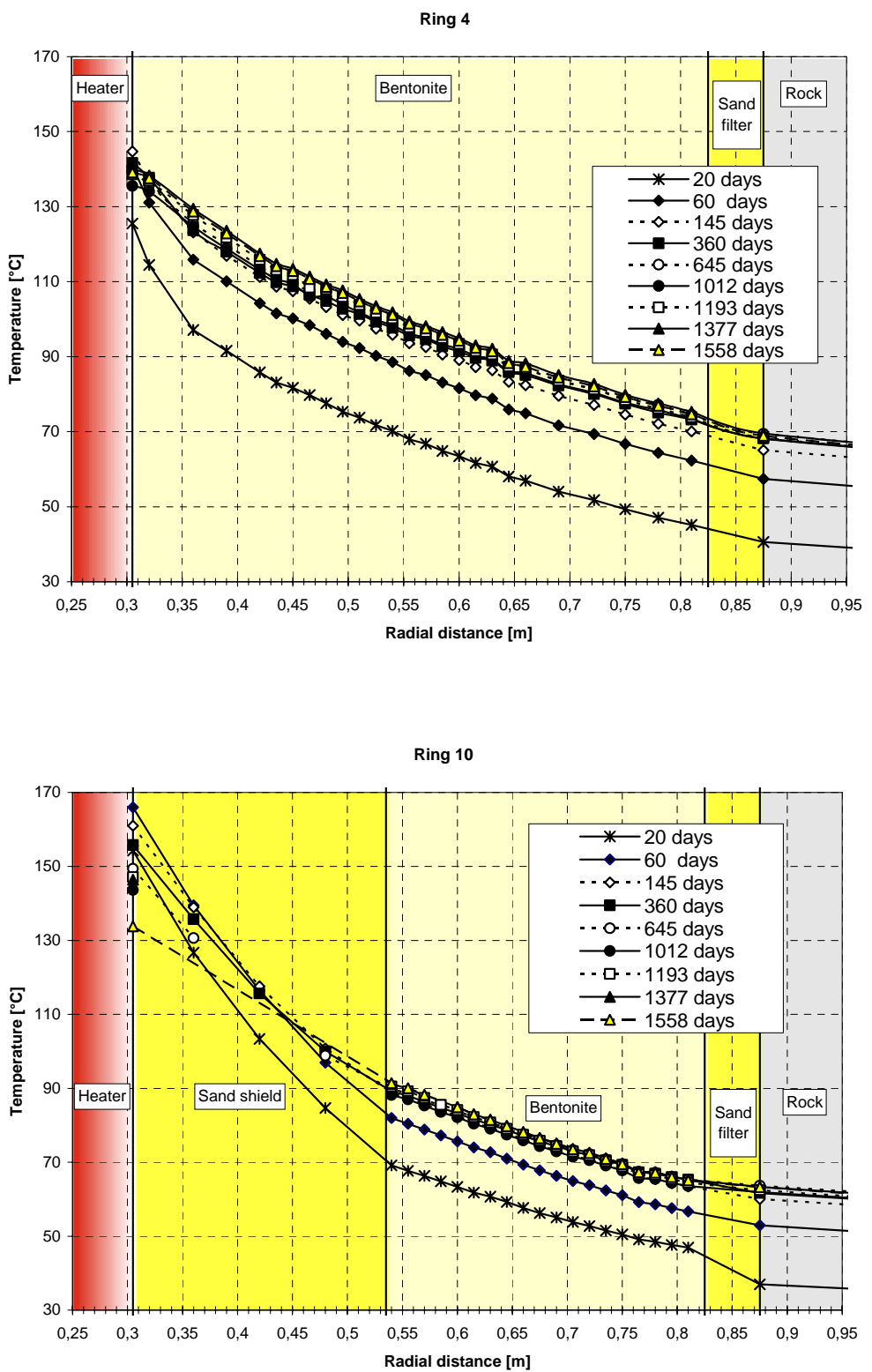


**Figure 5-4.** Temperatures measured at mid-height of heater 1 (Ring 4) and heater 2 (Ring 10).

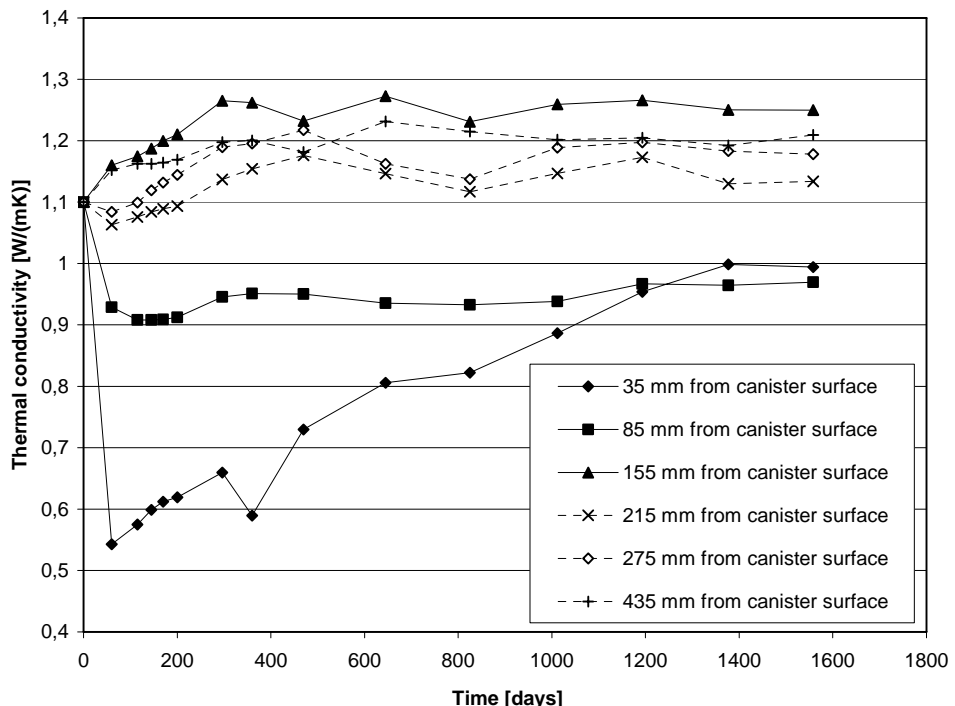


**Figure 5-5.** Thermal conductivity development in ring 4.

## 5.4 Relative humidity/suction

Recorded RH values and suctions indicate that moisture contents generally increase: RH from 72 to maximum 100 % (App.A\pages63-68); suction between 6 and 1 MPa (App.A\pages58-62).

A significant exception was the suction *increase* in Ring 10 at radius 785 and 735 mm after day 225 (App.A\page61). Although this increase correlated with a general decrease in stresses in parts of Ring 9, it was most likely caused by a shortage in water supply, resulting in a localized desiccation cycle to occur. The trend was also reversed when water injection through the upper tubes was introduced (see Section 5.2), which supports the water supply explanation for these observations.

The hydration of the buffer, as recorded by the RH-sensors, is illustrated in Figure 5-6. Occasions when capacitive sensor signals showing  $\text{RH} \approx 100\%$  (Vaisala and Rotronic), and all *active* signals from psychrometers, corresponding to  $\text{RH} > 95\%$  (Wescor), are compiled. These occasions have earlier been taken as indication of *buffer* saturation. Recent results from the pore pressure sensors have however led to a reassessment of this interpretation. The occasions are instead taken as indications of *vapour* saturation. The current understanding is that the process of reaching full saturation is slow, and that only the bentonite at the mid-section around the upper heater has yet reached this condition.

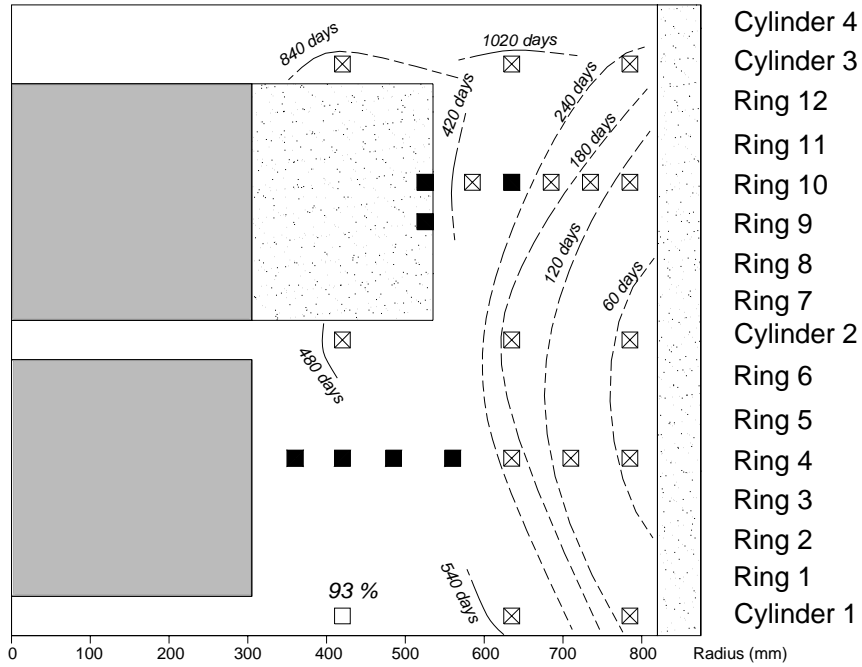


**Figure 5-6.** Occurrences of vapour saturation up till July 1, 2007. Boxes are sensor positions. Ticked boxes indicate saturation. Filled boxes indicate sensors out of order. Percentage is current RH values.

The activation of the filter mat between the upper cylinders is reflected by the most recent vapour saturation event in the upper part (see Figure 5-6).

The only capacitive sensor that still indicates unsaturated vapour is the innermost sensor in Cylinder 1. This sensor has showed a stable value of 93 % RH since the beginning of 2006. The innermost sensor in Ring 4 failed in April 2006. At that time it showed 91 % RH.

## 5.5 Pore pressure

Ideally, pore pressure sensors should give a zero signal as long as the condition isn't totally saturated. At present, four sensors, the outermost in Ring 3 and all sensors in Ring 9 located in the bentonite, clearly show positive values (App.A\pages69-70\), which indicates that these parts are saturated. The build-up of the outermost sensor in Ring 9 coincided with the filter pressure increase in the beginning of 2005, whereas the other sensors responded within 200 days.

The data from the sensors that have responded appears to be correlated with the pressure in the sand filter. The absolute level of the sensors is however higher than the sand filter pressure, which can put the accuracy of the pore pressure sensors into question.

## 5.6 Total pressure

Results from pressure monitoring are shown in App.A\pages49-57. A compilation of recent total pressures is shown in Figure 5-7. The conditions in the lower and the mid-section cylinders are quite isostatic, while the sections around the heaters are characterized by deviatoric stresses, with relatively lower radial stresses. This appears to reflect that the largest displacements occur in radial direction around the heaters. In these sections, the sand filter and the sand shield, and perhaps also the dehydration of the inner parts around the lower heater, enable the radial swelling of the hydrating buffer.

In general, all recorded total pressure is now quite stable. The main exception is the conditions in Cylinder 3, in which one remaining sensor still display an increasing trend (App.A\page57). This is also reflected by the increasing cable forces.

The injection of water into the sand shield resulted in a pressure drop in Ring 9 (see Section 5-2). The most significant difference between January 1 and July 1 was recorded by the innermost axial sensor, which decreased from 8.7 to 7.9 MPa.

Recent axial pressures, shown in Figure 5-7, appear to be quite similar in a band between radius 550 and 650 mm from Cylinder 1 to Ring 9. In contrast, the axial pressure in Cylinder 3 was significantly lower, although this can not be seen in Figure 5-7 due to the sensor failure in connection with the filter mat activation. The relation is further illustrated in Figure 5-8 in which results are shown from axial pressure sensors all located at radii 585 - 635 mm. Moreover, measured cable forces are here shown after conversion to pressures under the assumption that the forces are evenly distributed over the entire rock hole area ( $2.40 \text{ m}^2$ ).

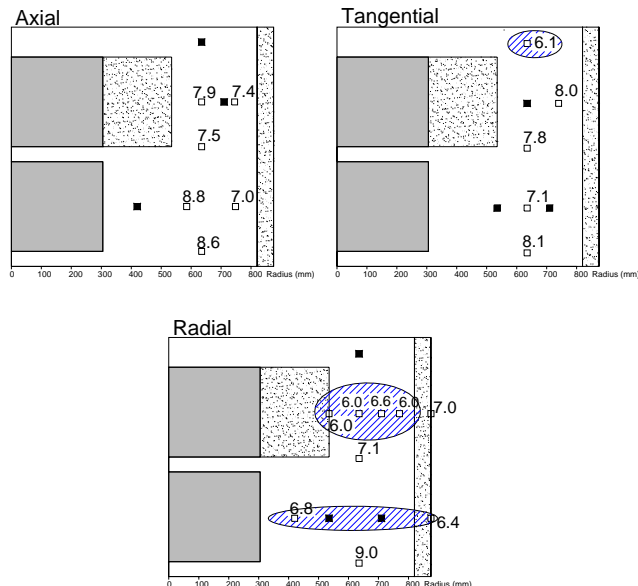


**Figure 5-7.** Total pressure distribution at July 1, 2007. Values in MPa. Boxes are sensor positions. Filled boxes indicate sensors out of order. Levels below 7 MPa marked blue.

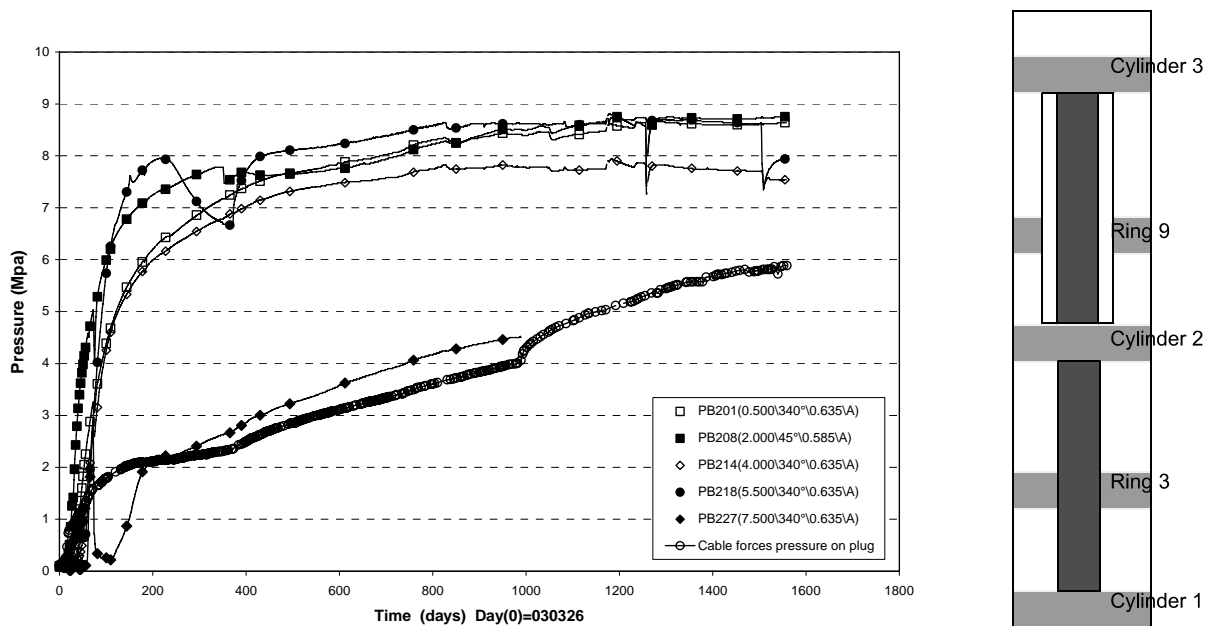


**Figure 5-8.** Axial pressure measured in different sections.

A fairly clear-cut grouping can be observed, which suggests that the vertical forces are predominantly transferred in a section corresponding to the buffer rings around the upper heater. The stress level around the heaters and in the lower cylinders has during the test period been significantly higher than the upper part of the experiment. This difference has however decreased during the test period. This has been further evaluated as a balance between the vertical forces acting on Ring 10 and the lid, respectively (/5-1/).

## **6 References**

**/4-1/ Sandén T and Börgesson L.** Report on instruments and their positions for THM measurements in buffer and rock and preparation of bentonite blocks for instruments and cables. Temperature Buffer Test, Report R5 , 2002. SKB ITD-02-05

**/4-2/ Garcia-Sineriz, J.L and Fuentes- Cantillana.** Feasibility study for the heating system at the TBT test carried out at the Äspö HRL in Sweden. Temperature Buffer Test , October 2002. SKB IPR-03-18

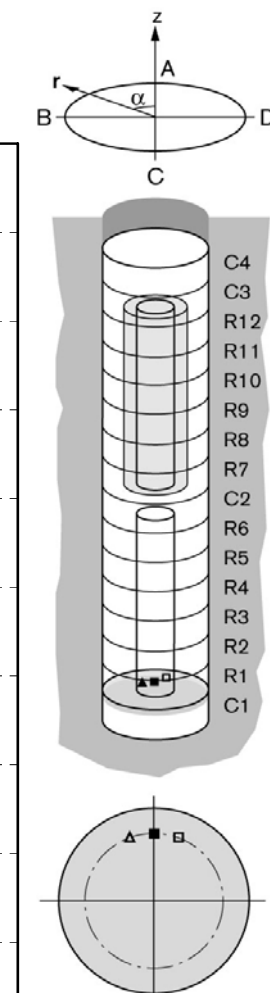
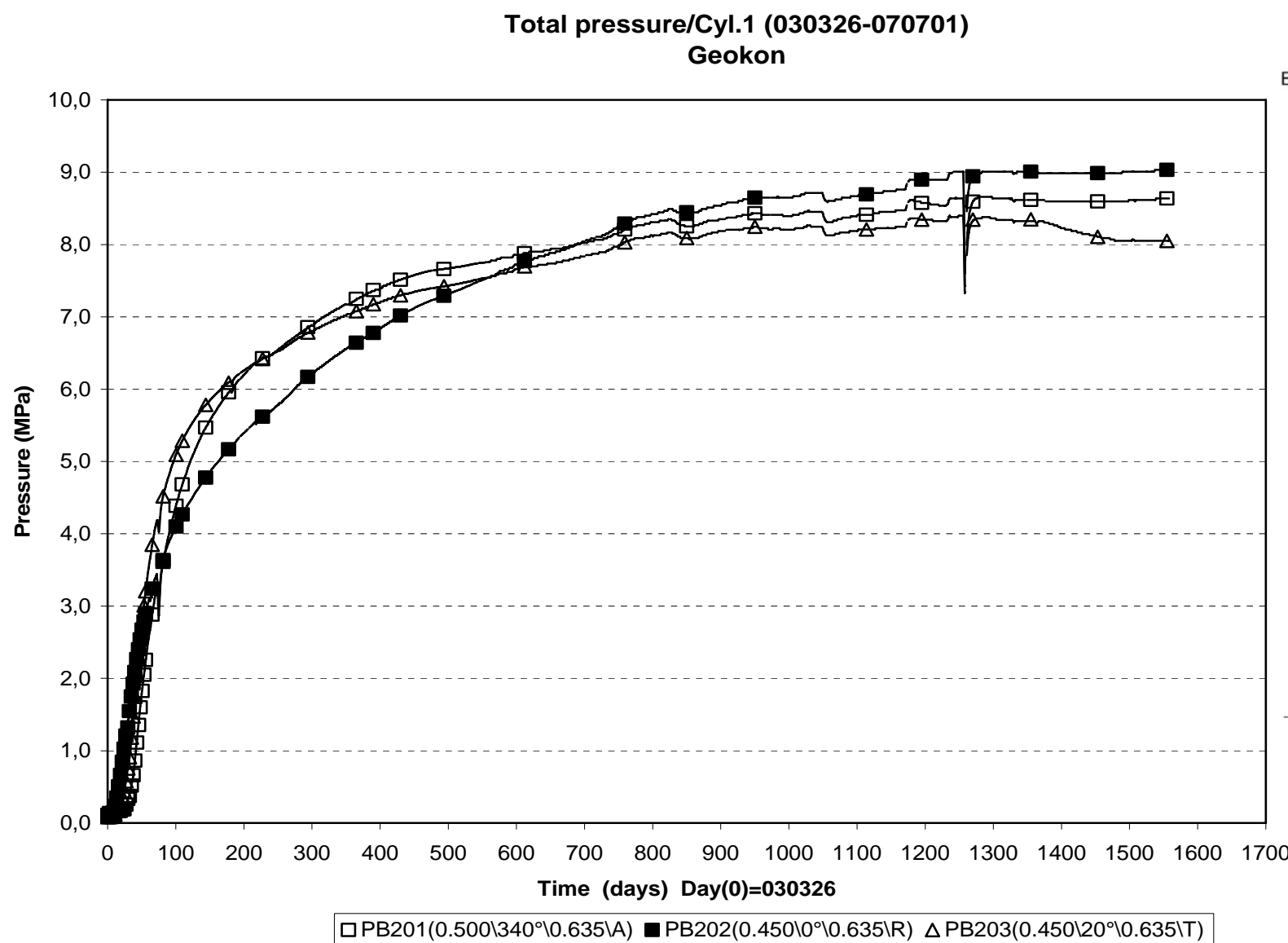
**/5-1/ Goudarzi R., Åkesson M., Hökmark H.** Äspö Hard Rock Laboratory. Temperature Buffer Test. Sensors data report (period 030326-060701) Report No:8, 2006, SKB IPR-06-27.

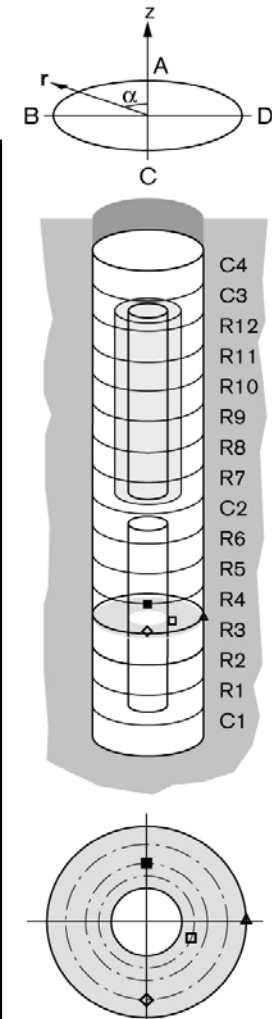
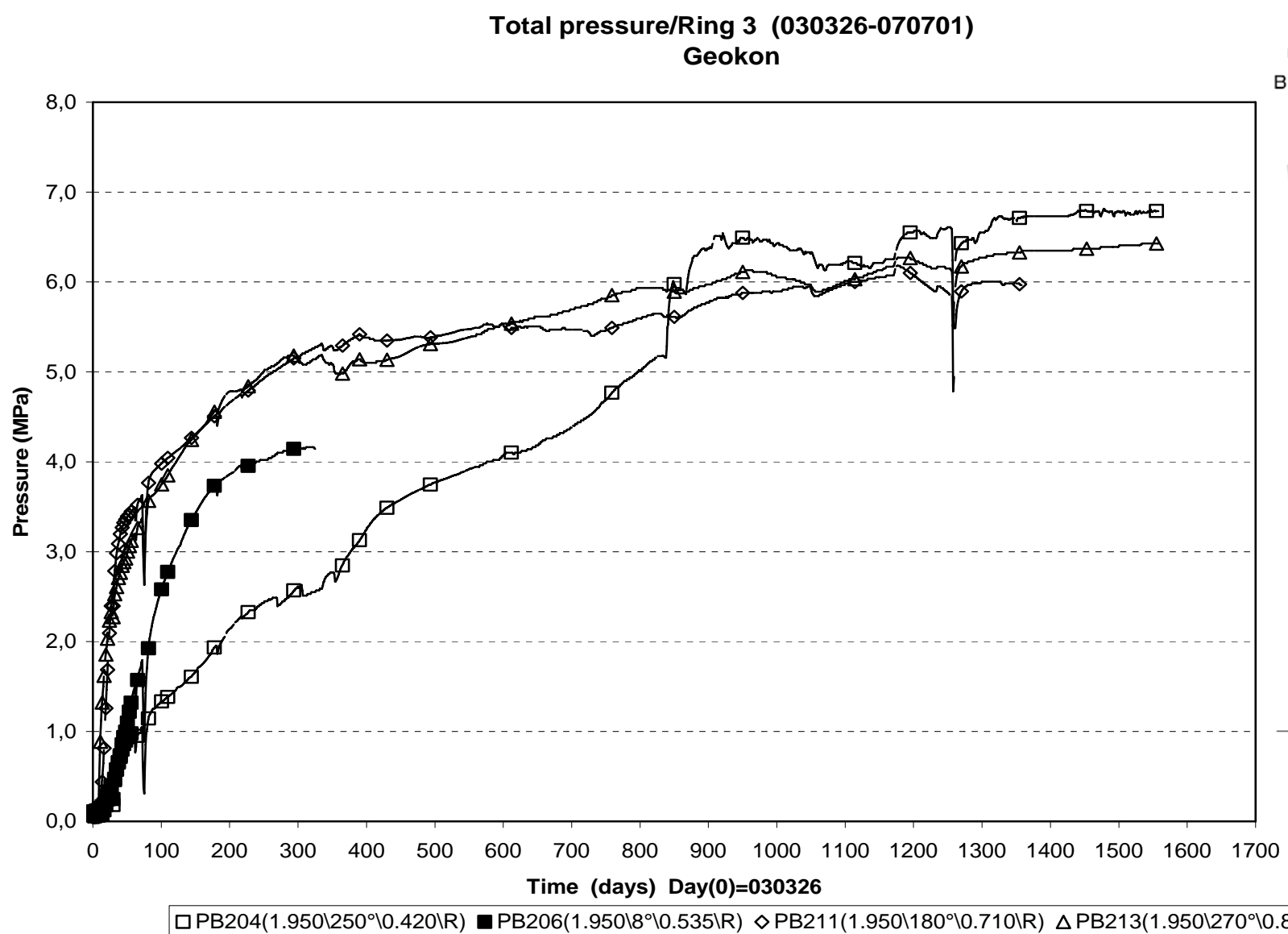


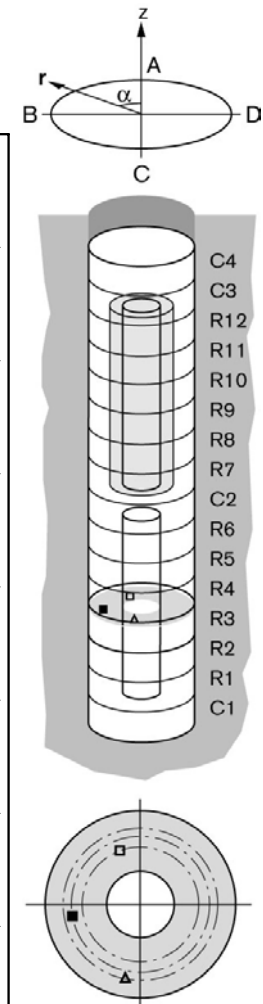
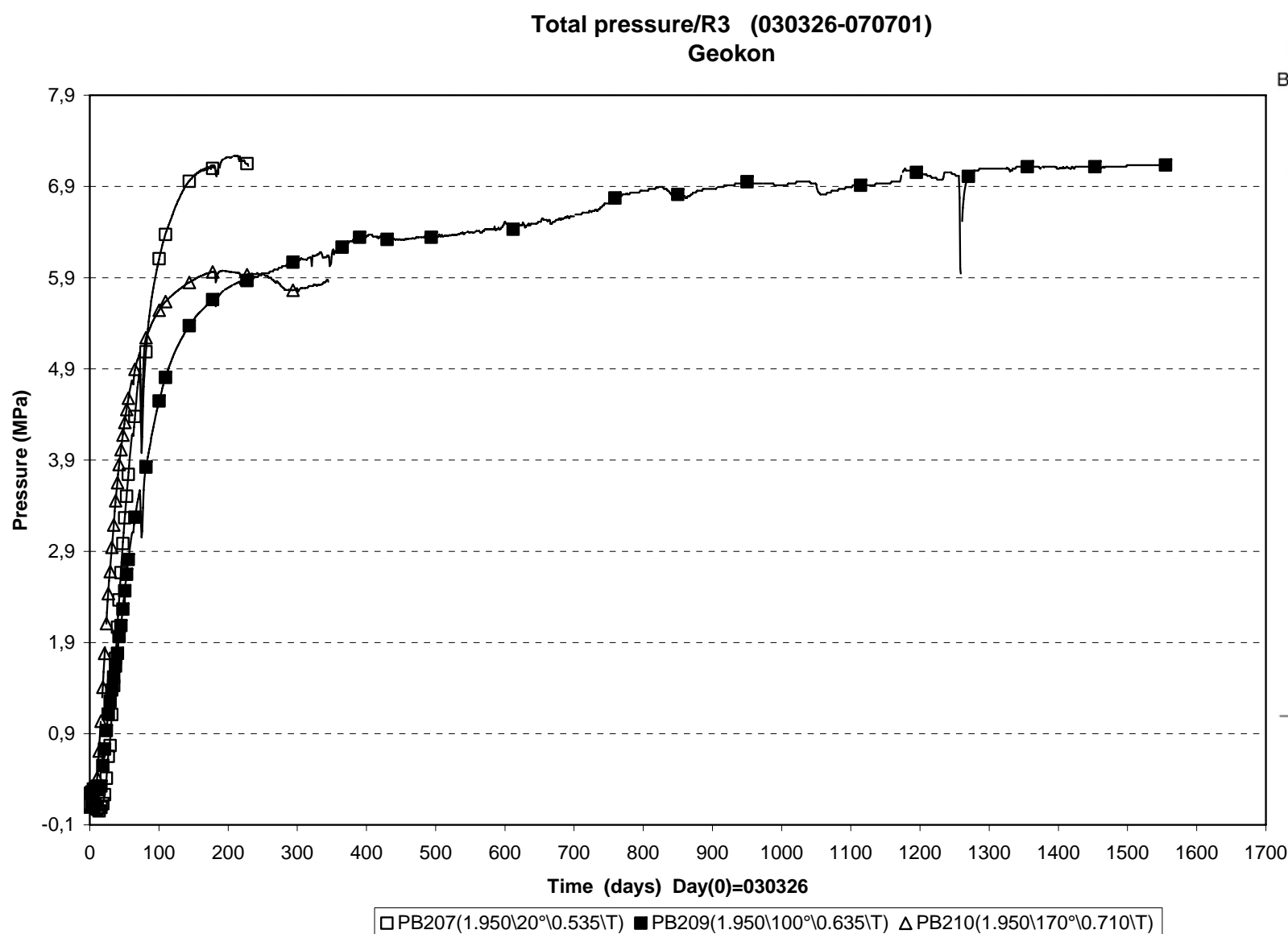
# **Appendix A**

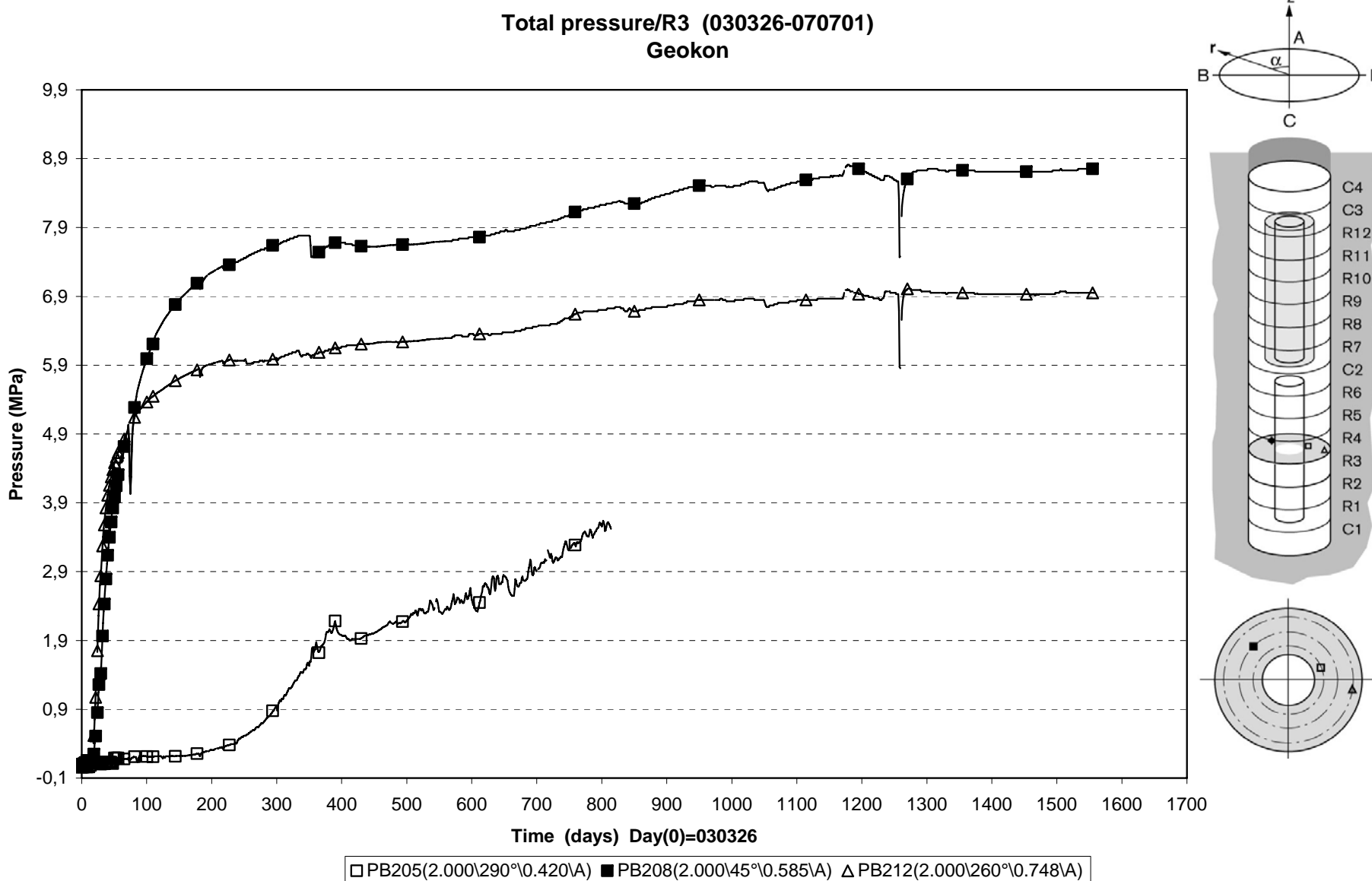
## **Measured data**

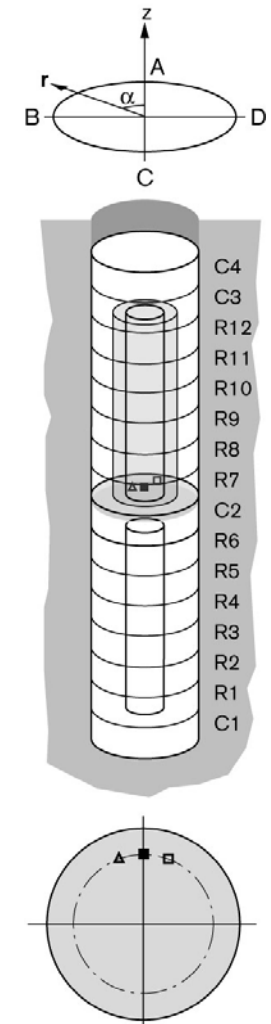
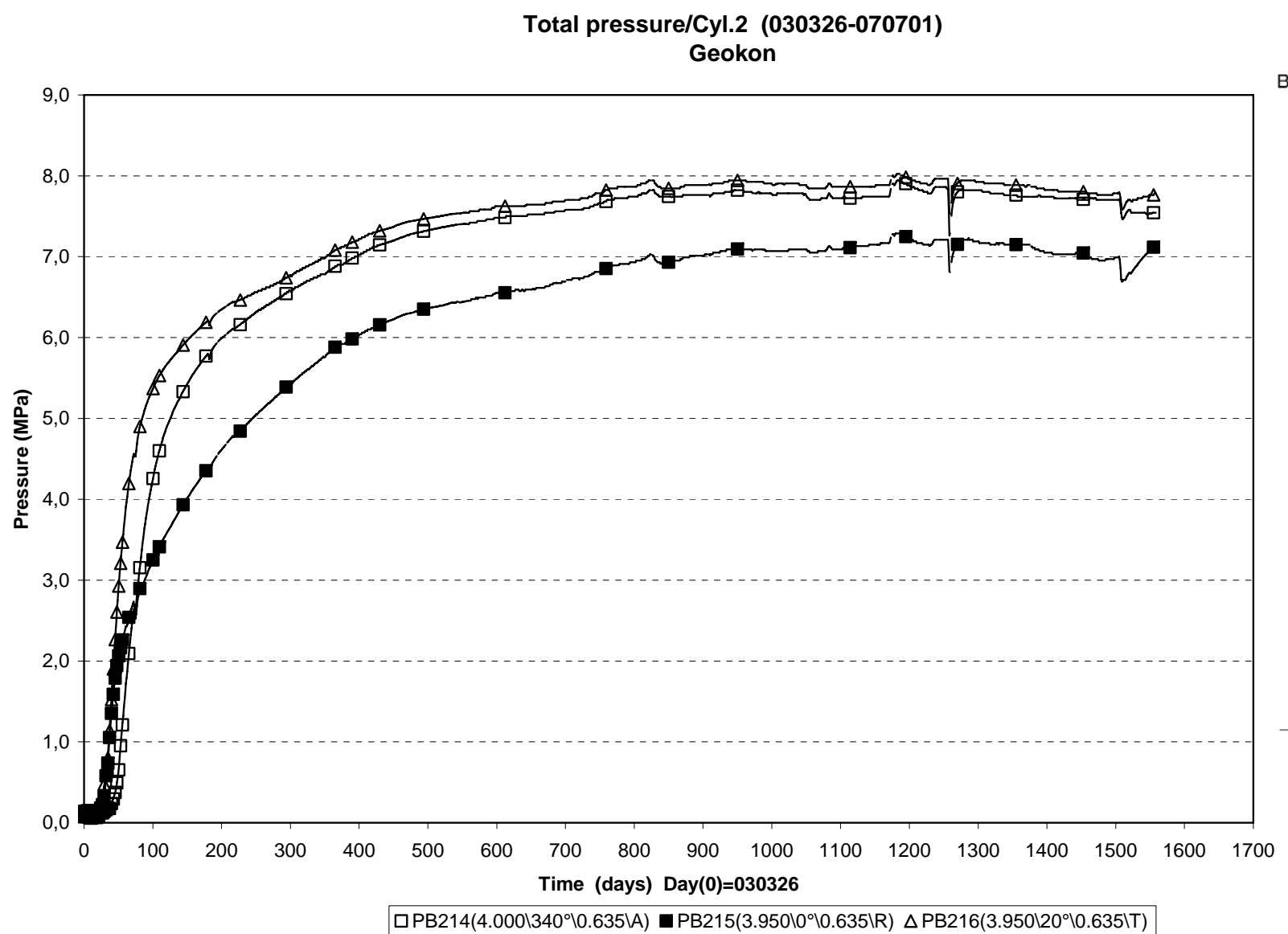


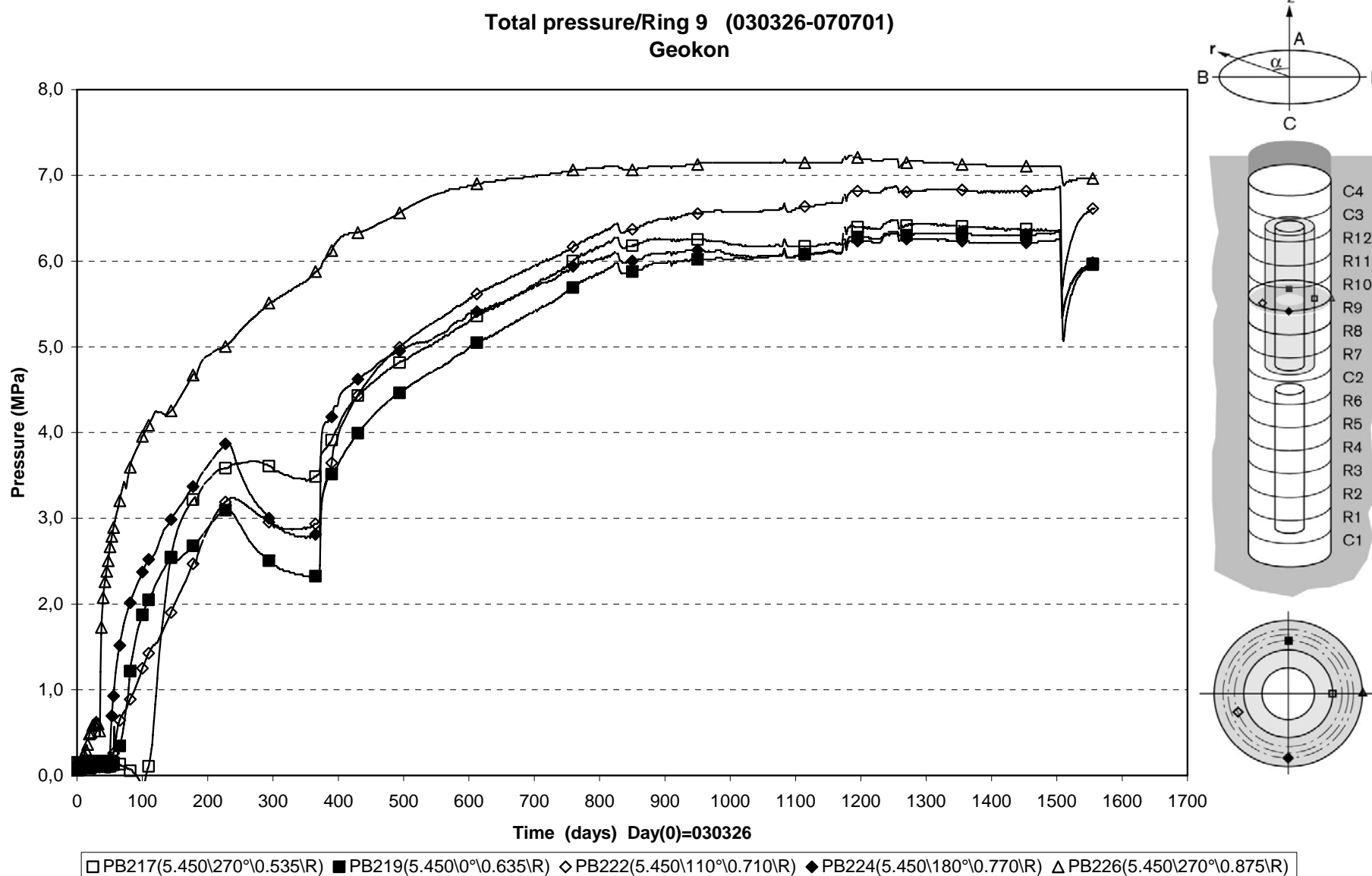


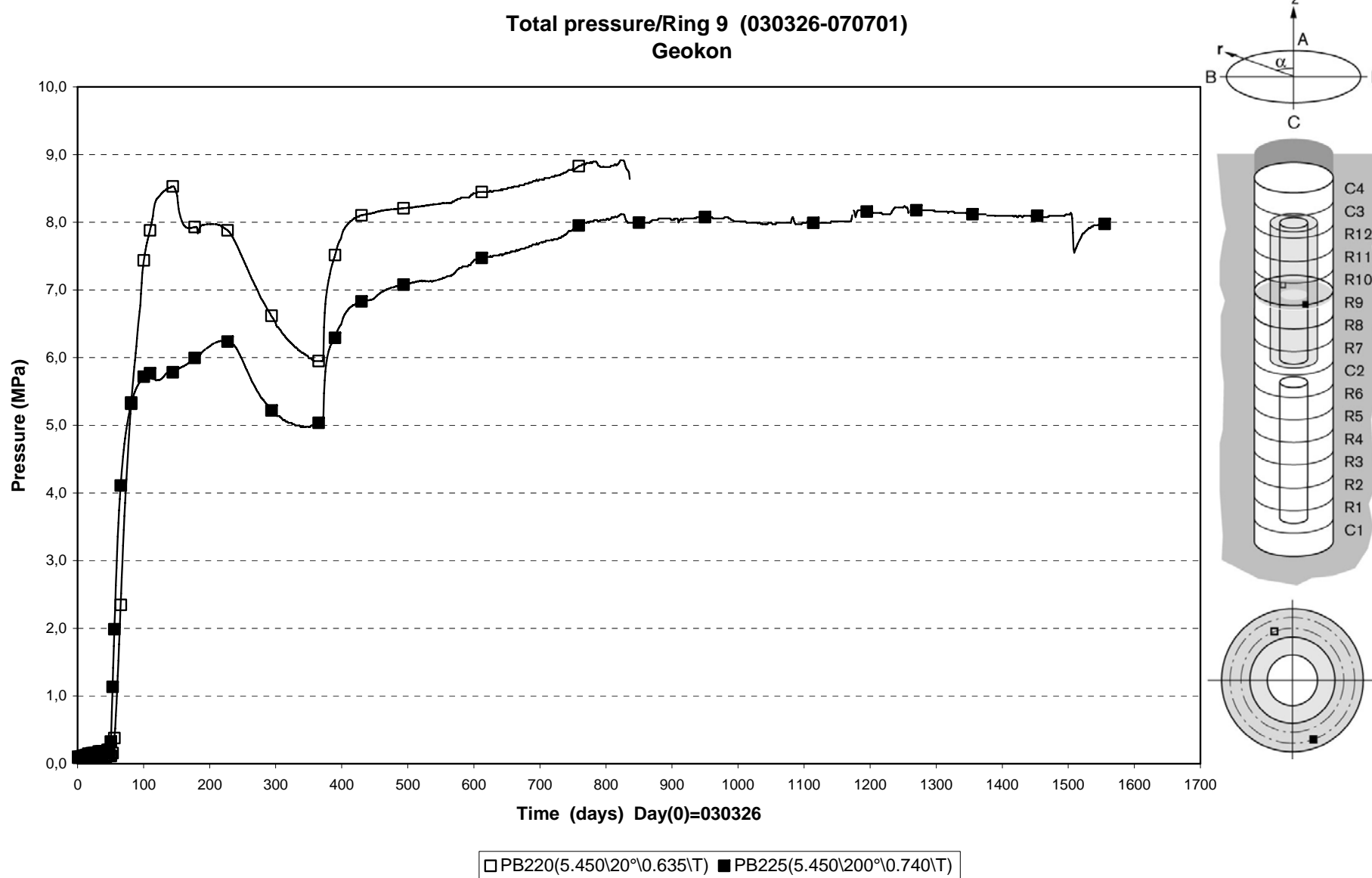


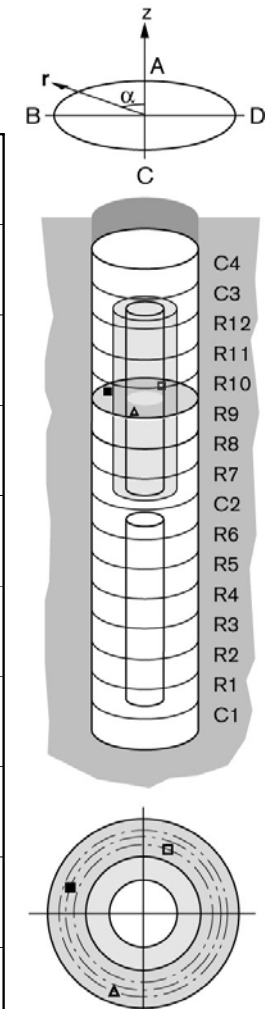
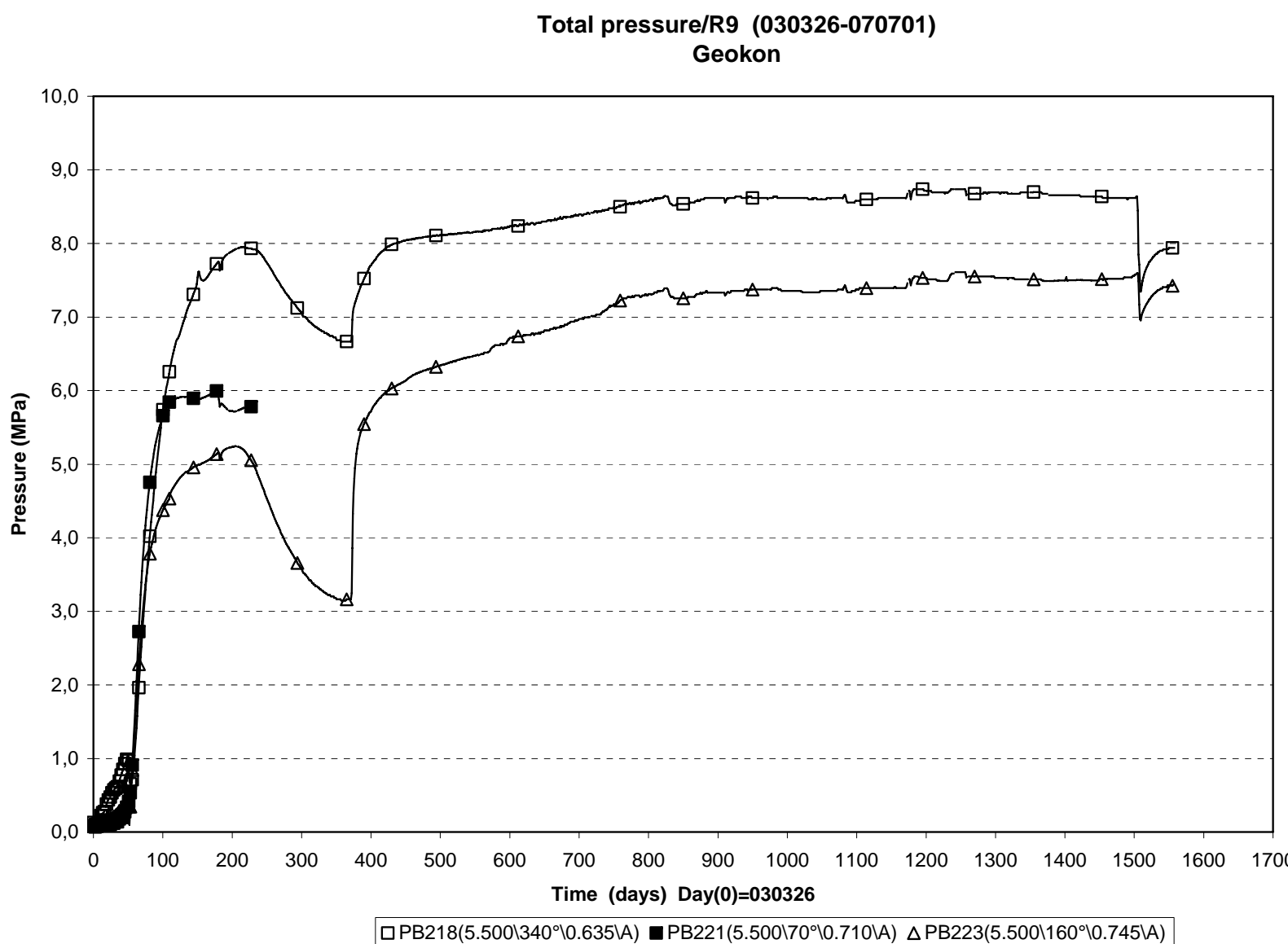


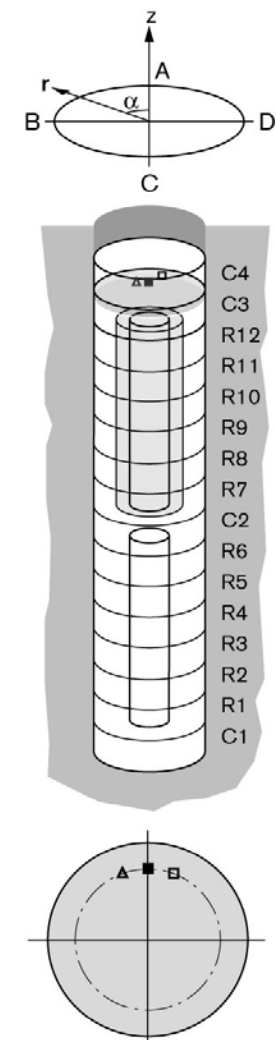
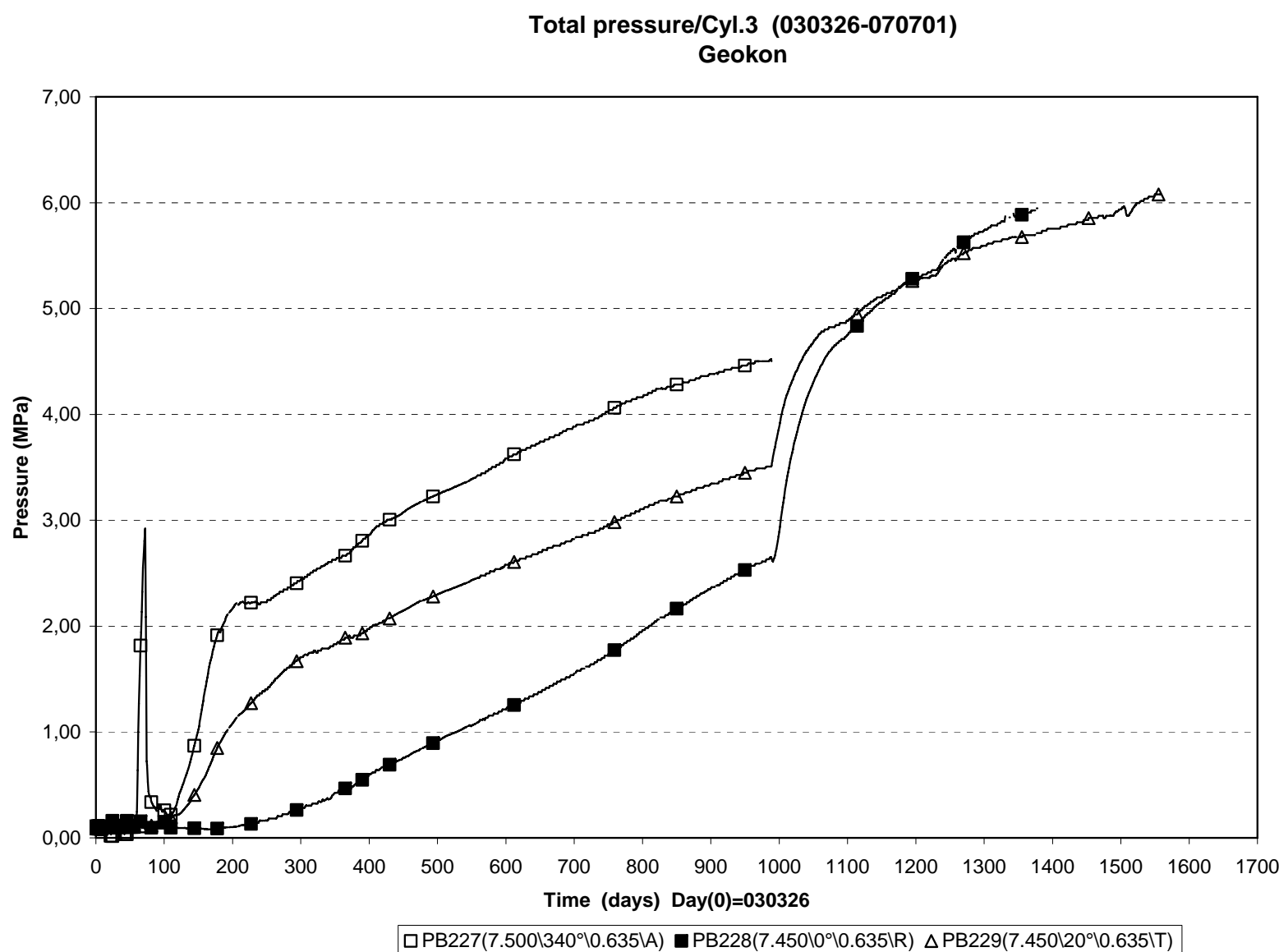


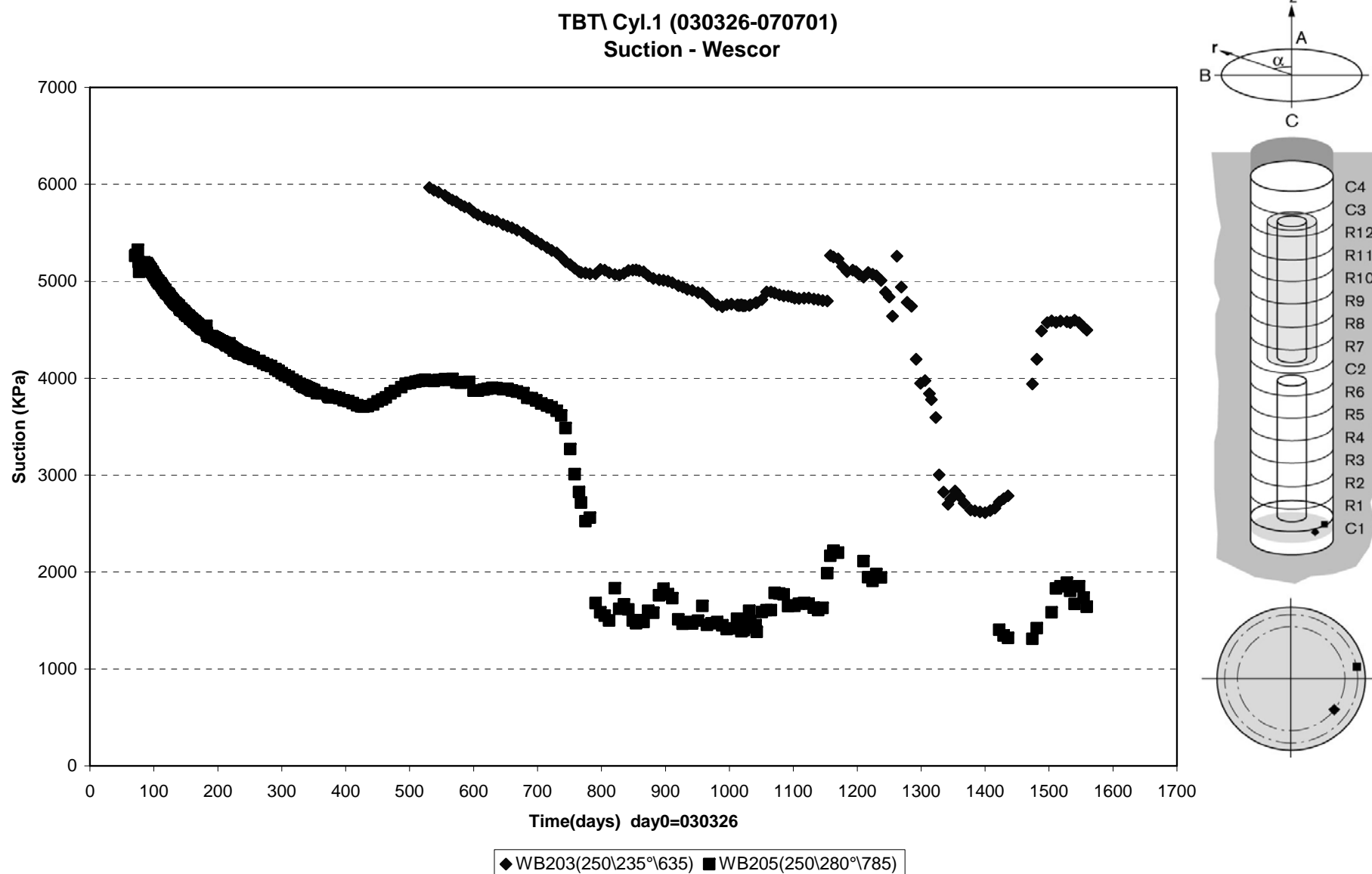


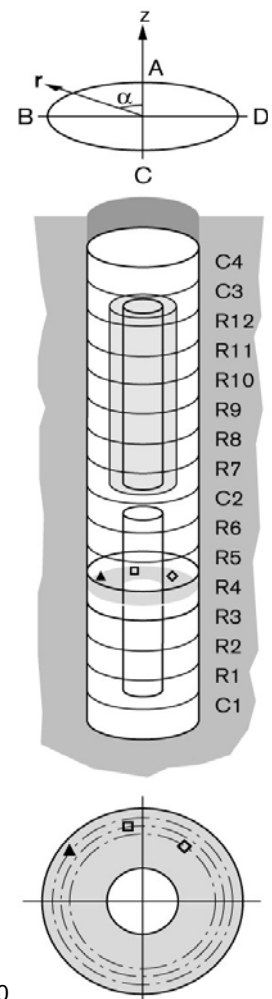
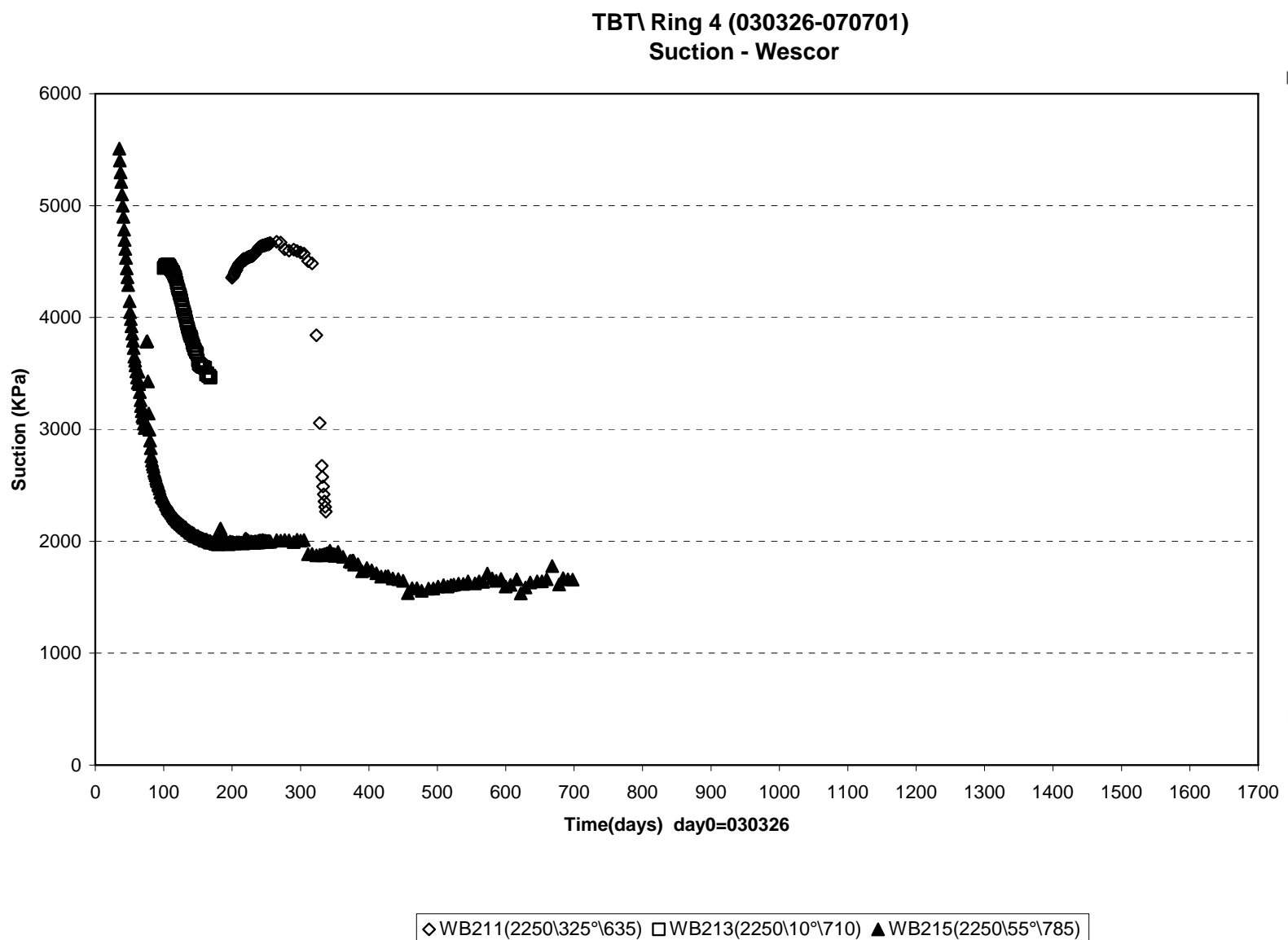


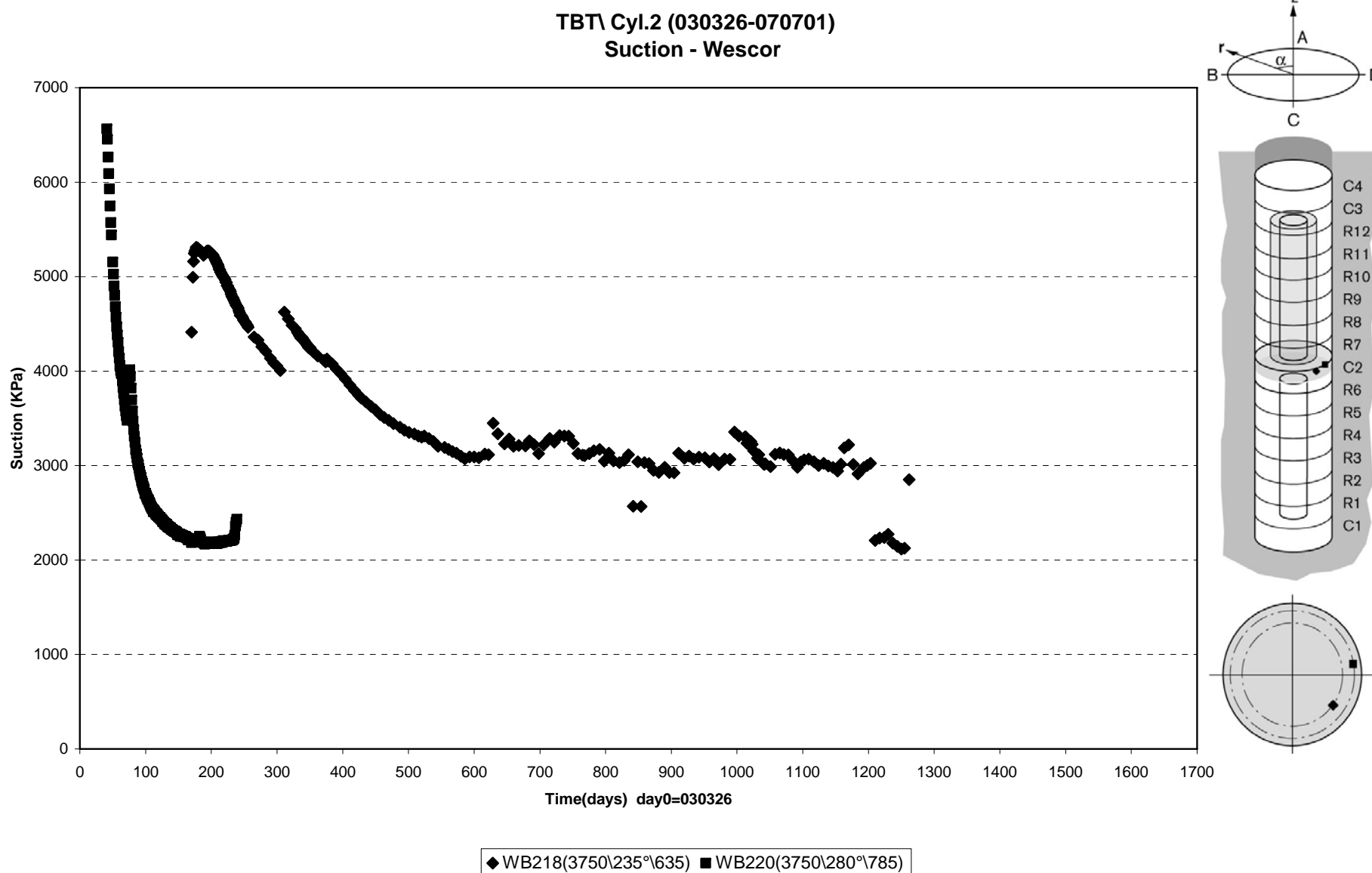


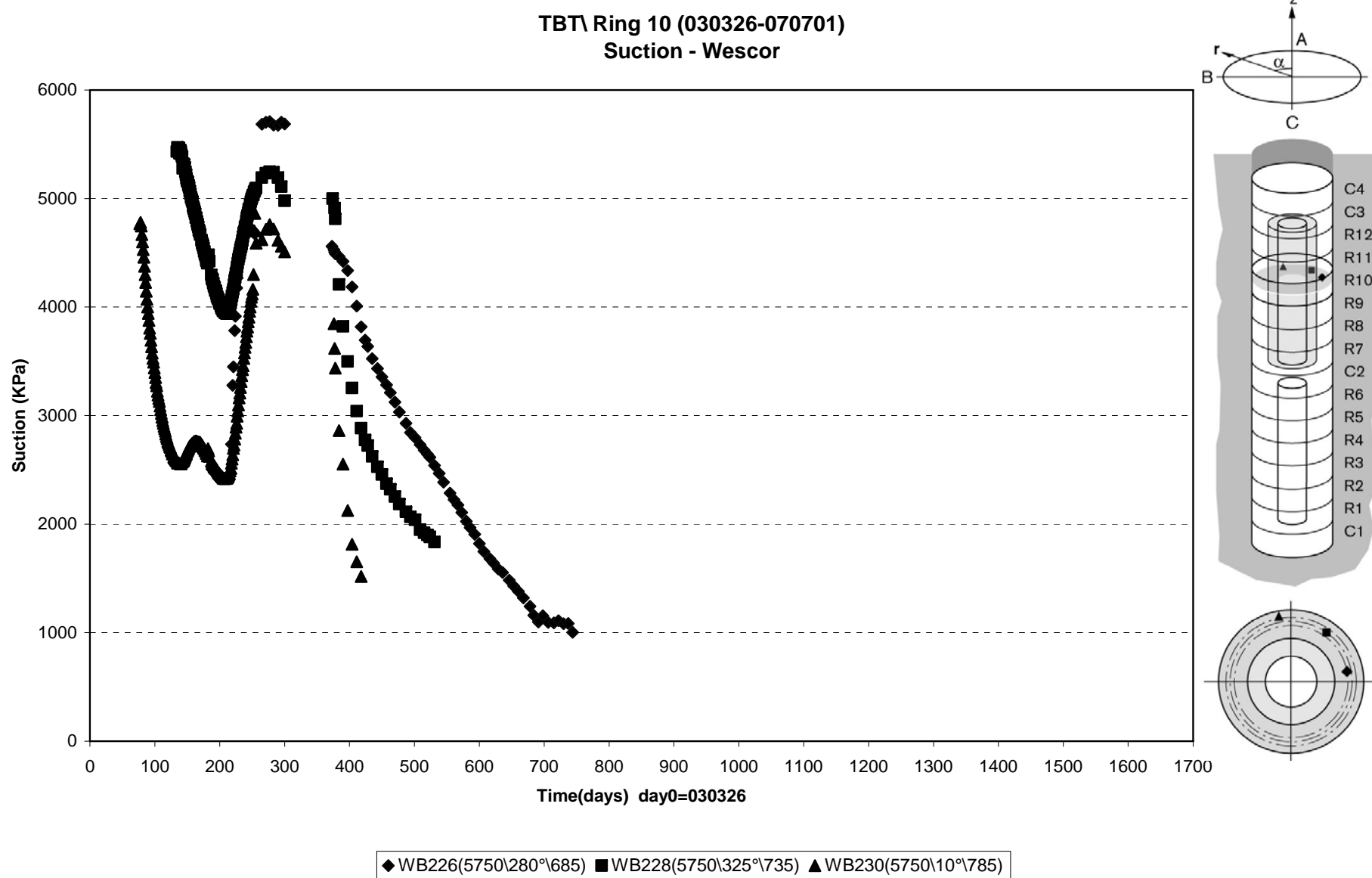


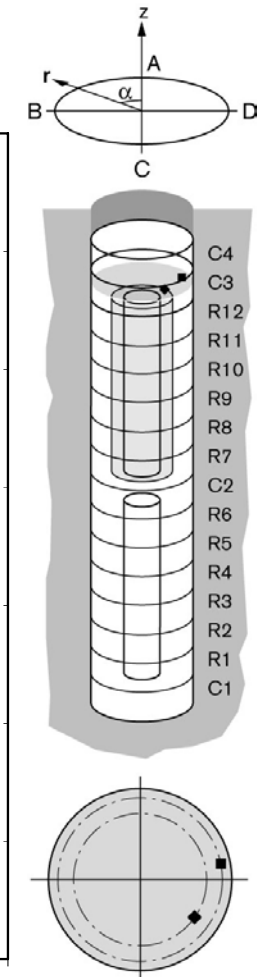
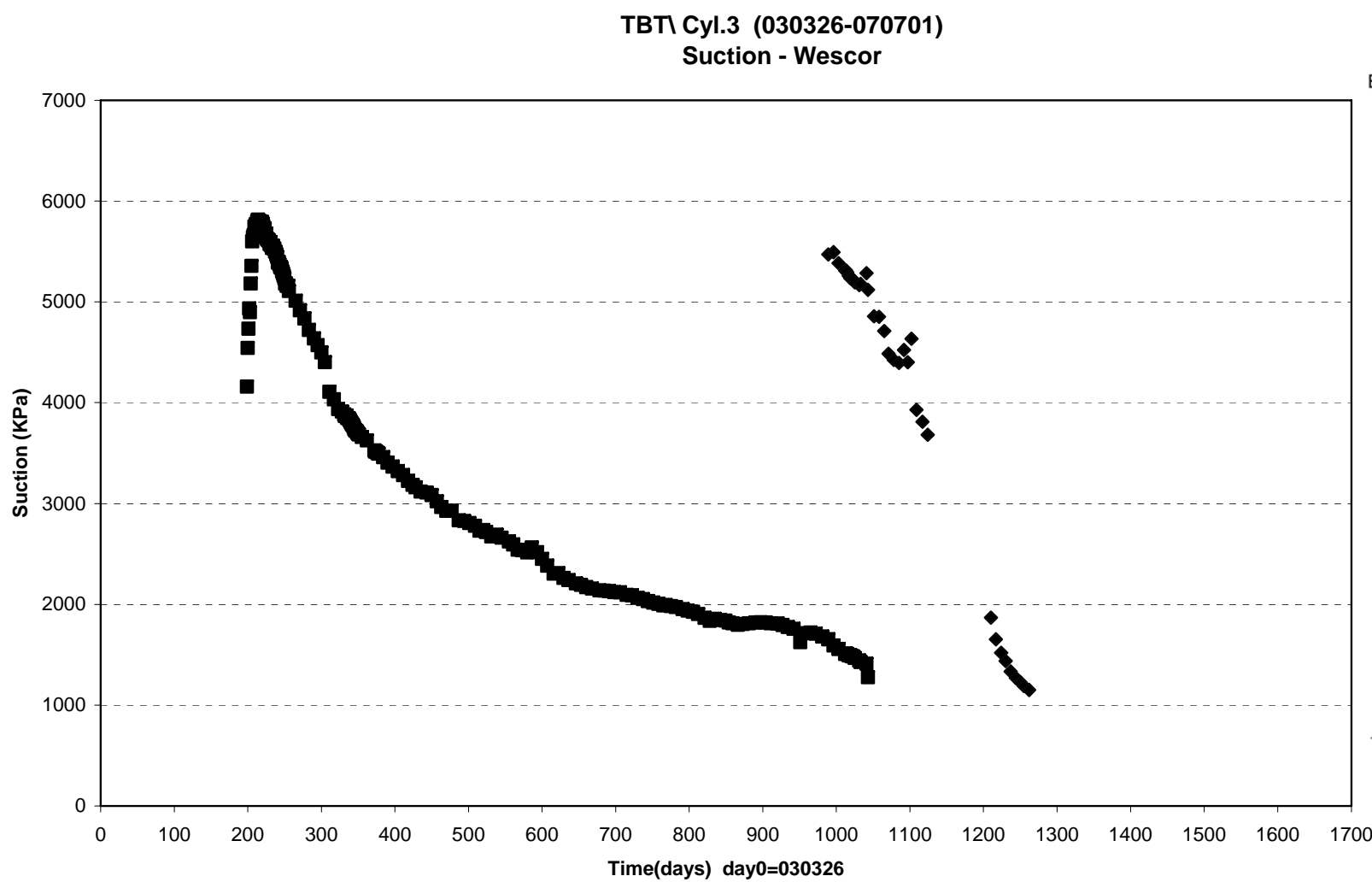


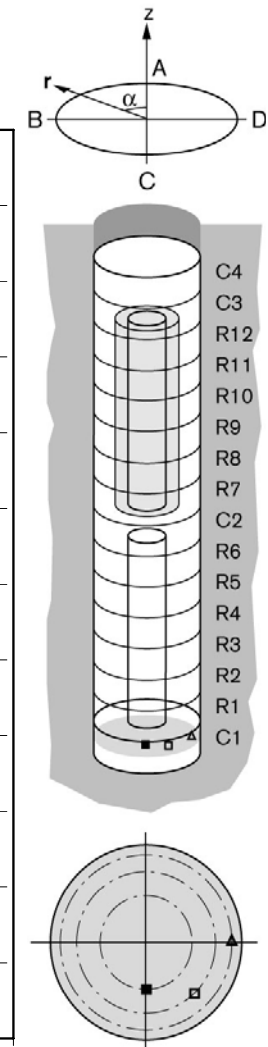
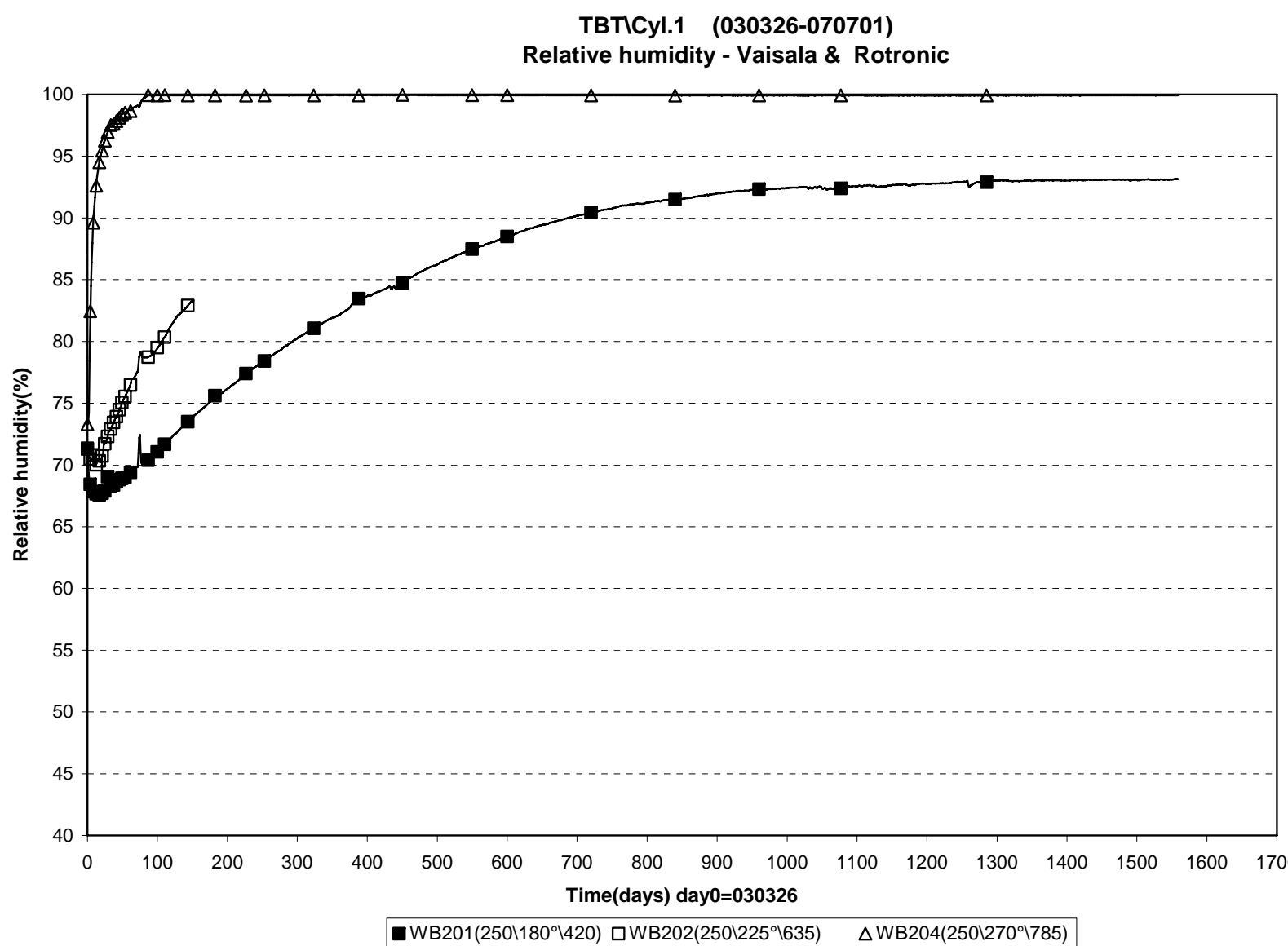


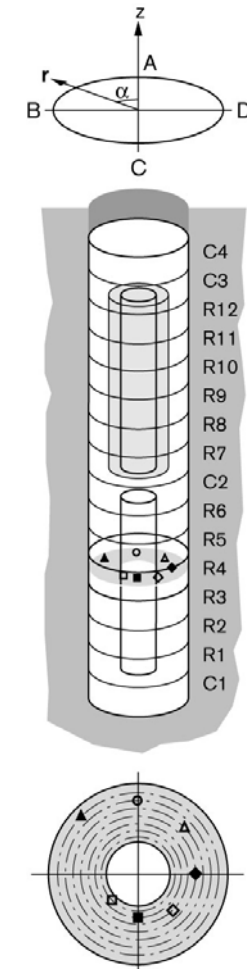
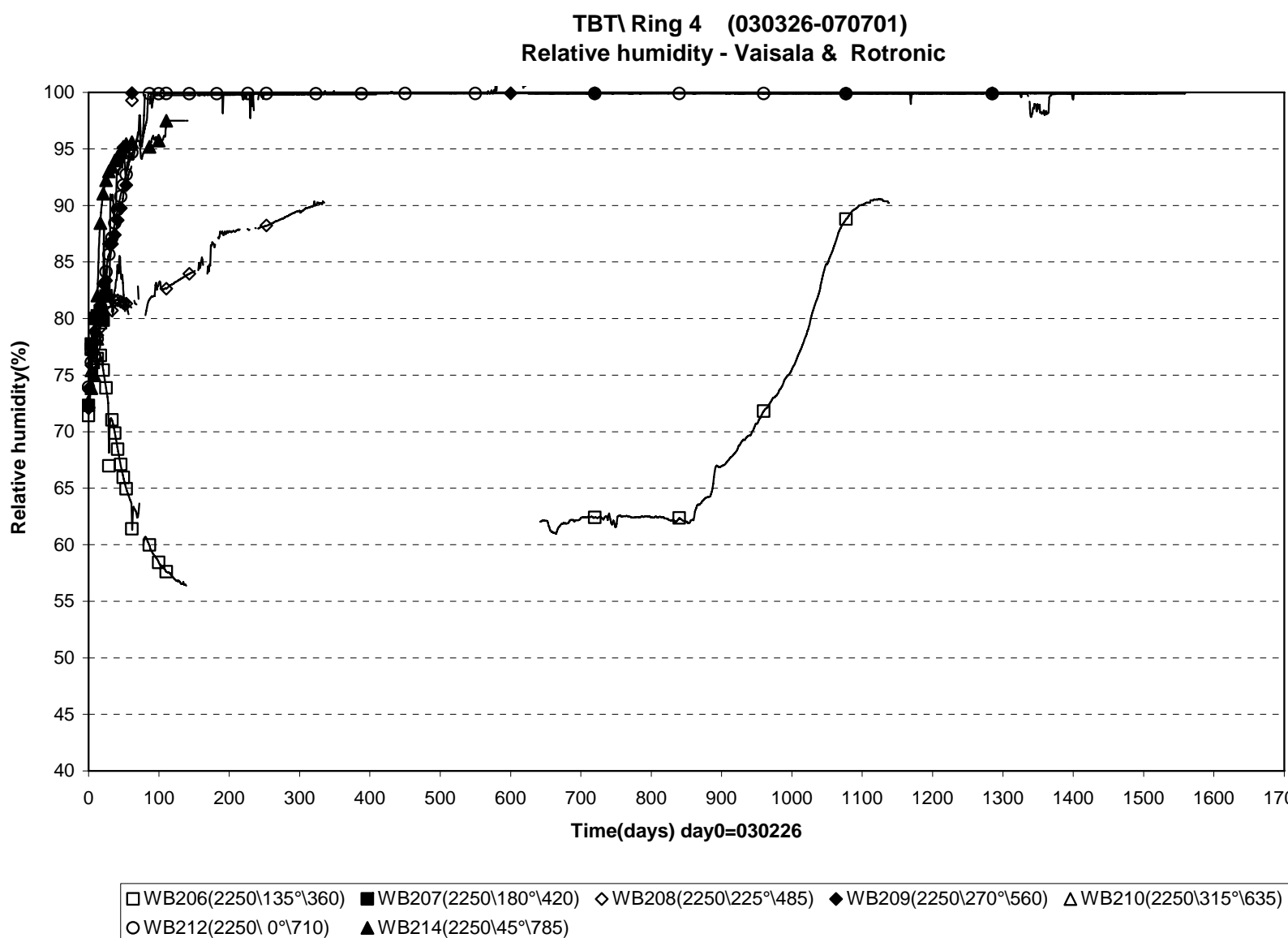


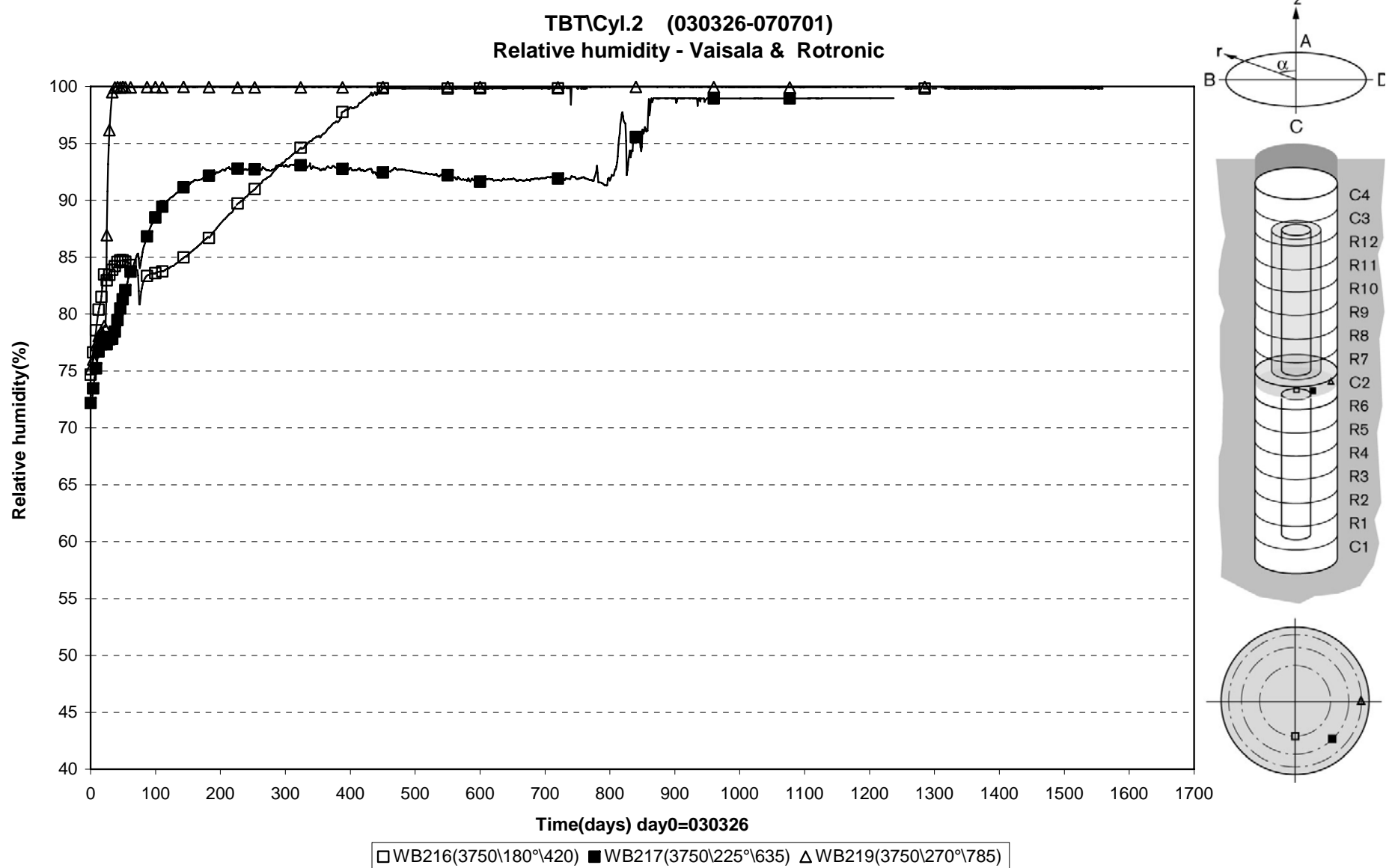


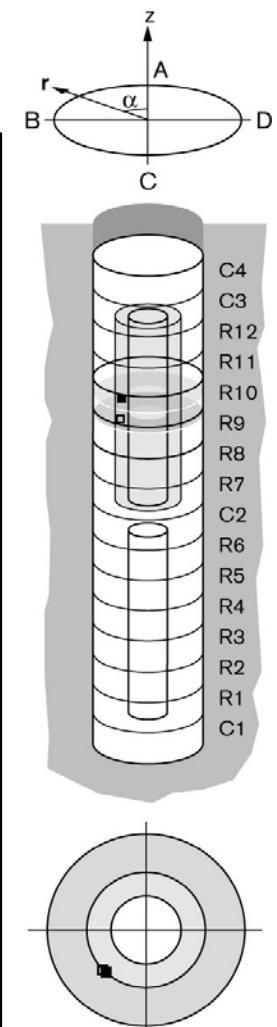
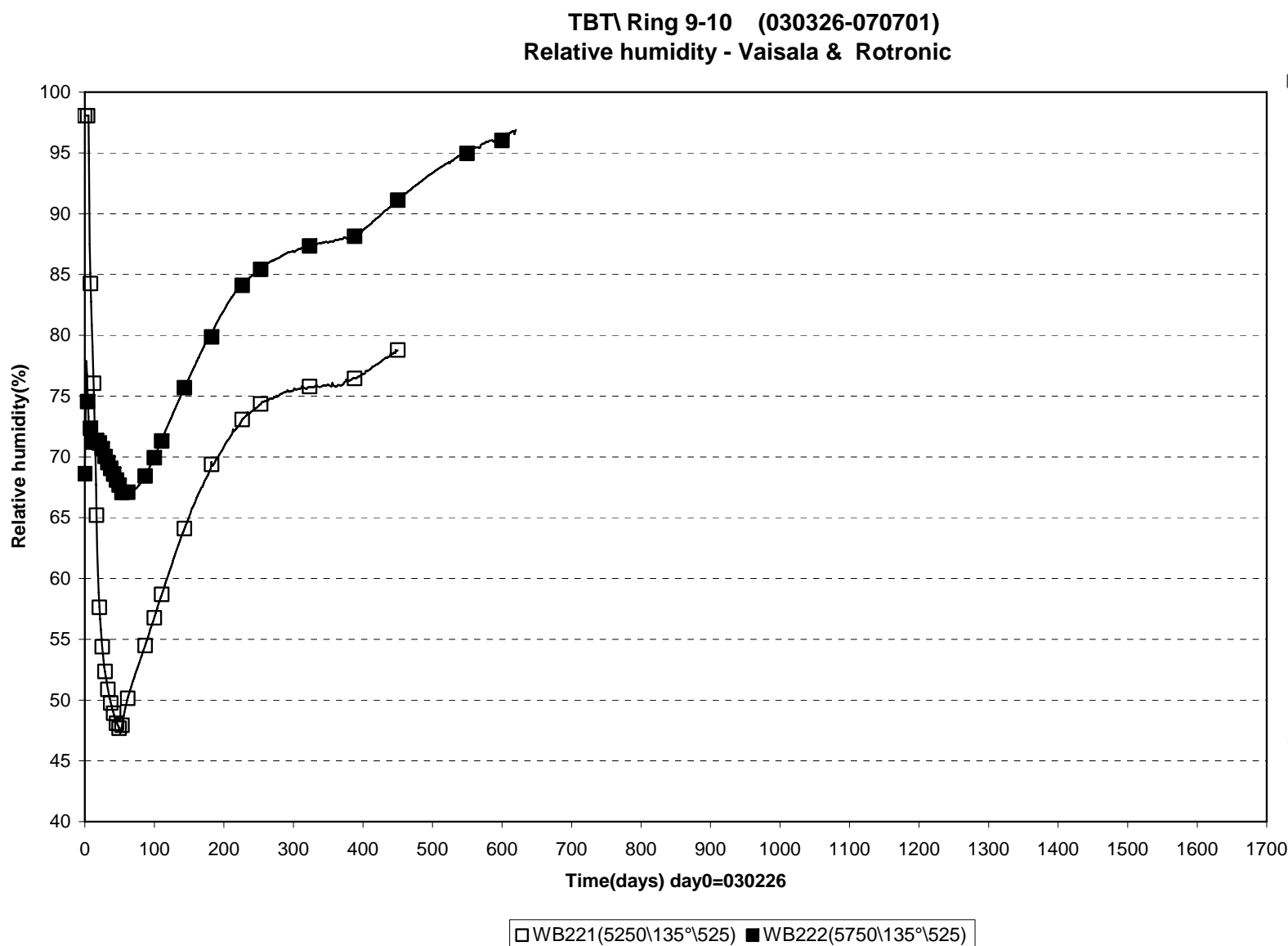


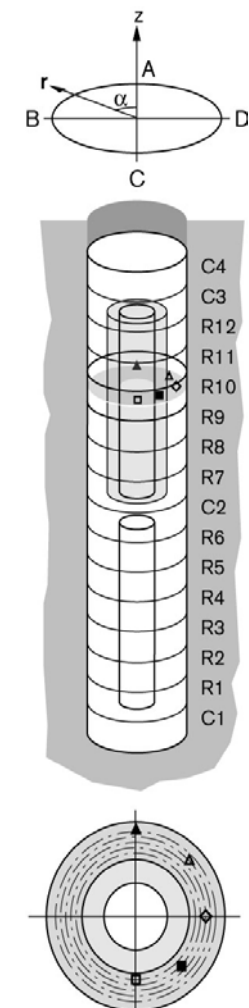
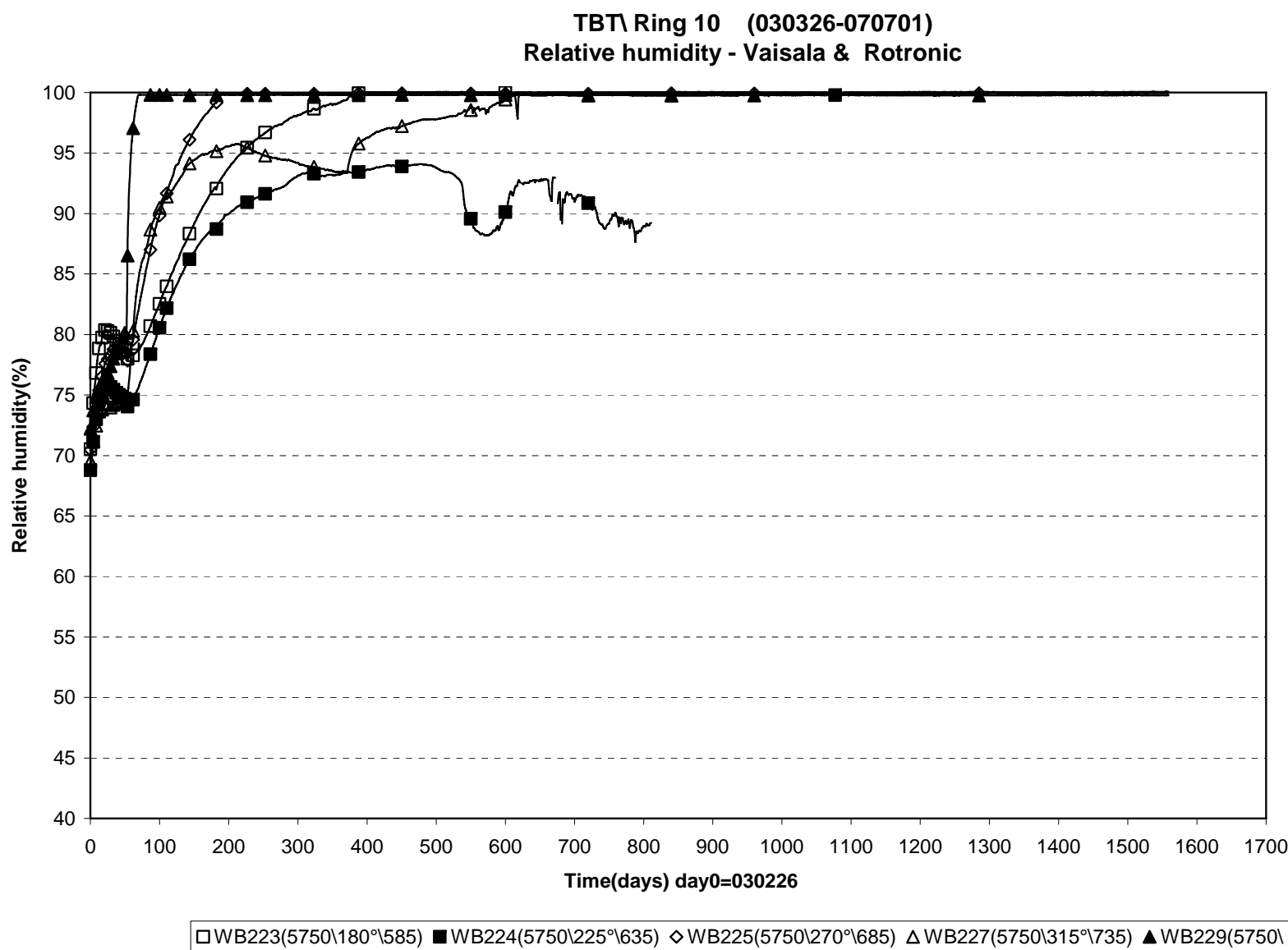


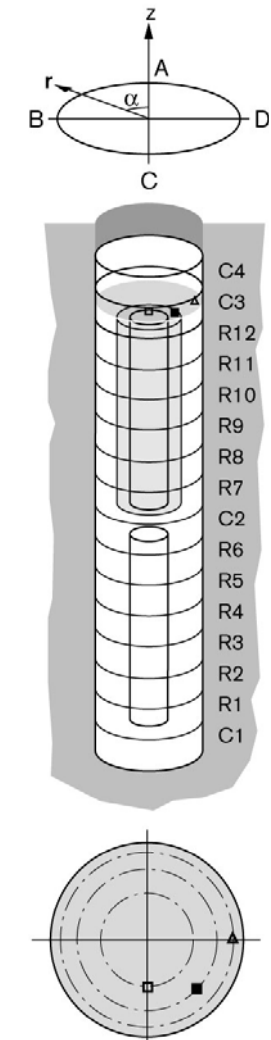
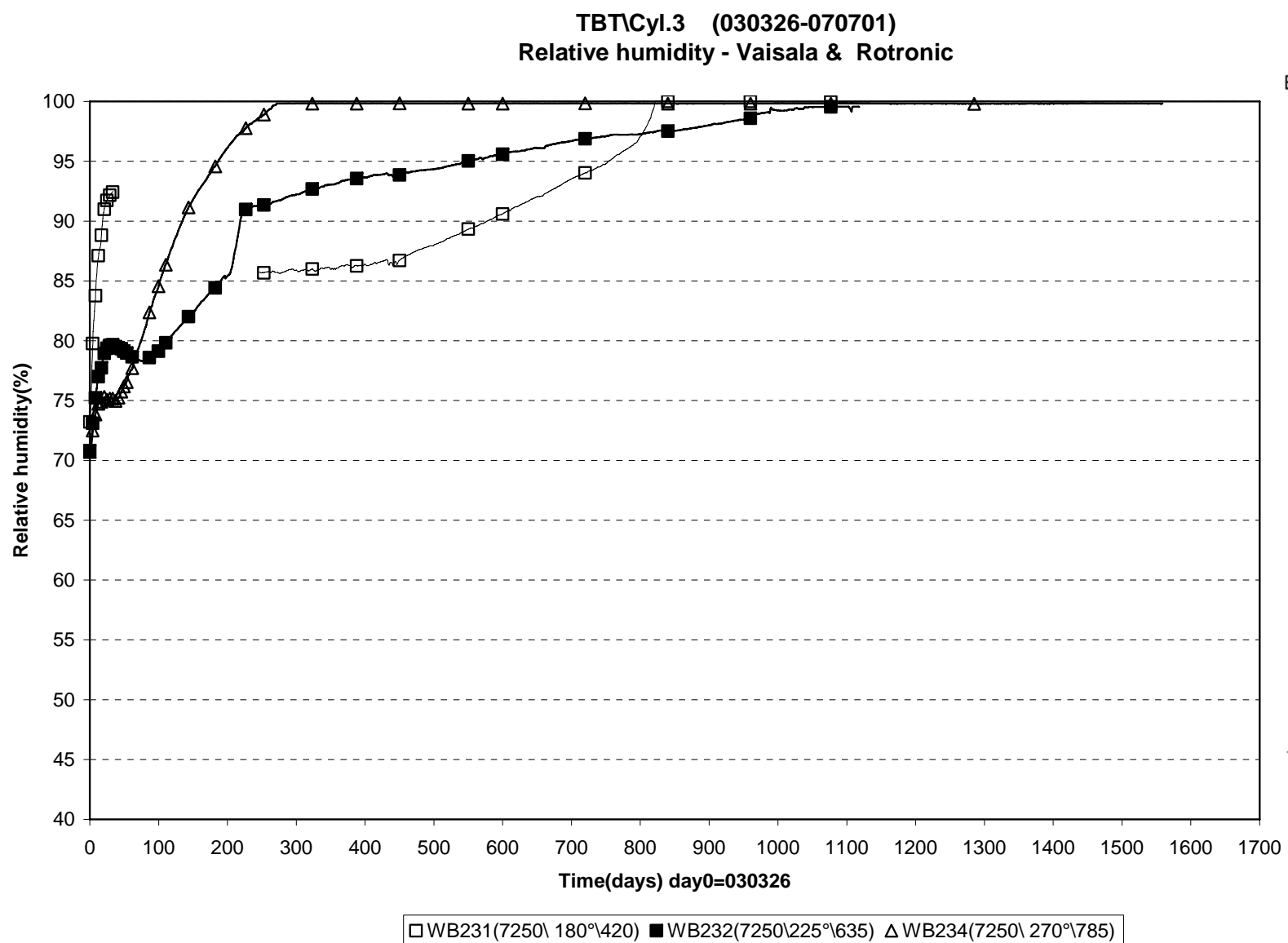


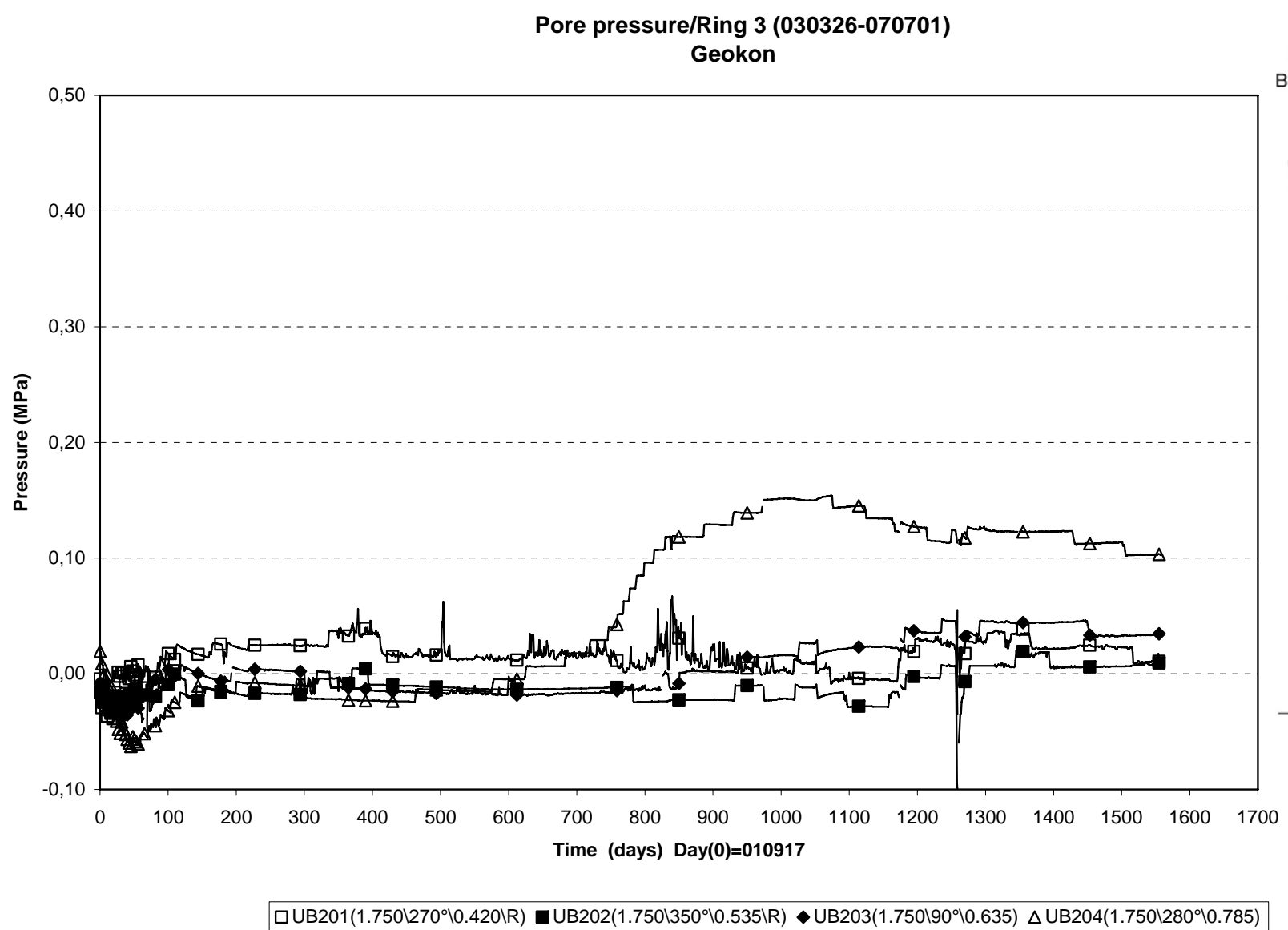


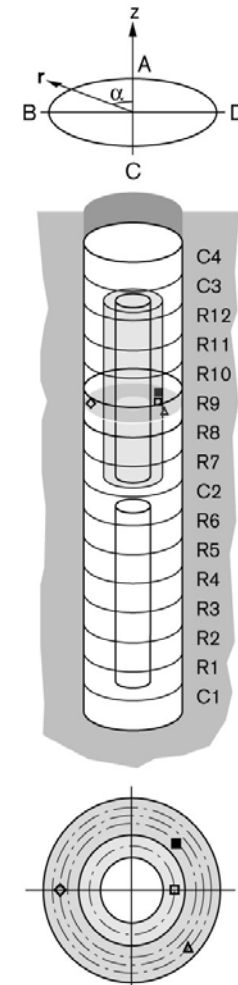
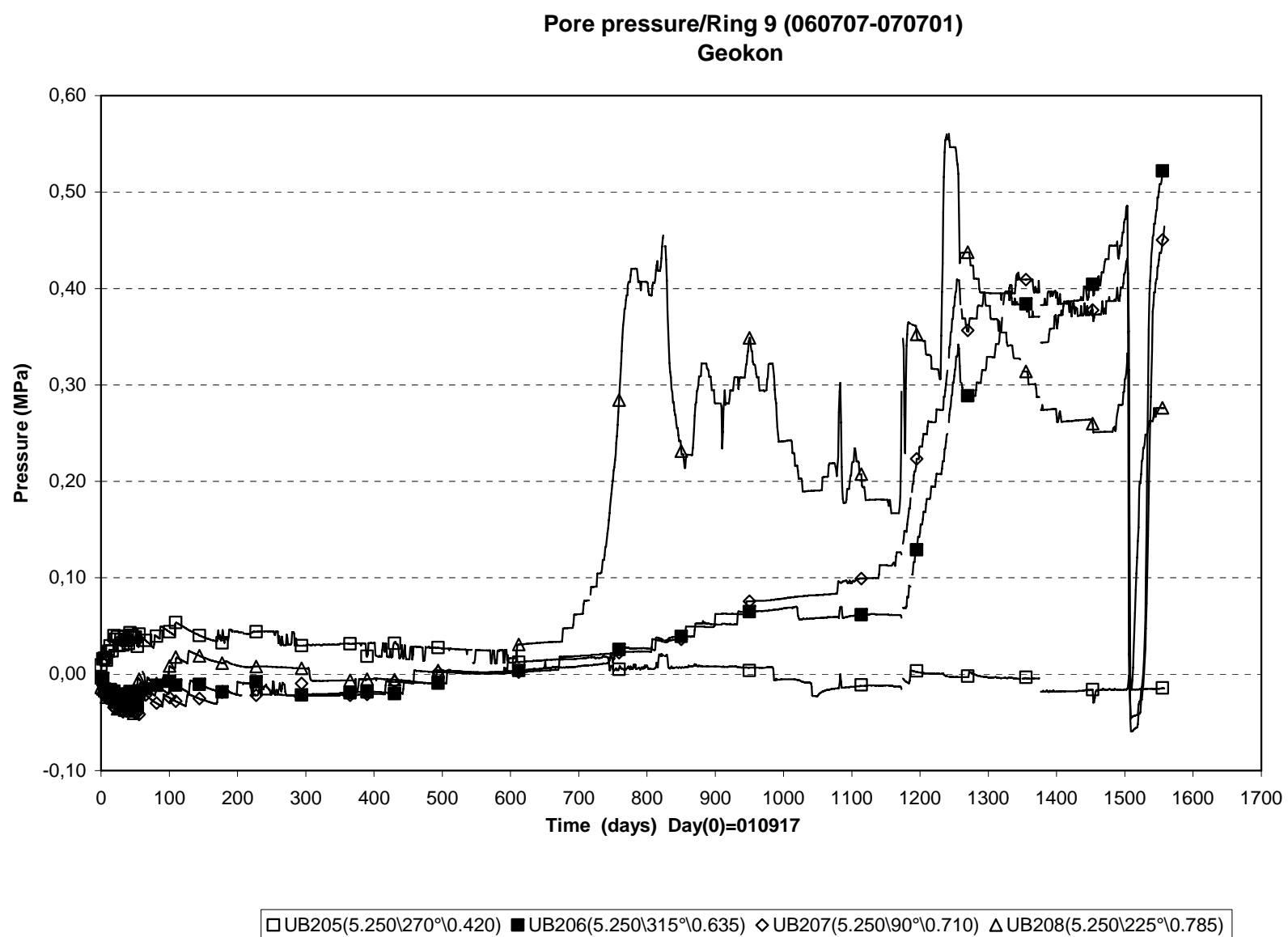




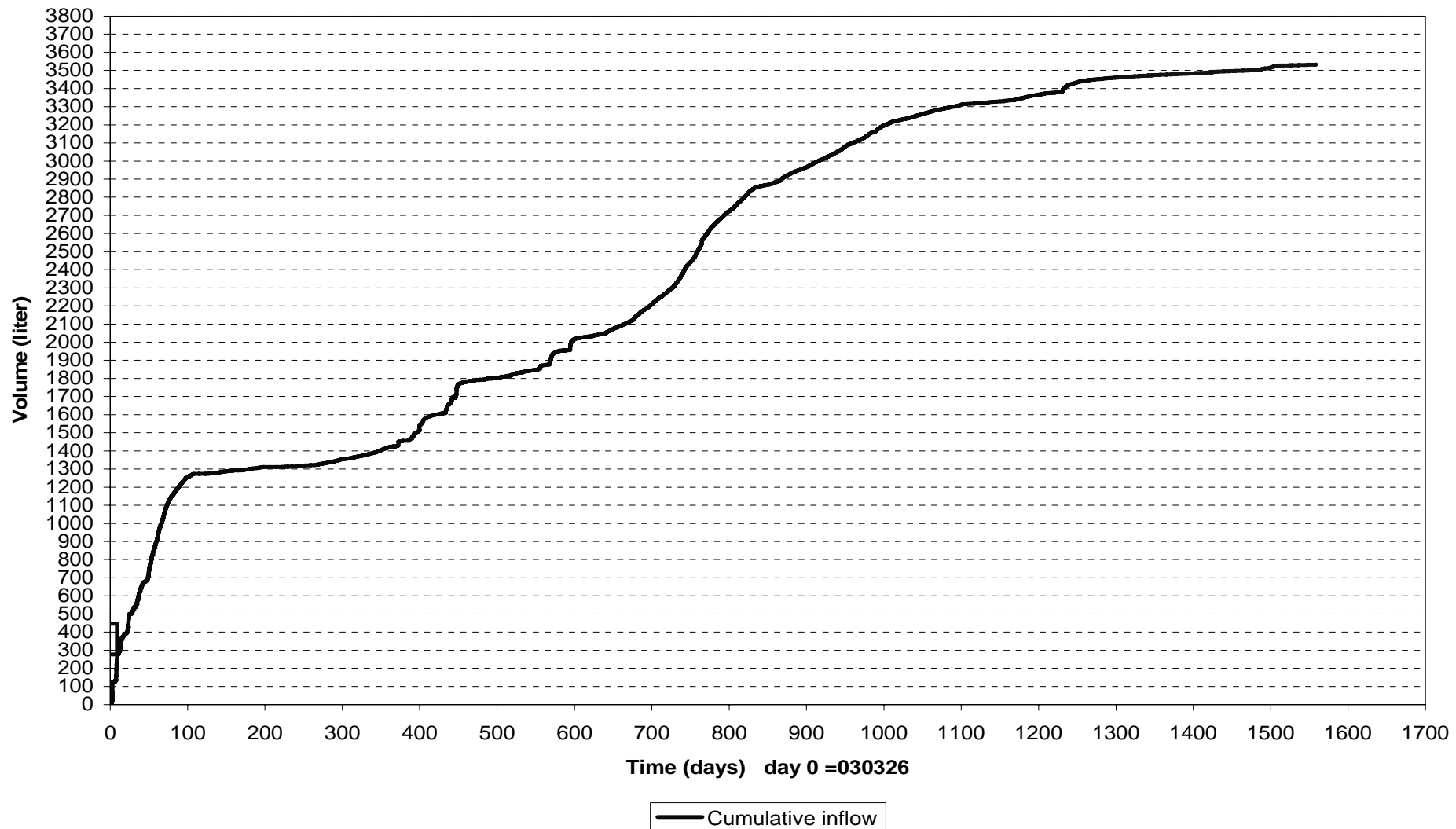




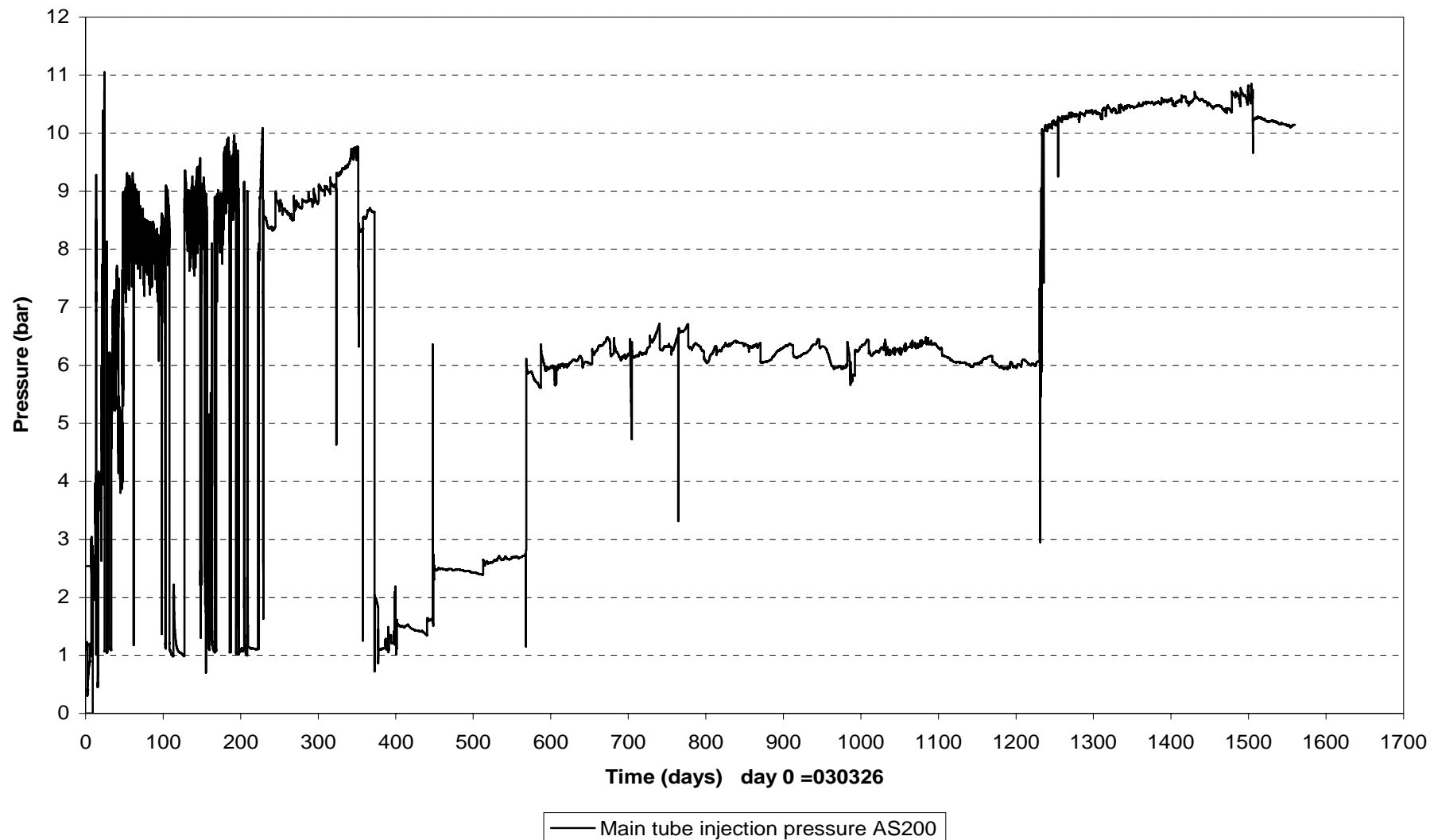




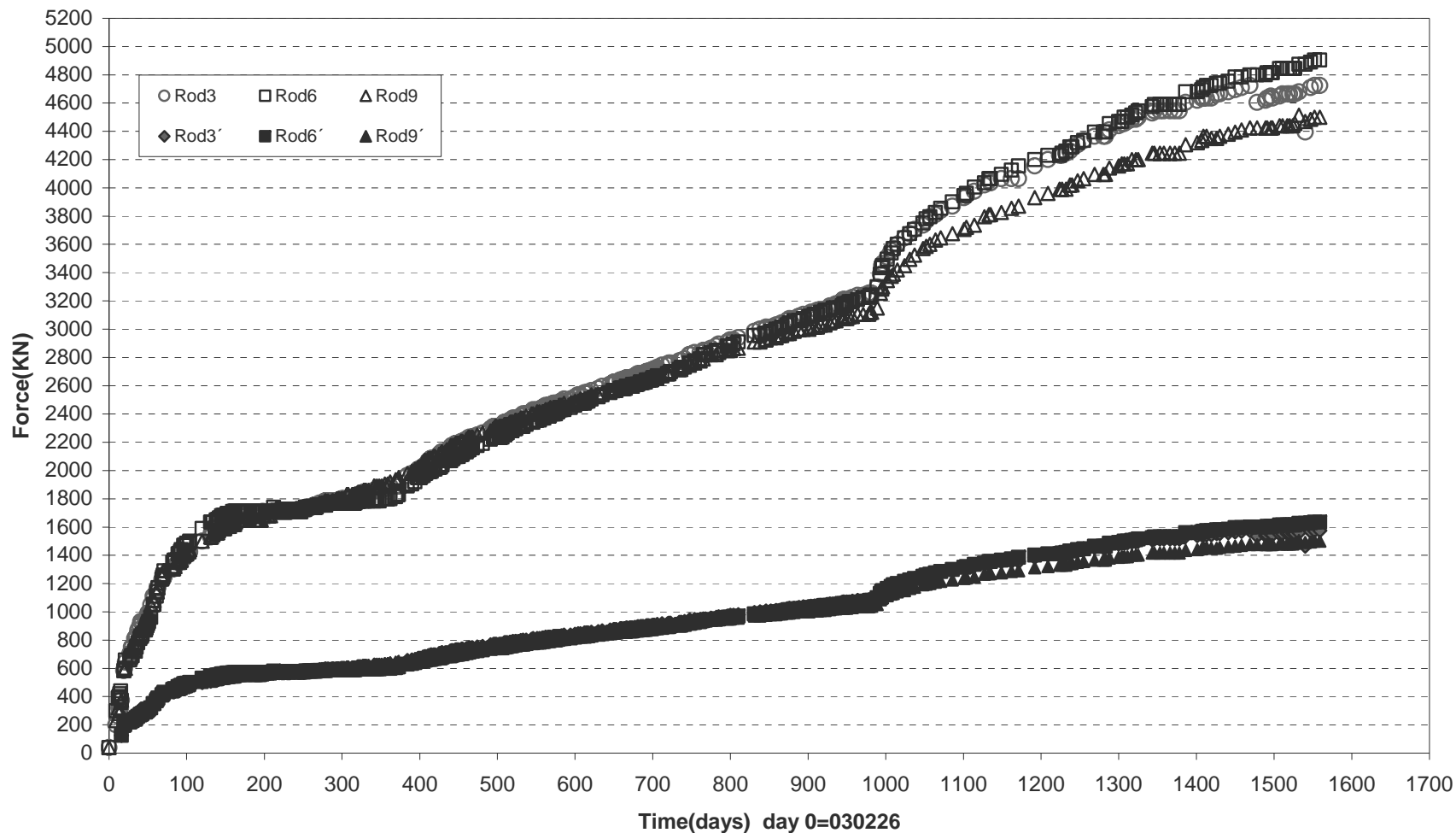
### Inflow of water (030326-070701)



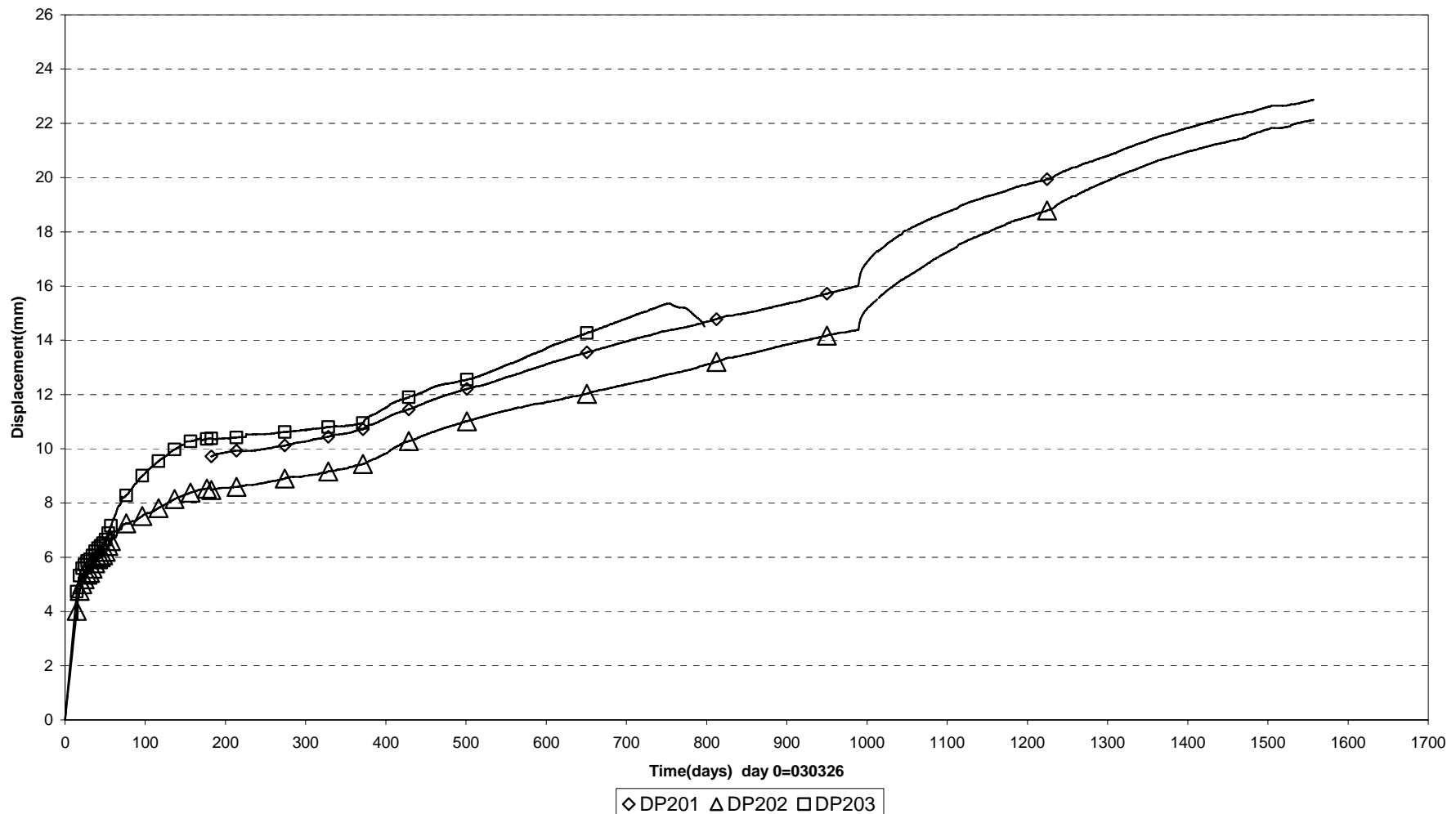
**Injection pressure upstream the filter tips (030326-070701)**



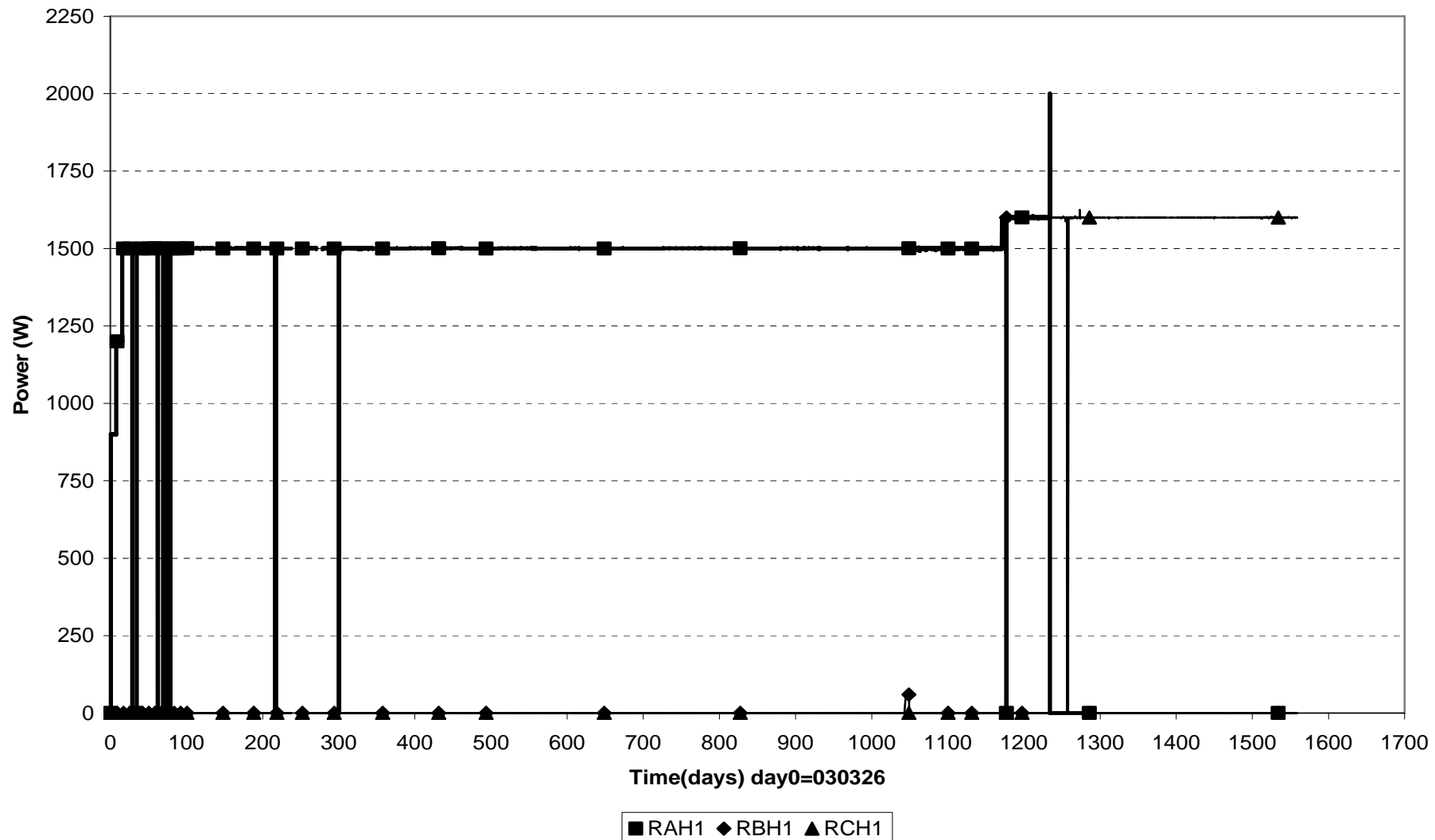
### Forces on plug (030326-070701)



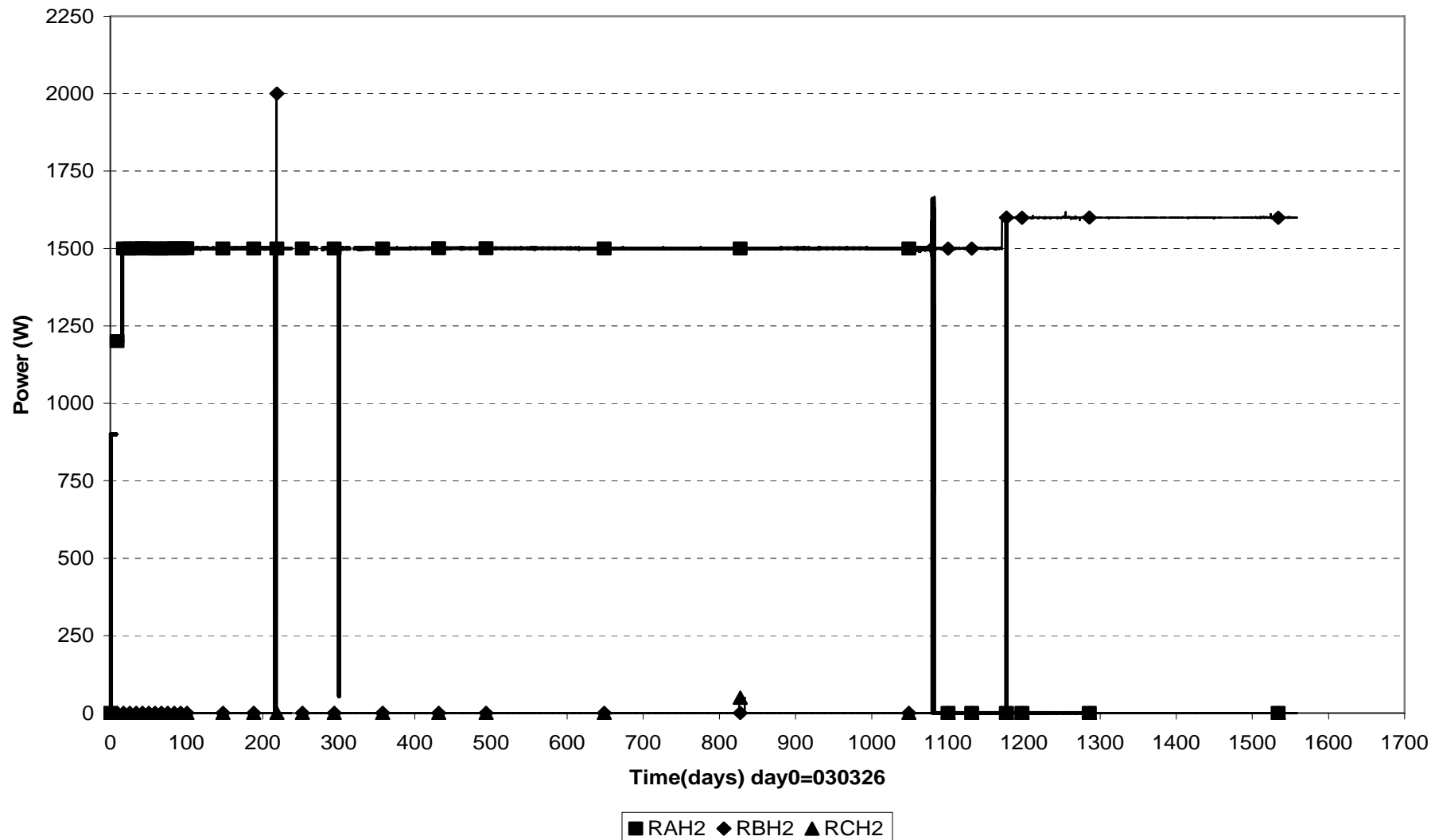
### Displacement of plug (030326-070701)



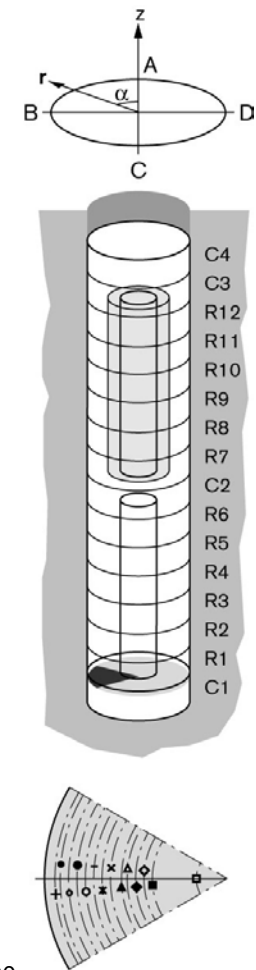
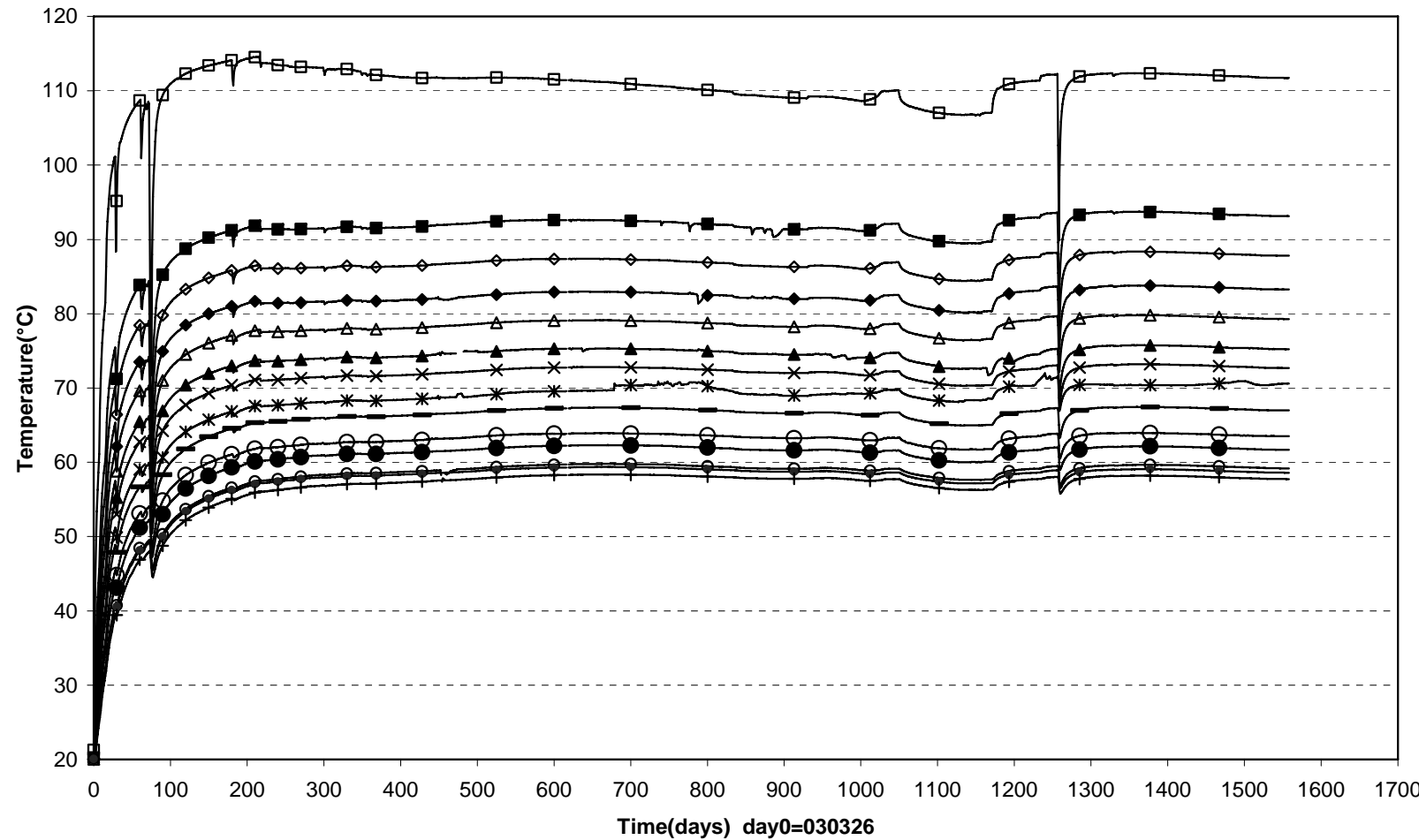
### Power Heater 1 (030326-070701)

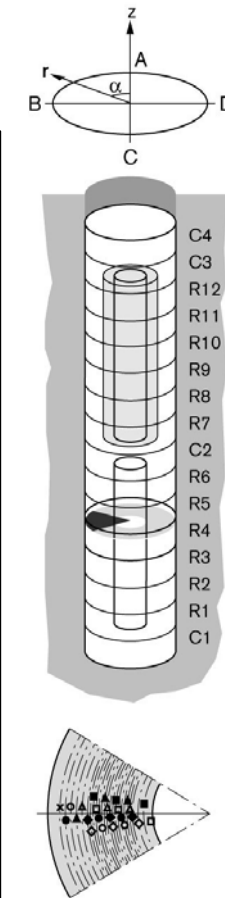
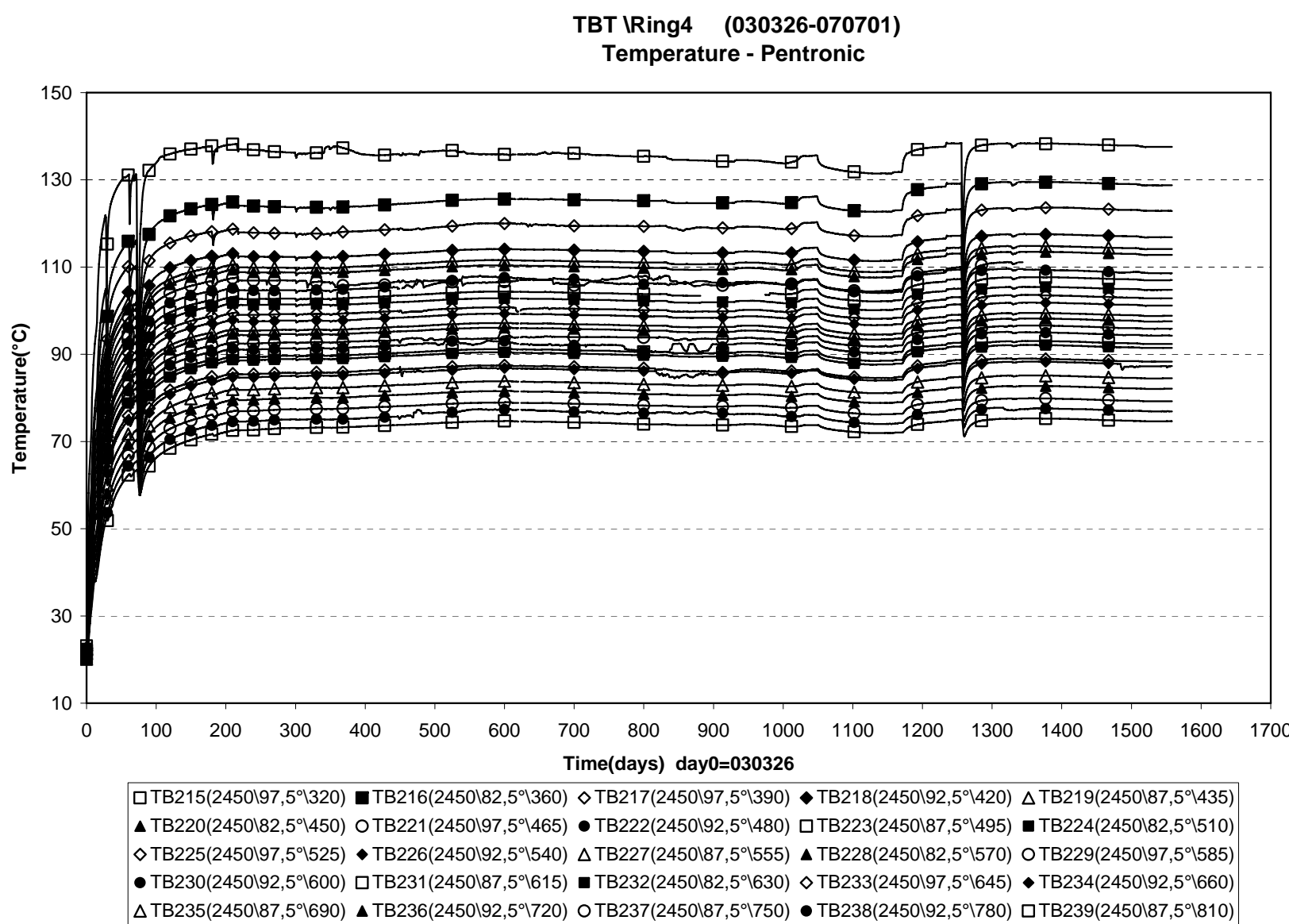


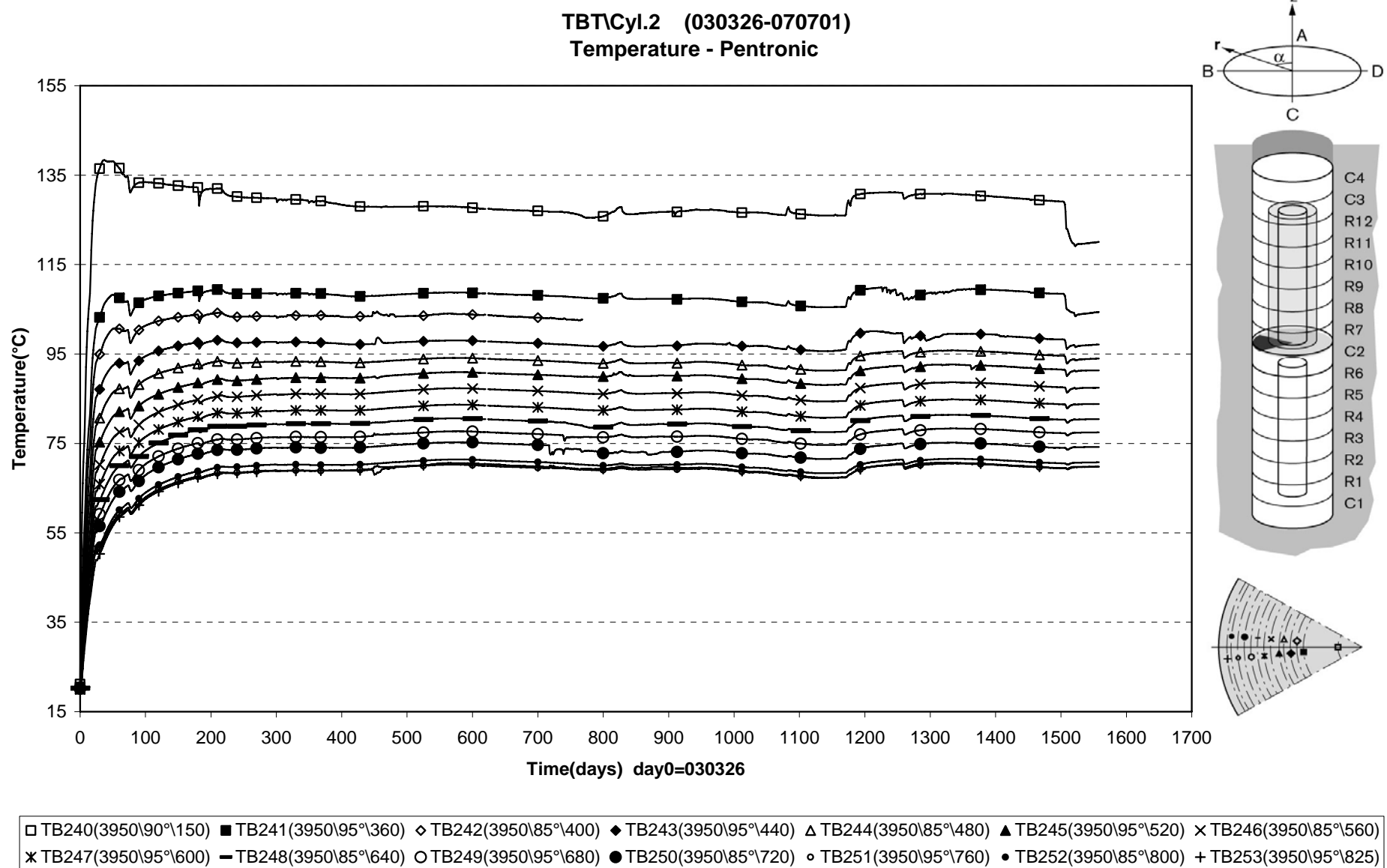
### Power Heater 2 (030326-070701)

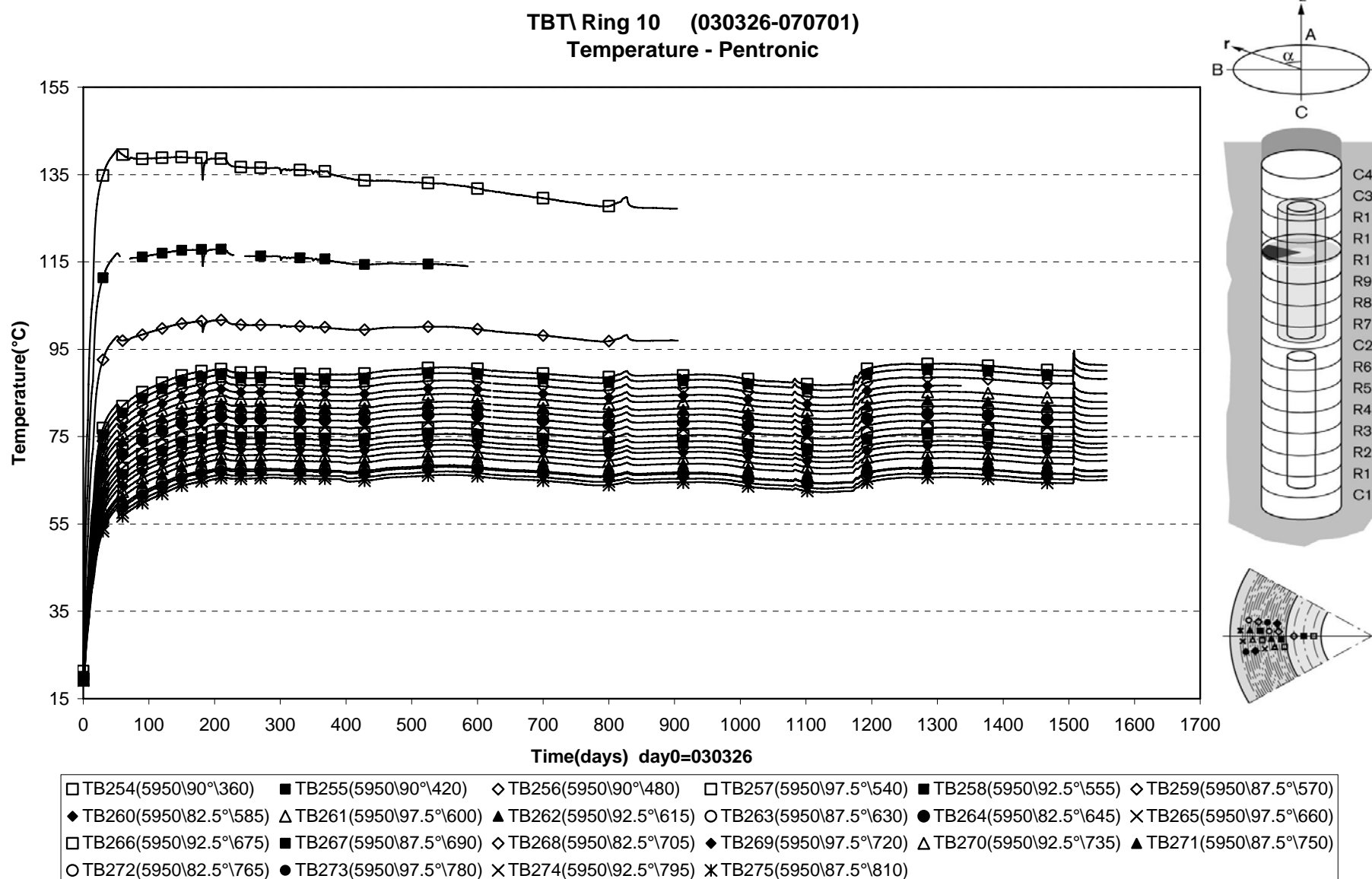


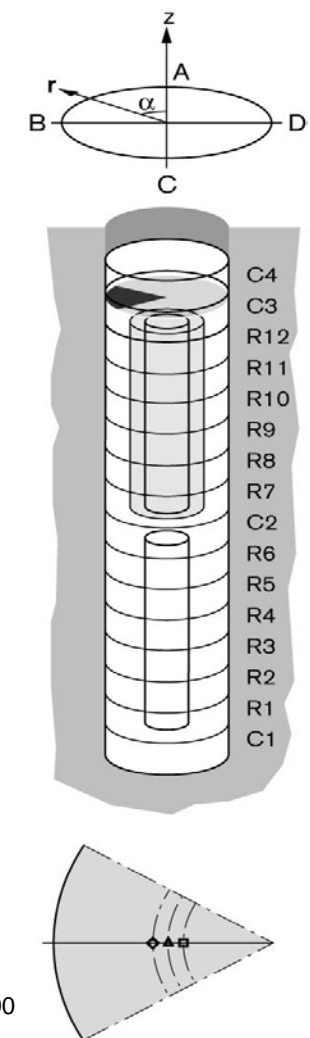
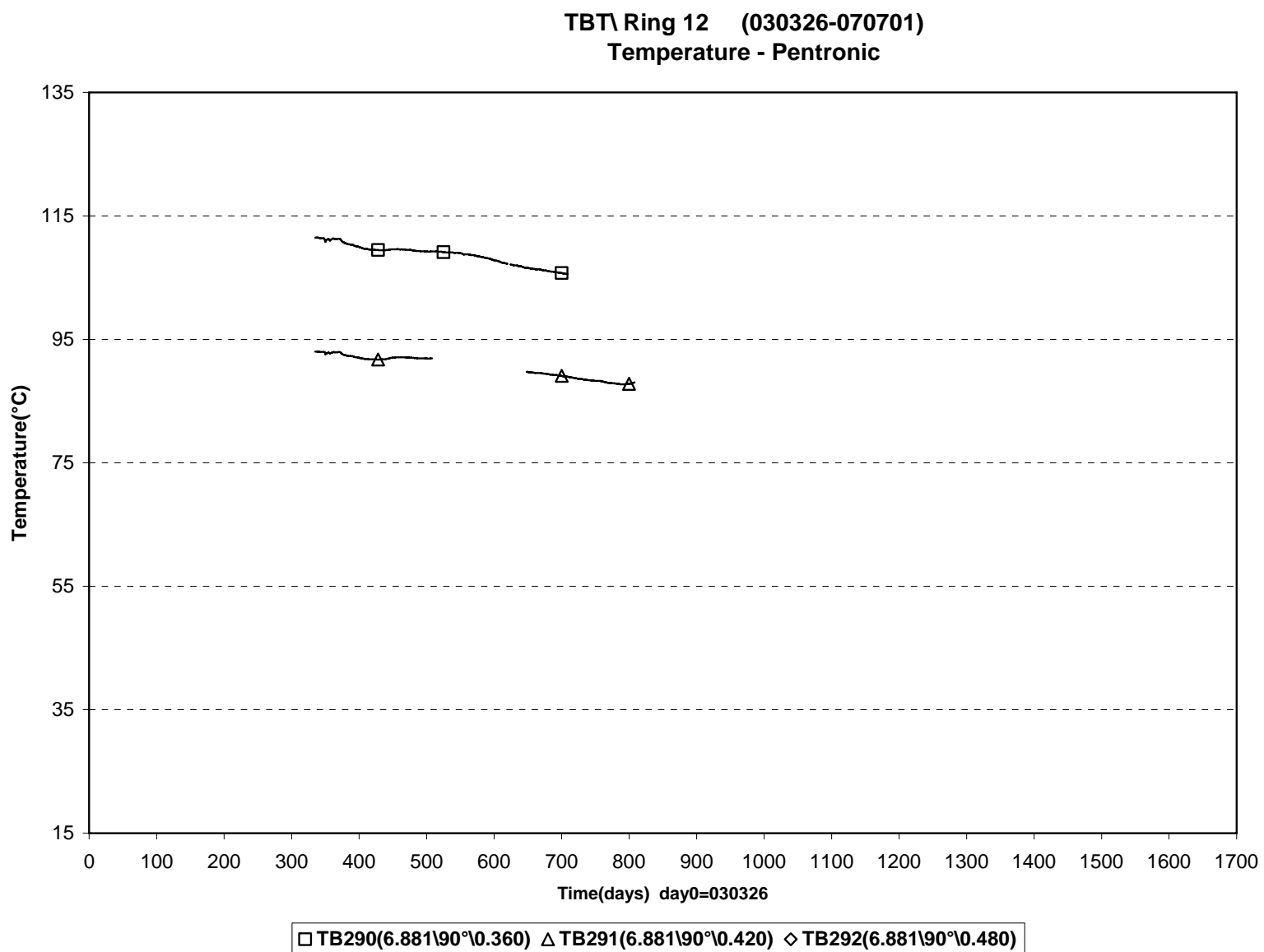
TBT\Cyl.1 (030326-070701)  
Temperature - Pentronic



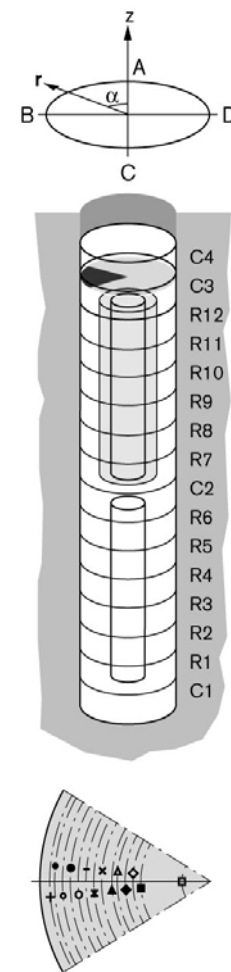
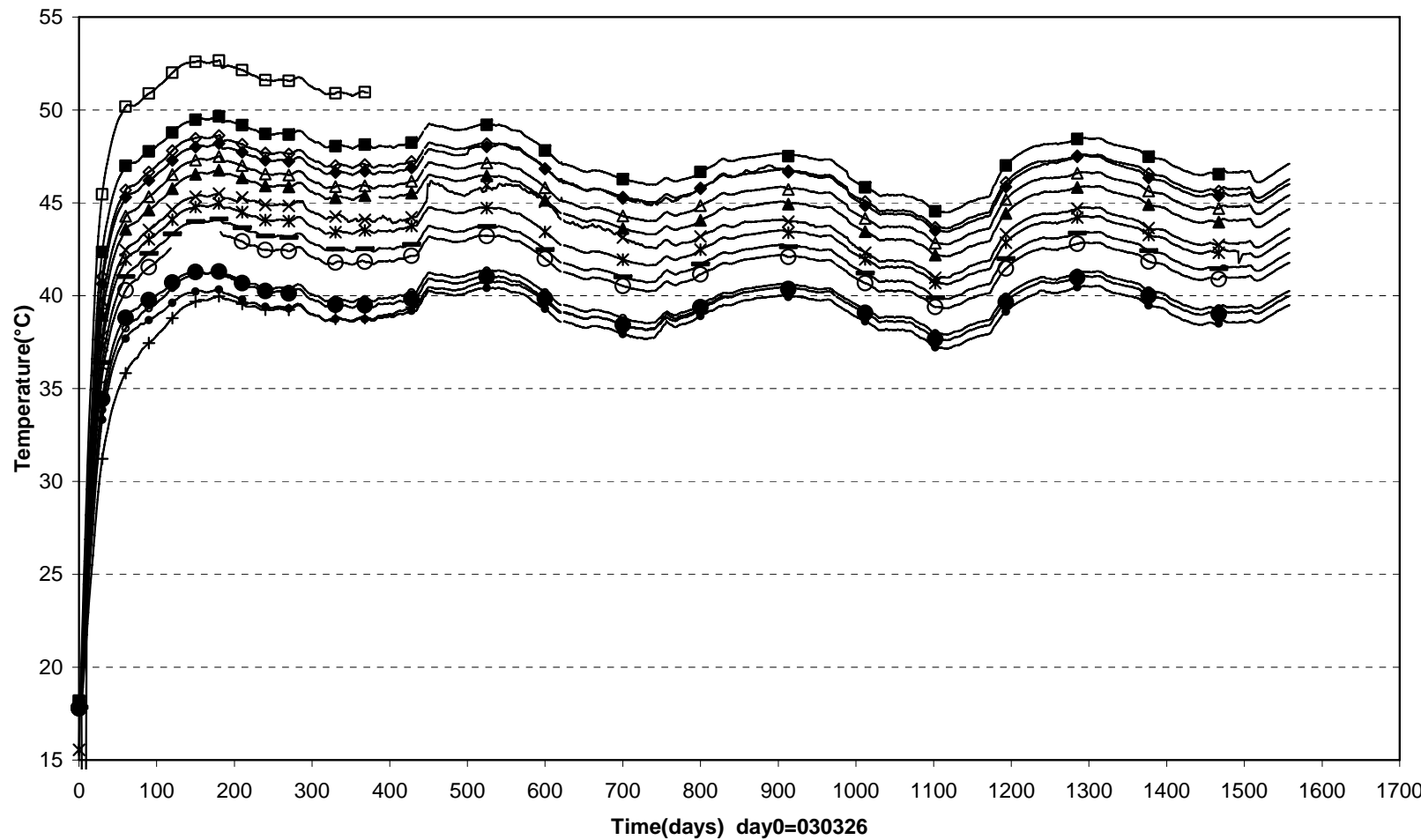




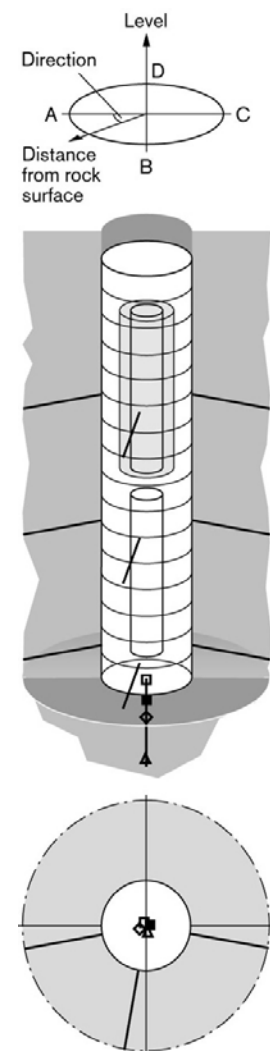
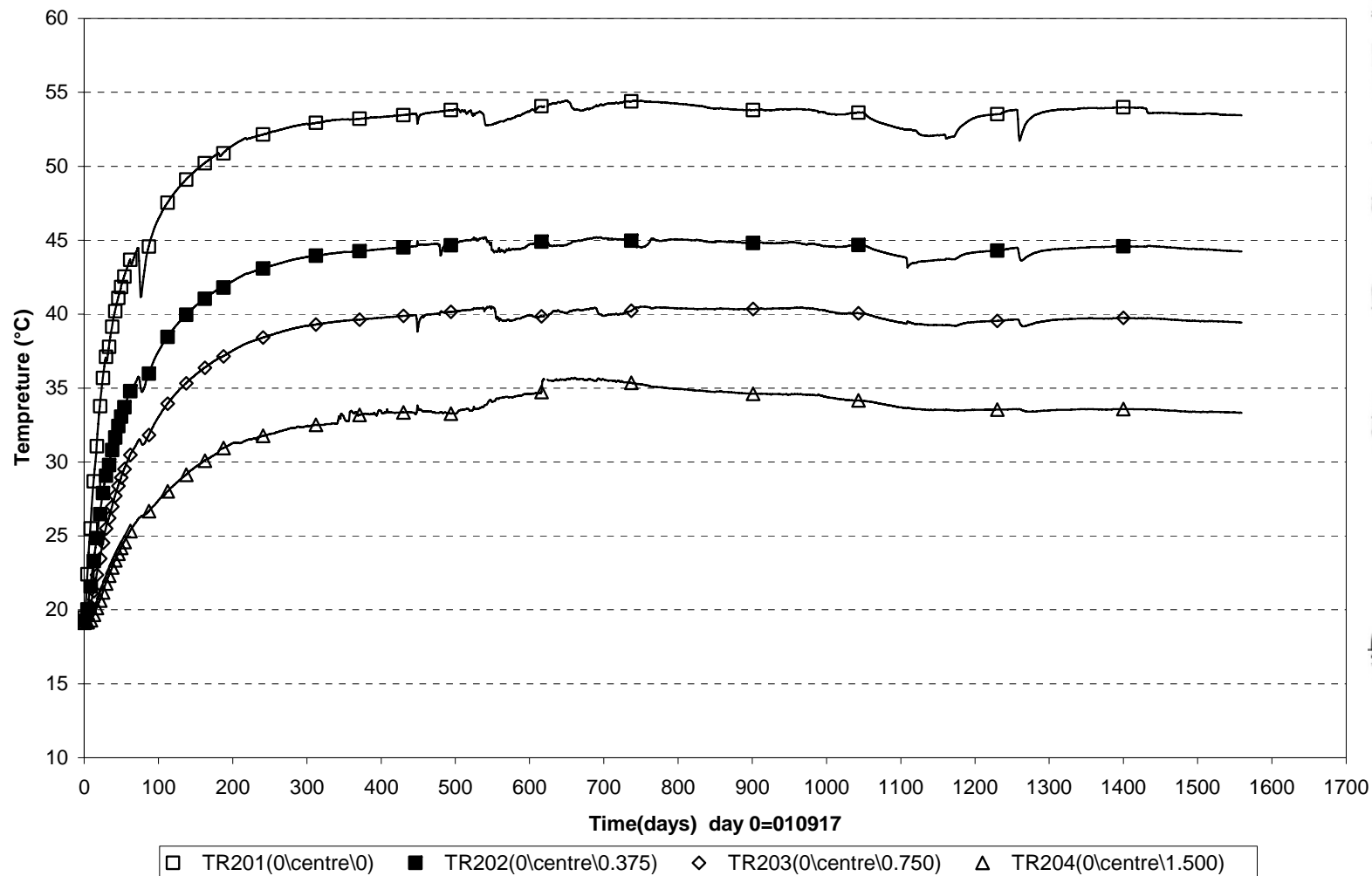




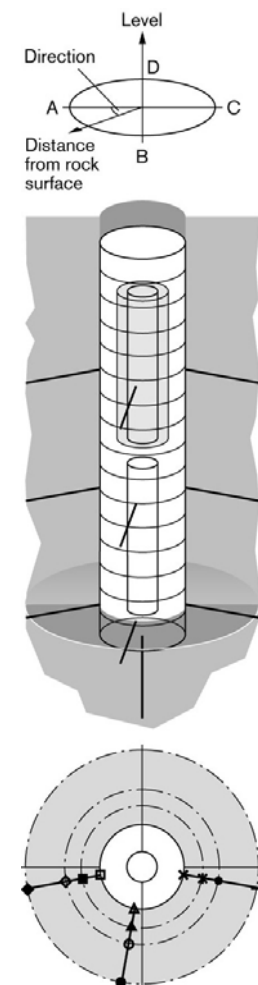
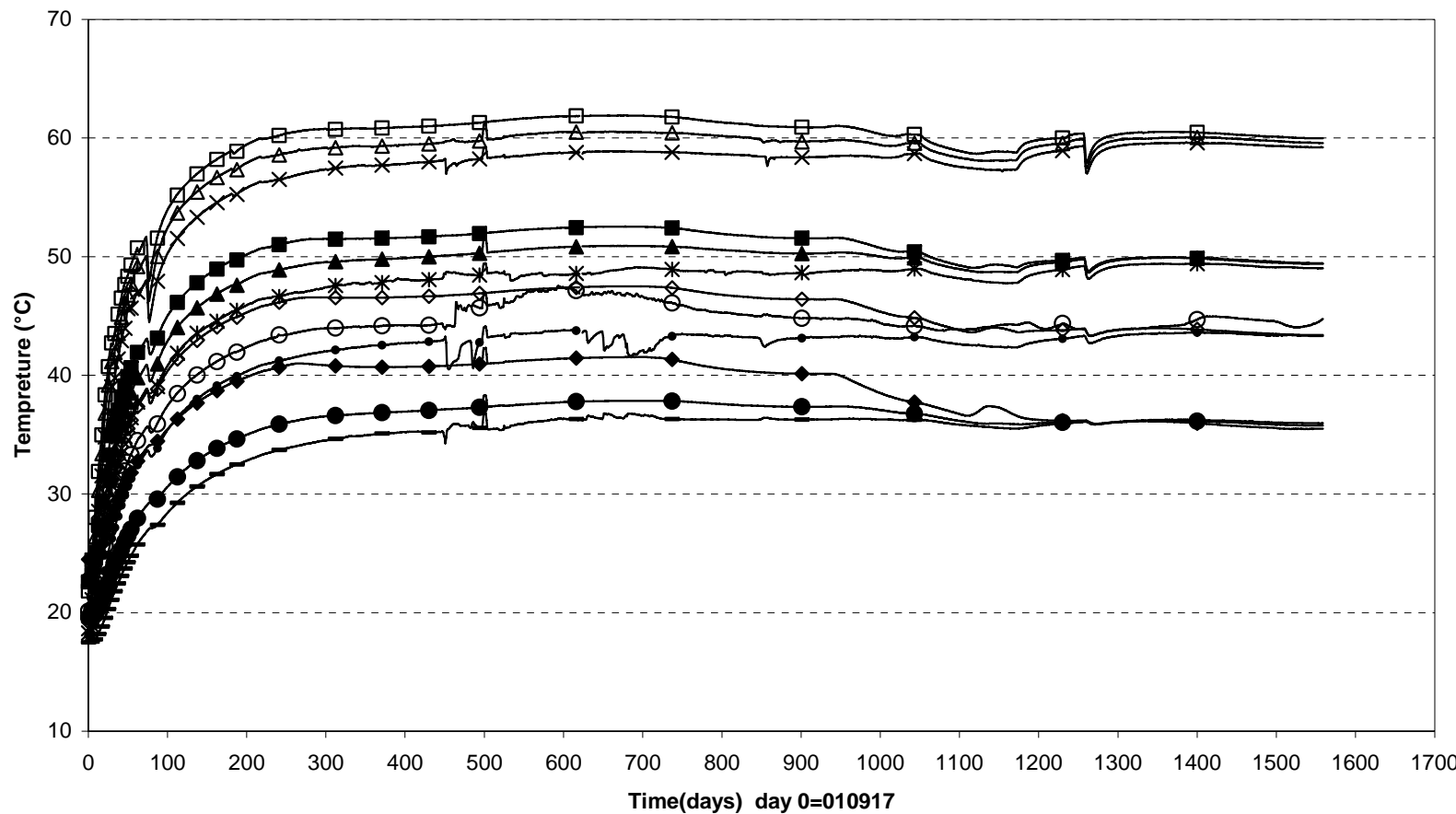
TBT\Cyl.3 (030326-070701)  
Temperature - Pentronic



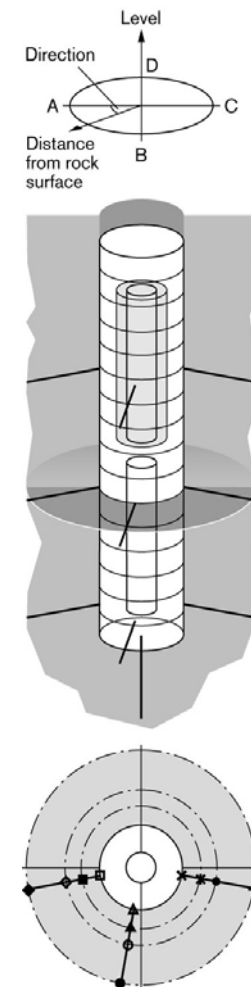
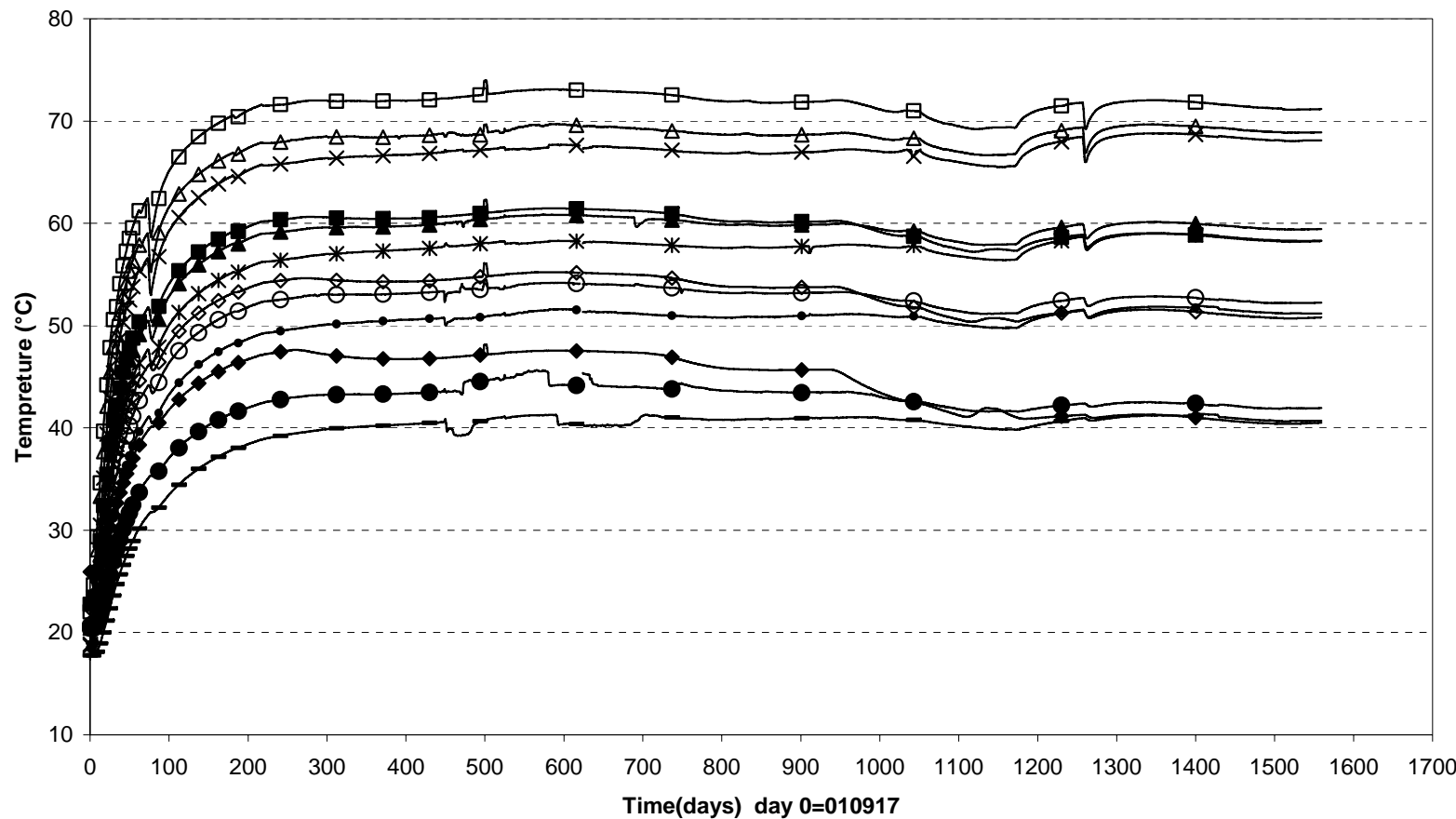
**TBT\ Temperature in the rock-below the dep.hole (030326-070701)**  
**Temperature - Pentronic**



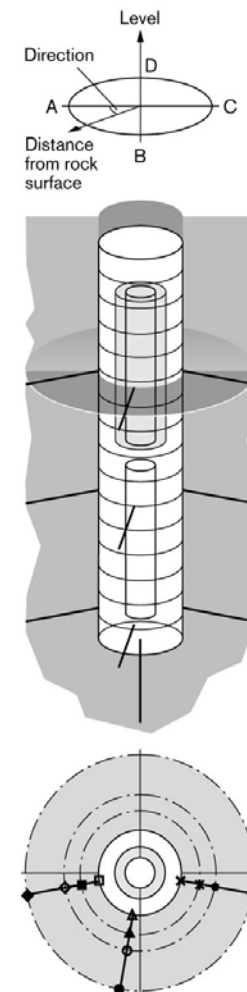
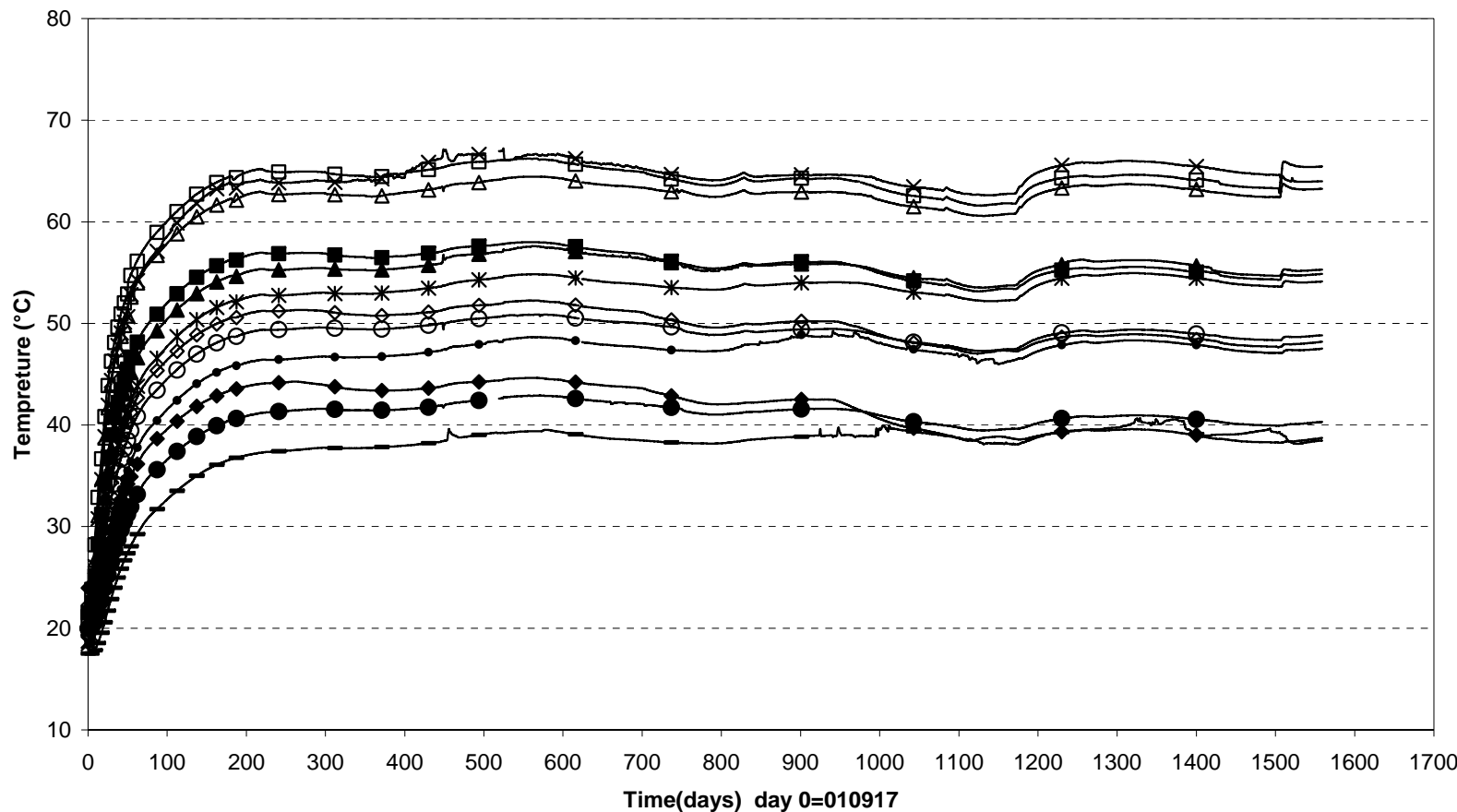
TBT\ Temperature in the rock-level 0,61 m (030326-070701)  
 Temperature - Pentronic



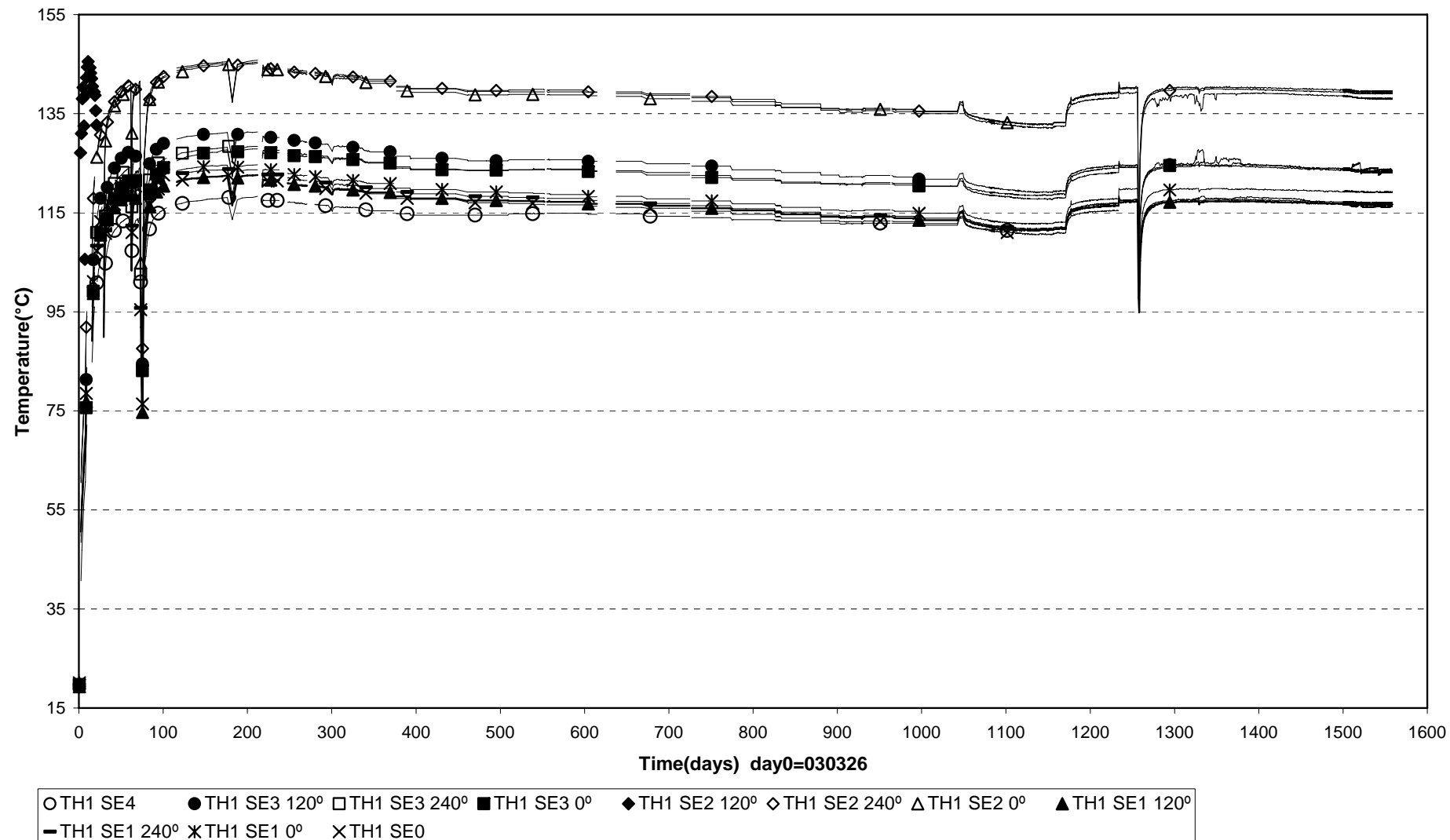
TBT\ Temperature in the rock-level 3,01 m (030326-070701)  
 Temperature - Pentronic



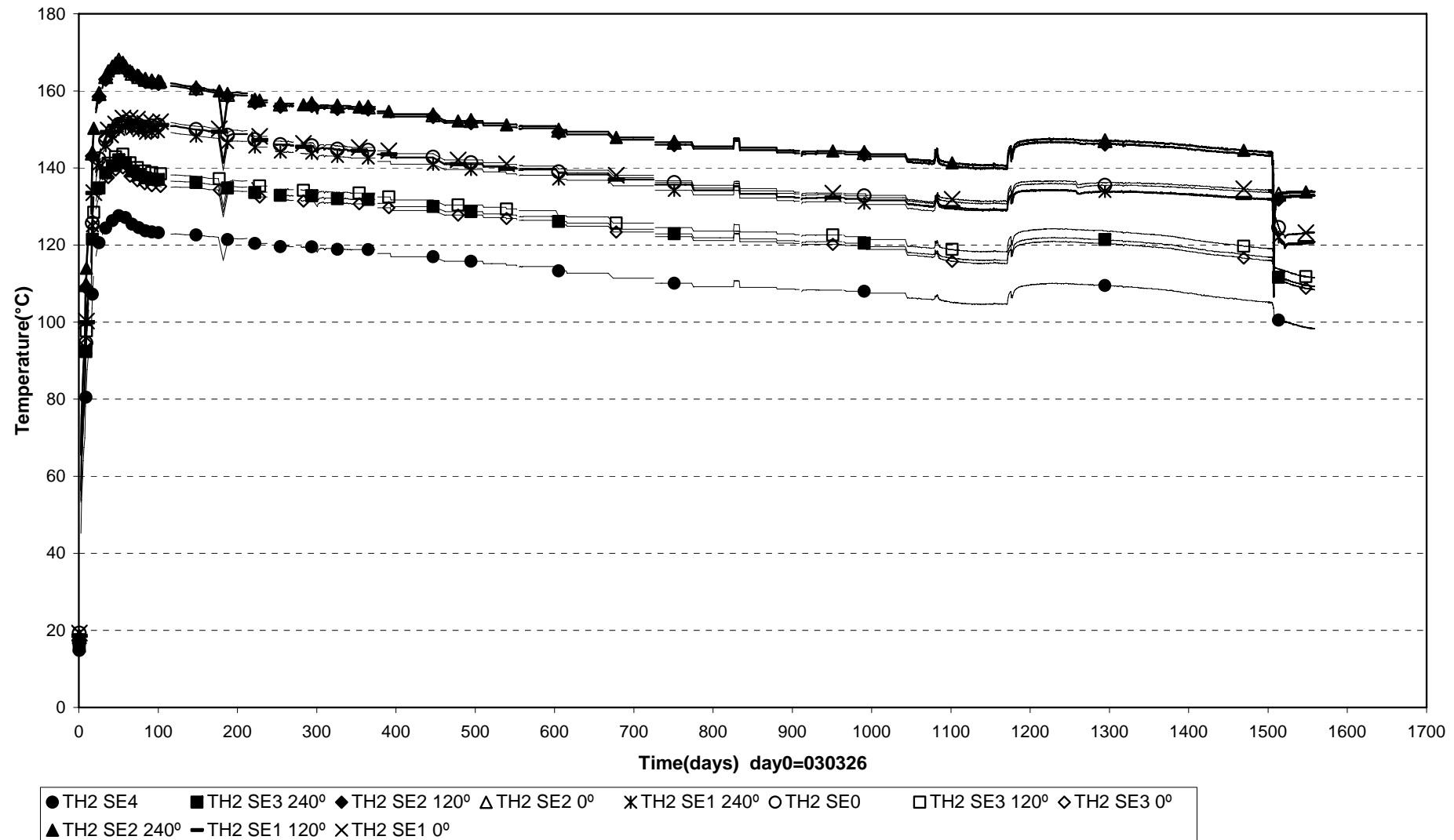
TBT\ Temperature in the rock-level 5,41 m (030326-070701)  
 Temperature - Pentronic



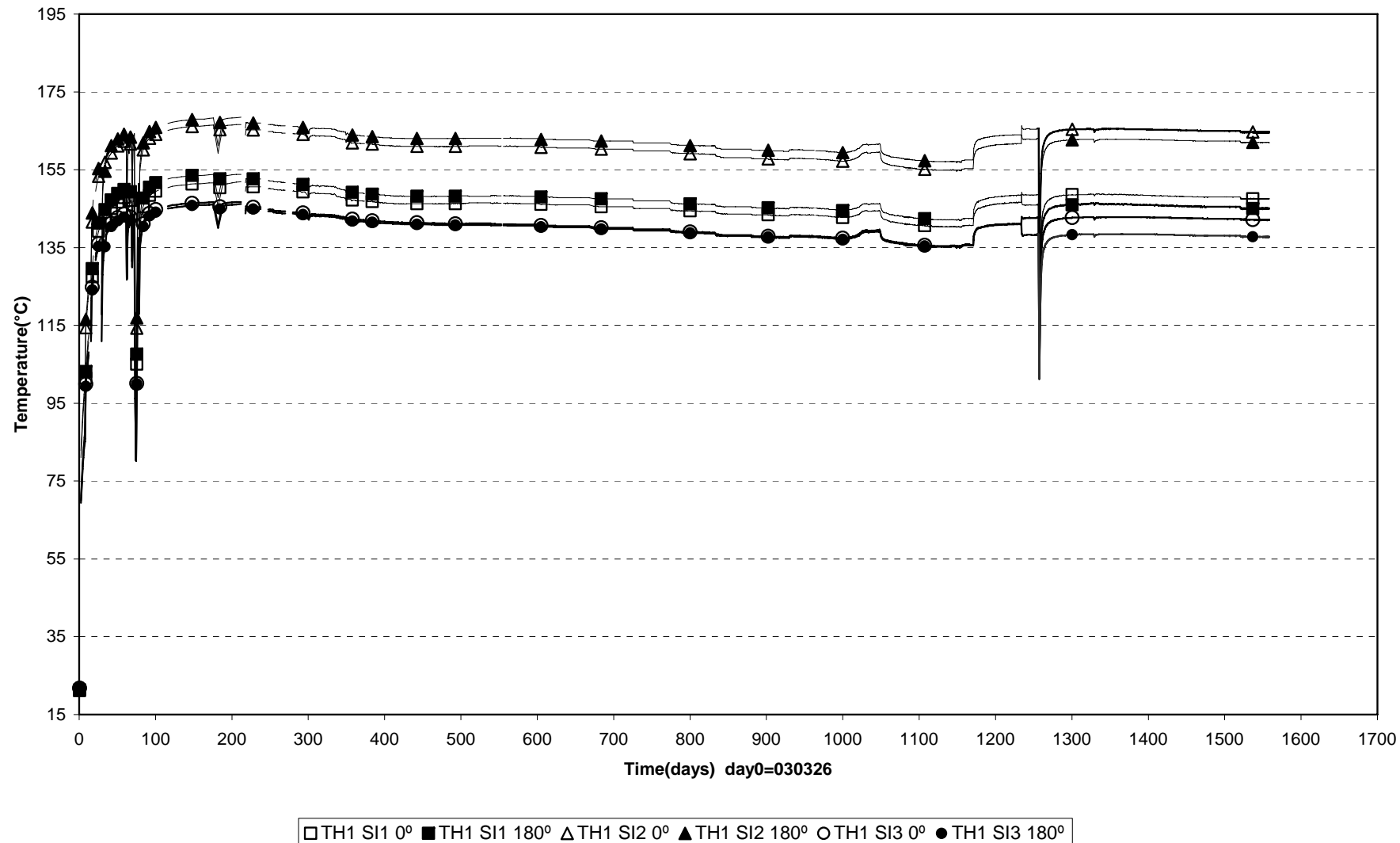
### External temperatures Heater 1 (030326-070701)



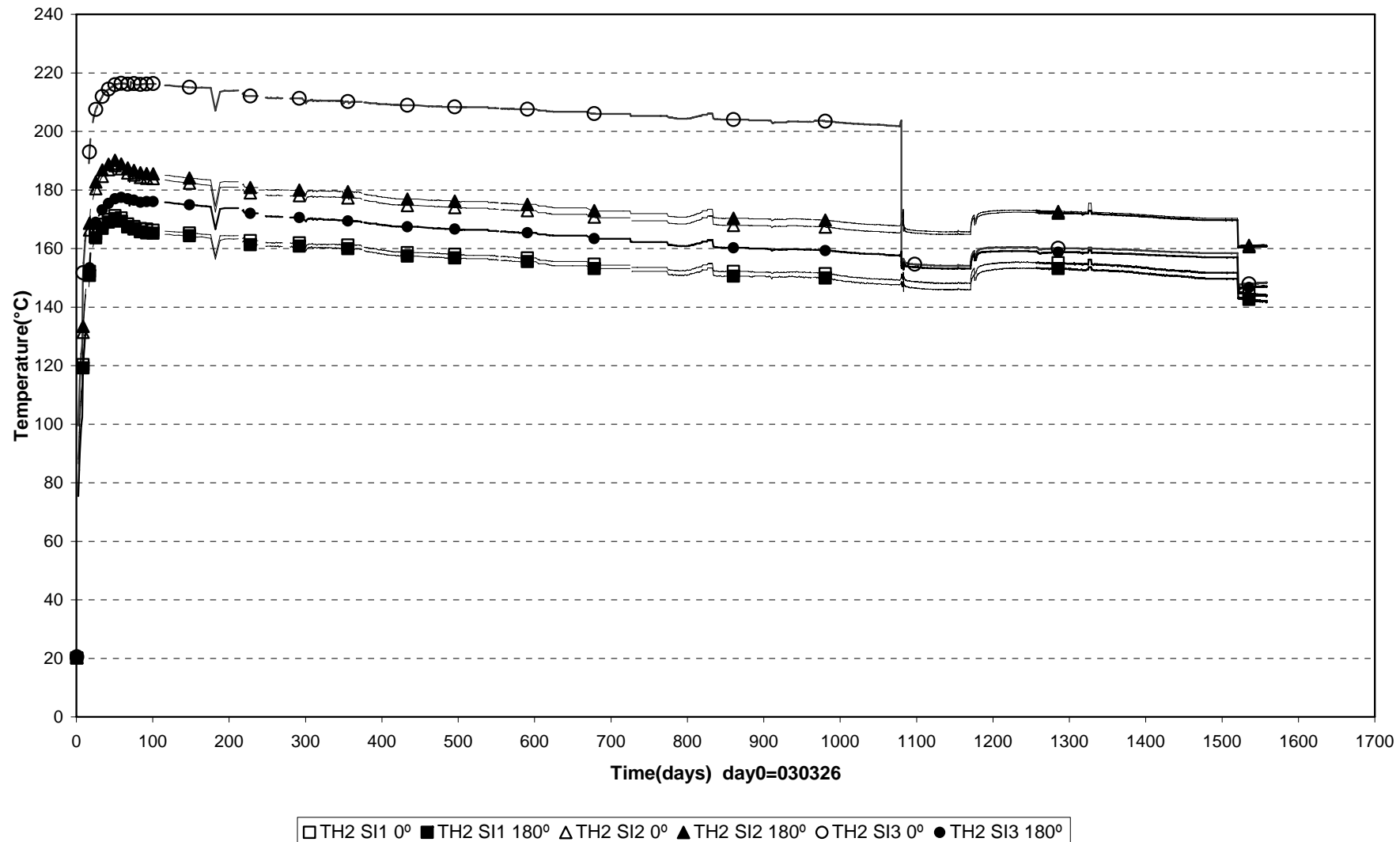
### External temperatures Heater 2 (070504-070701)



### Internal temperatures Heater 1 (030326-070701)



### Internal temperatures Heater 2 (070504-070701)



## **Appendix B**

**Measurement from optiska sensors**

*DBE Technology*



## Fiber Optic sensors in TBT

The high temperatures and the corrosive environment yield extreme requirements on the sensor material. Never before fiber optic sensors from DBE have been implemented under these conditions and thus a few optical pressure and temperature sensors have been installed for evaluation purposes.

Two pressure sensors and two pore water pressure sensors have been installed each including a low resolution temperature grating for compensation purposes. Figure 1 and 2 show the location of each sensor in addition to all the other sensors.

Data from PB231 has presented in this report .The other three sensors are out of order.

**Table 1. Numbering and position of the instruments referred to in this report.**

Instrument number	Measuring section	Block	$\alpha$ [deg]	r [mm]	z [mm]	Remark
PB204	2	Ring3	250	420	1950	Total pressure radial
PB205	2	Ring 3	290	420	2000	Total pressure axial
PB206	2	Ring 3	0	535	1950	Total pressure radial
PB207	2	Ring 3	20	535	1950	Total pressure tangential
PB208	2	Ring 3	45	585	2000	Total pressure axial
PB209	2	Ring 3	100	635	1950	Total pressure tangential
PB210	2	Ring 3	170	710	1950	Total pressure tangential
PB211	2	Ring3	180	710	1950	Total pressure radial
PB212	2	Ring 3	260	770	2000	Total pressure axial
PB213	2	Ring 3	270	875	1950	Total pressure radial on the rock
<b>PB230a</b>	<b>2</b>	<b>Ring 3</b>	<b>180</b>	<b>376</b>	<b>1950</b>	<b>Fiber Optic total pressure radial</b>
<b>PB230b</b>	<b>2</b>	<b>Ring 3</b>	<b>180</b>	<b>428</b>	<b>950</b>	<b>Fiber Optic temperature</b>
PB217	5	Ring 9	270	535	5450	Total pressure radial against sand
PB218	5	Ring 9	340	635	5500	Total pressure axial
PB219	5	Ring 9	0	635	5450	Total pressure radial
PB220	5	Ring 9	20	635	5450	Total pressure tangential
PB221	5	Ring 9	70	710	5500	Total pressure axial
PB222	5	Ring 9	110	710	5450	Total pressure radial
PB223	5	Ring 9	160	770	5500	Total pressure axial
PB 224	5	Ring 9	180	770	5450	Total pressure radial
PB225	5	Ring 9	200	770	5450	Total pressure tangential
PB226	5	Ring 9	270	875	5450	Total pressure radial on the rock
<b>PB231a</b>	<b>5</b>	<b>Ring 9</b>	<b>180</b>	<b>573</b>	<b>5450</b>	<b>Fiber Optic total pressure radial</b>
<b>PB231b</b>	<b>5</b>	<b>Ring 9</b>	<b>180</b>	<b>608</b>	<b>5450</b>	<b>Fiber Optic temperature</b>

UB201	2	Ring 3	270	420	1750	Pore pressure
UB202	2	Ring 3	350	535	1750	Pore pressure
UB203	2	Ring 3	90	635	1750	Pore pressure
UB204	2	Ring 3	280	785	1750	Pore pressure
<b>UB209a</b>	<b>2</b>	<b>Ring 3</b>	<b>190</b>	<b>495</b>	<b>1750</b>	<b>Fiber Optic pore pressure</b>
<b>UB209b</b>	<b>2</b>	<b>Ring 3</b>	<b>190</b>	<b>555</b>	<b>1750</b>	<b>Fiber Optic temperature</b>
UB205	5	Ring 9	270	420	5250	Pore pressure
UB206	5	Ring 9	315	635	5250	Pore pressure
UB207	5	Ring 9	90	710	5250	Pore pressure
UB208	5	Ring 9	225	785	5250	Pore pressure
<b>UB210</b>	<b>5</b>	<b>Ring 9</b>	<b>160</b>	<b>420</b>	<b>5250</b>	<b>Fiber Optic pore pressure and temp.</b>
TB215	3	Ring 4	97.5	320	2450	Pentronic thermocouple thermometer
TB216	3	Ring 4	82.5	360	2450	Pentronic thermocouple thermometer
TB217	3	Ring 4	97.5	390	2450	Pentronic thermocouple thermometer
TB218	3	Ring 4	92.5	420	2450	Pentronic thermocouple thermometer
TB222	3	Ring 4	92.5	480	2450	Pentronic thermocouple thermometer
TB229	3	Ring 4	97.5	585	2450	Pentronic thermocouple thermometer
TB235	3	Ring 4	87.5	690	2450	Pentronic thermocouple thermometer
TB239	3	Ring 4	87.5	810	2450	Pentronic thermocouple thermometer
TB254	6	Ring 10	90	360	5950	Pentronic thermocouple thermometer
TB255	6	Ring 10	90	420	5950	Pentronic thermocouple thermometer
TB256	6	Ring 10	90	480	5950	Pentronic thermocouple thermometer
TB260	6	Ring 10	82.5	585	5950	Pentronic thermocouple thermometer
TB267	6	Ring 10	87.5	690	5950	Pentronic thermocouple thermometer
TB275	6	Ring 10	87.5	810	5950	Pentronic thermocouple thermometer

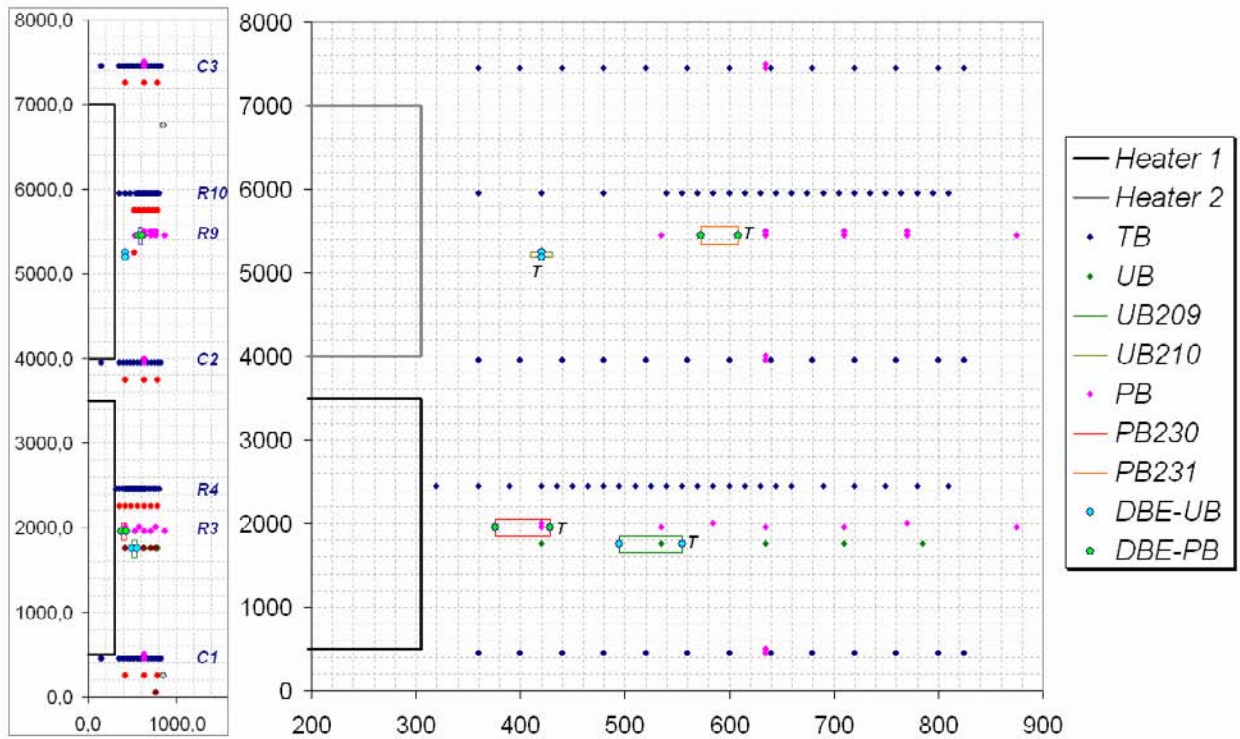


**Fig. 1.** Vertical location and radial distance of each sensor in mm.

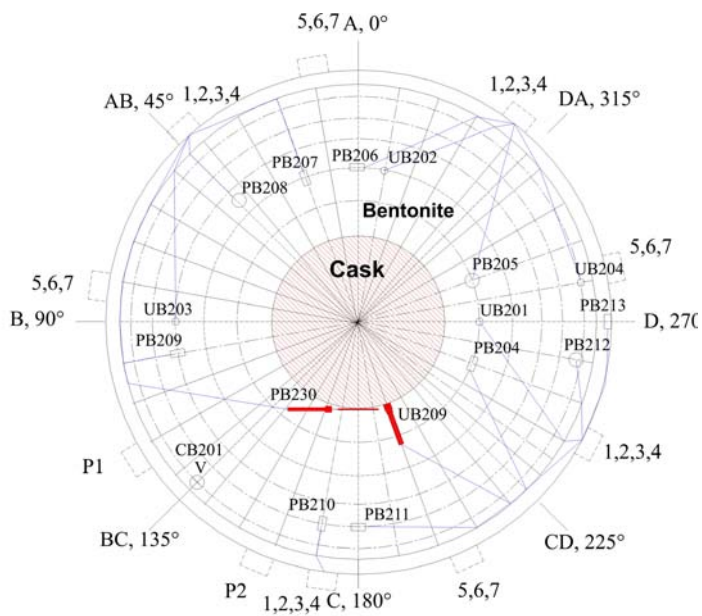


**Fig. 2a.** Radial location of sensors in Ring 3 horizontal cross-sections of the lower canister.

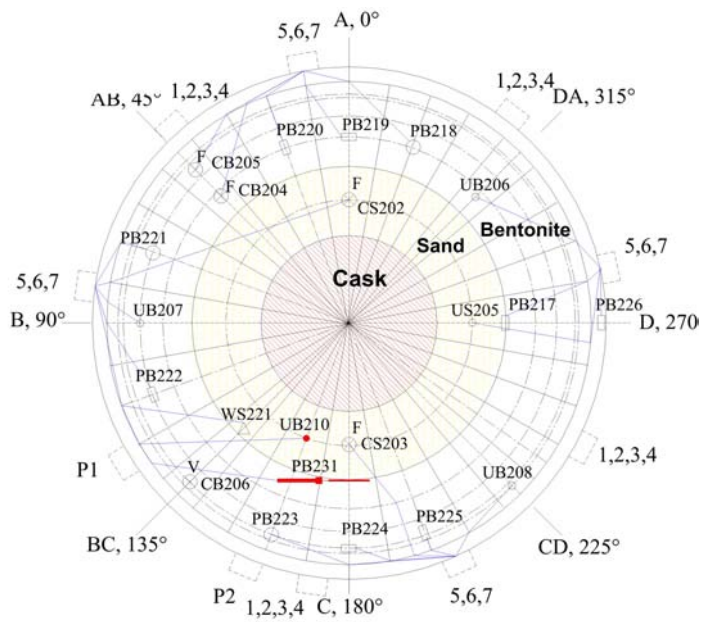
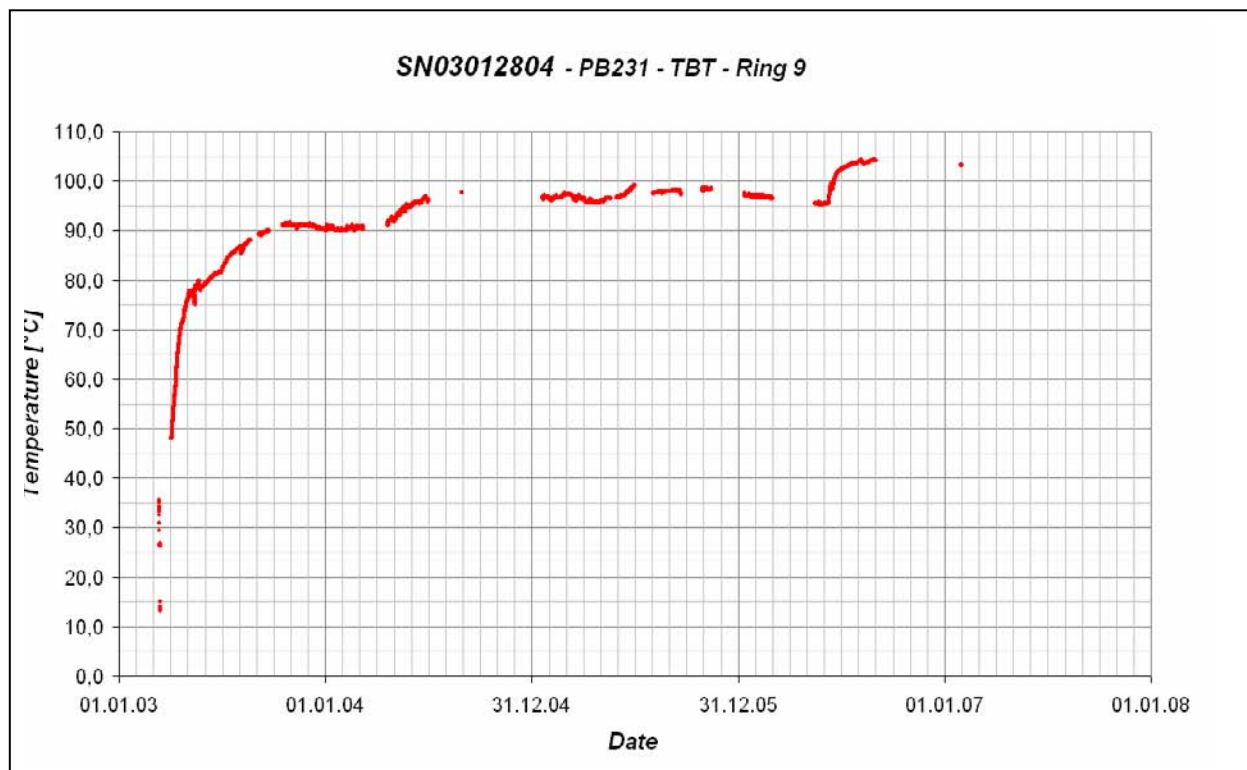


**Fig. 2b.** Radial location of sensors in Ring 9 horizontal cross-sections of the upper canister

Data update of FO-sensor PB231 (the other three sensors failed)



*SN03012804 - PB231 - TBT - Ring 9*

